Is the grass always greener on the other side? Comparing vegetation dynamics of a protected area and adjacent communal rangeland during growing seasons with extreme climatic events

---

Alekzandra Marí Szewczuk

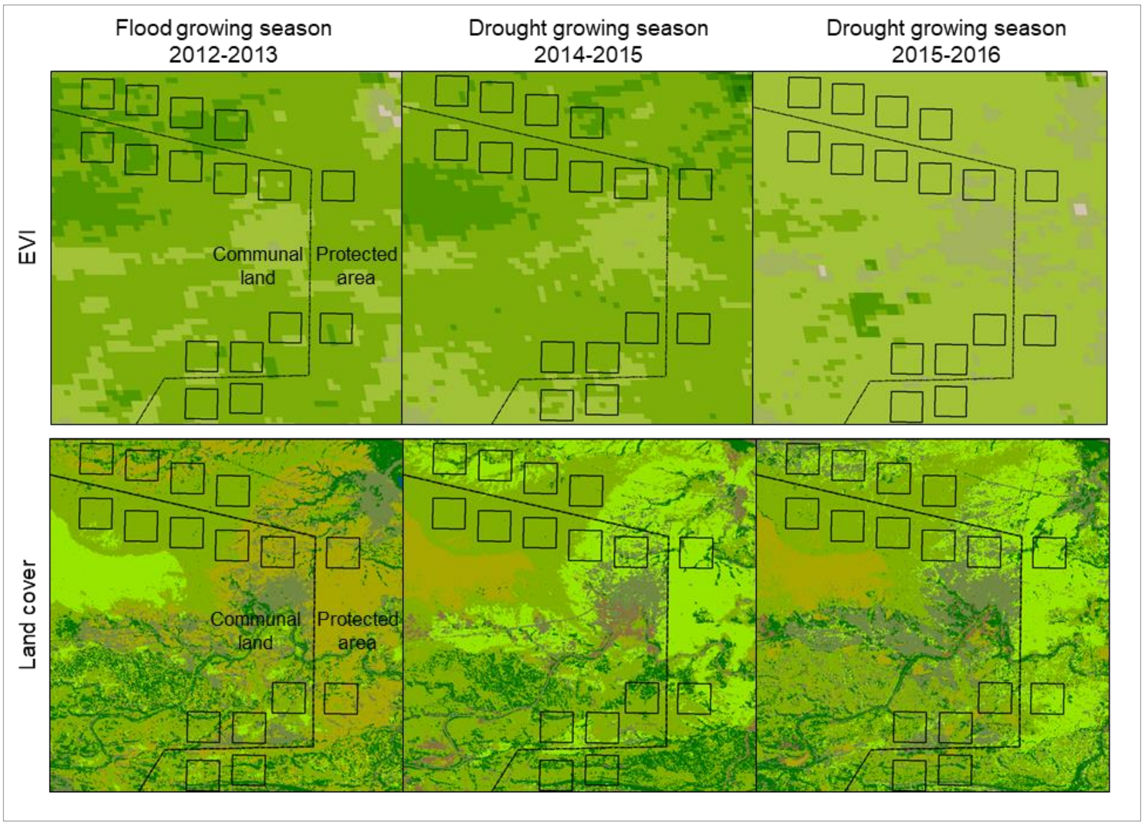

Master of Science Dissertation: School of Animal, Plant and Environmental Sciences, University of the Witwatersrand, Johannesburg

WITS UNIVERSITY

AP&ES

May 2019

Declaration

I declare that this dissertation is my own unassisted work, which is being submitted for the degree of Master of Science at the University of the Witwatersrand, Johannesburg. It has not been previously submitted for any degree or examination in any other university.

Supervisors:

Prof Ed Witkowski

Dr Melissa Whitecross

University of the Witwatersrand, Johannesburg

____

Alekzandra Marí Szewczuk
29 May 2019

Table of contents

Abstract

Recent changes in global climate have led to an increase in the severity and frequency of climatic events with current climate models predicting that global temperatures and regional rainfall patterns will continue changing in the future. Annually, the initiation of any phenological event is triggered by seasonal changes in temperature, photoperiod and rainfall. Enhanced Vegetation Index (EVI), a measure of vegetation greenness, obtained from remotely sensed MOD13Q1 16-day composite imagery (250 m resolution), was used to extract phenological time series data and the associated phenometrics of growing seasons. Six consecutive growing seasons (2011-2017) were assessed, during which two "extreme" events occurred. These were a flood in 2013 (annual rainfall = 757.8 mm) and a drought from 2014-2016, in 2014-15 (annual rainfall = 343.7 mm) and 2015-16 (annual rainfall = 307.5 mm). To test if land use and extreme climatic events had an influence on the phenometrics of a mopane dominated region, phenological responses of vegetation to these extreme events was assessed. This was conducted at multiple sites, within a communal rangeland and a protected area- on either side of the north-western fence line of the Greater Kruger National Park, near Pafuri, with a total area of 1250 ha on either side of the fence. The phenological dynamics were compared to rainfall, temperature and photoperiod. Lastly, land cover was determined using three different remote sensing platforms (MODIS MCD12Q1, 500 m resolution; Landsat 8 OLI and TIRS, 30 m resolution; Sentinel-2A, 10 m resolution) for both sides of the fence and the change across the growing seasons was assessed. Results showed that differences in phenology and the associated phenometrics measured within the communal land and protected area were driven by land use, rather than by vegetation type. The start of greenup and the length of the growing season were significantly earlier (six days; $p<0.001$) and longer (five days; $p<0.001$) in the communal land. However, the end times did not differ notably for the two sites ($p = 0.410$). Although the communal land had slightly greater productivity (1%, $p<0.05$), the protected area had slightly more seasonally active vegetation (1%, $p<0.01$). EVI was not as strongly influenced by rainfall (protected area: $R^2 = 0.180$; communal land: $R^2 = 0.190$) yet, the phenometrics derived from EVI were more susceptible to changes in seasonal rainfall. The flood year had the longest growing season (protected area = 229 days; communal land = 244 days; $p<0.05$) and greatest vegetation productivity (flood year to first drought year: protected area = 13% decrease; communal land = 13% decrease, $p<0.05$; flood year to second drought year- protected area = 9% decrease; communal land = 8% decrease, $p<0.05$). All the phenometrics were significantly influenced by change in austral years. The end time of the growing season was the only phenometric to not be significantly influenced by land use ($p = 0.405$). Land use had a significant effect on the response of the $Start_T$, $Peak_T$ and Mid_T to conditions associated with the flood year and first drought year. Dense shrub was the most dominant land cover class for both sides of the fence as detected by the finer scales of Landsat 8 (communal land = 50%, protected area = 42%) and Sentinel (communal land = 43%, protected area = 28%). The MODIS assessment, however, showed significant differences across the fence line for the two common land cover classes between the two sides of the fence, with grass being the most dominant cover class (communal land = 83%, protected area = 95%, $p<0.01$) followed by deciduous broadleaf trees (communal land = 12%, protected area = 95%, $p<0.05$). All three datasets showed change in land cover across most of the austral seasons. More importantly, Landsat 8 and MODIS showed land cover to change considerably after the flood year, and Landsat 8 and Sentinel-2 showed change after the drought years.This study highlights the impacts of extreme climatic events and the response of vegetation under different land management strategies to these events. As well as providing important insight for land managers and conservation practitioners, given the prediction of more frequent extreme climatic events across South Africa in the future.

Keywords: Drought, Enhanced Vegetation Index (EVI), flood, Greater Kruger National Park, land use, land cover change, phenology, remote sensing, semi-arid savanna, vegetation response.

Acknowledgments

Thank you to the National Research Foundation (NRF), from whom I received a Block Grant for both years of this study (2017-2018) and the University of the Witwatersrand for funding for the 2019 SAAB conference.

Thank you to my supervisors, Prof Ed Witkowski and Dr Melissa Whitecross for their endless support and guidance all the way through this project. Thank you to Dr Joleen Fisher for endless advice, especially on remote sensing aspects and Chevonne Reynolds for advice and guidance on several of the statistical analysis. Thank you to Anastashia Chetty for taking me along to Venda as her field assistant for her research, which allowed me a brief visit of my study area, where I met Hennie van der Colff from Awelani Lodge who provided much needed information on the area.

Lastly, I thank my family, particularly my parents, for their constant interest, support, motivation and above all patience. To my Dziadzui (7 May 1929- 26 December 2018), so much of where I am today is because of you, thank you for your endless encouragement to learn and expand my knowledge.

Abbreviations

ANOVA – Analysis of covariance

CHIRPS – Climate Hazards Group InfraRed Precipitation

CV – Coefficient of variation

ENSO – El Niño Southern Oscillation

EVI – Enhanced Vegetation Index

KNP – Kruger National Park

LEDET – Limpopo Economic Development, Environment and Tourism

LRB – Limpopo ridge bushveld

MMB – Musina mopane bushveld

MODIS – Moderate Resolution Imaging Spectroradiometer

MSB – Makuleke sandy bushveld

NDVI – Normalized Difference Vegetation Index

SE – Standard error

SWIR – Short wave infrared

NIR - Near wave infrared

Symbols

Phenometrics:

$Start_T$ – Start time

Mid_T – Mid time

$Peak_T$ – Peak time

End_T – End time

SI – Small integral

LI – Large integral

GU rate – Rate of greenup

Sen rate – Rate of senescence

EVI_{max} – Maximum EVI value

EVI_{min} – Minimum EVI value

Chapter 1

General Introduction

1. Background

Recent changes in global climate have led to an increase in the severity and frequency of extreme climatic events and current climate models predict that global temperatures, atmospheric CO_2 concentrations and regional rainfall patterns will continue changing in the future (Bloor *et al.* 2010). Floods and droughts are two severe disturbances experienced in southern African savannas and can initiate shifts in vegetation dynamics such as changes in biomass production, species distribution, abundance and compositional changes in species assemblages (Stephenson 1990, Mueller *et al.* 2005).

Drought, as experienced in southern African savannas, is a period with extremely low rainfall during the wet season for an extended period of months or years (Viljoen 1995, Rouault and Richard 2005, Dai 2011). Extreme extended droughts can result in the widespread mortality of both herbaceous and woody vegetation (Mueller *et al.* 2005). With the decline in forage availability during droughts, herbivore densities decrease (Ogutu and Owen-Smith 2003). At a national scale, the drought of 2014-2016 in South Africa was not as severe as the droughts experienced in the early 1980s and 1990s. However, at a regional scale the drought was equally severe, particularly in areas such as north eastern Bloemfontein, north eastern Mpumalanga, northern Kwa-Zulu Natal, and parts of the Western Cape (Swemmer *et al.* 2018). Droughts are a recurrent event in southern African savannas (Rouault and Richard 2005, Ogutu *et al.* 2008, Dai 2011), while floods are relatively infrequent (Ogutu *et al.* 2008).

A flood event occurs when high rainfall falls across a catchment region and results in a river or several rivers rising to peak flow and the water spilling over into the surrounding flood plain (Baruch 1994, Heritage *et al.* 2001). In South Africa, the flood event of early 2013 occurred in the northern region of Kruger National Park during mid-January. The flood was as a result of rainfall that fell over nearly ten days with 290 mm falling over 24 hours. The total rainfall in the region for 2013 was 757.8 mm. Although this flood event was not as severe in South Africa, it was devastating in Mozambique, resulting in over 100 deaths and vast damage to property and infrastructure (Manhique *et al.* 2015). The occurrence of the flood two years before a drought provides an opportunity to study the response of vegetation to two different extreme climatic events over a relatively short period.

Phenology is the study of the seasonal timing of biological events and the abiotic and biotic triggers of these events (Lieth 1974, Badeck *et al.* 2004). With regard to vegetation phenology, the initiation of these events is primarily driven by environmental factors including temperature, rainfall and photoperiod (Cleland *et al.* 2007, Fitchett *et al.* 2015). Vegetation phenology in semi-arid savannas may be sensitive to flooding and drought events, as water availability is one of the main drivers of productivity in these systems (Briggs and Knapp 1995, Knapp *et al.* 2001).Savannas support commercial and private industries including wildlife farming and preservation, as well as livestock farming. The wildlife and livestock industries are of key importance for the local economy, tourism and livelihoods respectively (Scholes and Walker 2004).

The Kruger National Park (KNP), is the largest protected area in South Africa and was established in 1903 with the amalgamation of the Sabie and Singwitsi Game Reserves. Since then there have been several major managerial shifts due to the compound history of socio-political pressures, as well as ecosystem complexities (Venter *et al.* 2008). The socio-political aspect is strongly linked to internal management choices and to a lesser extent to South Africa's political history (McLoughlin *et al.* 2011). Management of ecosystem complexities including wildlife population control and vegetation dynamics were based on a paradigm focused on conservation at the species level (McLoughlin *et al.* 2011) and maintaining equilibrium and carrying capacity which was largely derived from commercial agricultural concepts (Peel *et al.* 1998). In the past few years, KNP management has shifted to biodiversity conservation at an ecosystem level (McLoughlin *et al.* 2011). This has developed a broader understanding of how to control dynamics such as patch burning, artificial water points and elephant populations (Venter *et al.* 2008) and their associated effects. Although KNP went through many managerial shifts, the greater goal of conserving and maintaining a savanna system was still achieved.

The northern half of KNP borders on to the Vhembe district of Venda, which encompasses several protected areas and reserves, one being the Madimbo Corridor, another being the Makuya Nature Reserve which borders onto KNP and forms part of the Greater Kruger National Park. The Madimbo Corridor is a military owned stretch of land boarding KNP and extending along the Limpopo River, South Africa's northern boundary. A land claim by local communities made in 1994 is still unresolved for this piece of land to which there is still restricted access (News24 2017). With local communities unable to access the corridor, the vegetation has remained mostly unchanged with wildlife still roaming (Pers. Com, van der Colff 2017). Makuya Nature Reserve is roughly 18 000 ha and was founded in 1987 when several Venda Chiefs relinquished land for conservation purposes

(Medvey 2010). The fences between Makuya Nature Reserve and KNP were dropped when the Makuya Nature Reserve was established. Previously, the land was utilized for grazing, fishing, hunting and the collection of building material and medicinal plants. Prior to 1994 the reserve was managed by the provincial government. Today, the reserve operates under a tourism and conservation manager that coordinates with KNP management. However, any major decisions are required to be approved by a Forum. This Forum consists of representatives from provincial government, Limpopo Economic Development, Environment and Tourism (LEDET), SANParks, as well as the three tribes (Medvey 2010).

The Vhembe district is a former homeland and has a population of approximately 1.2 million people (van Marrewijk 2011). The economy of this region is largely dependent on mining, tourism and agriculture (van Marrewijk 2011). Agricultural produce includes citrus, macadamia nut, sub-tropical fruit and avocado. However, these products are typically sold locally as poor infrastructure and remoteness limits the transport of these goods. Although the Tshikondeni Coal Mine, which borders the Makuya Nature Reserve, is one of the largest contributors to employment opportunities, unemployment in the area is still extremely high (Medvey 2010). Most households rely on social grants and their natural environment for the harvesting of fruits, vegetables, medicinal plants, firewood and fodder (van Marrewijk 2011). Furthermore, crop agriculture may be difficult due to very low rainfall (Paumgarten *et al.* 2018) and this region has soils that are prone to erosion (Van Marrewijk 2011). This, added to unsustainable resource use or overgrazing often leads to land degradation (Fisher *et al.* 2009). The land neighbouring the western side of the Makuya Nature Reserve is still predominantly used as grazing lands for domesticated livestock, such as cattle and goats and the surrounding villages are prone to overgrazing (Venter and Witkowski 2013).

The collection methods for obtaining information for vegetation mapping have progressed from ground surveys to satellite remote sensing surveys which allow for more accurate, and objective measures at greater scales (Tucker *et al.* 1985, Sibanda *et al.* 2017). This allows for the assessment of the impacts that disturbances including drought (Peters *et al.* 2002, Ji and Peters 2003) and floods (Horritt 2003, Chen *et al.* 2017) have on vegetation dynamics. There are several different data products available from remote sensing satellites and sensors that are used for vegetation mapping and the analysis of vegetation dynamics. These sensors have varying spatial and temporal resolutions and spectral characteristics, thus it is essential to select appropriate sensors when mapping vegetation (Xie *et al.* 2008). Several of the main sensors are: Advanced Very High-Resolution Radiometer (AVHRR); Landsat TM; Moderate Resolution Imaging Spectroradiometer (MODIS); SPOT (Satellite Pour l'Observation de la Terre); Very High-Resolution Satellites (VHR) and Sentinel-2 (Table

1). MODIS is a commonly used sensor and provides the means for vegetation mapping and phenological assessments.

Developing an understanding of phenological responses to climate change may help to further predict the occurrences of extreme events, such as flooding and drought in the future (Cleland *et al.* 2007, Chambers *et al.* 2013, Fitchett *et al.* 2015) and aid in the establishment of better strategies to combat the negative effects of climate change.

2. Rationale

Extreme climatic events are episodes of intense natural happenings, largely driven by the changes in a region's climate and are typically classified as "extreme" due to the rarity, intensity and impact (environmentally and economically) of the event (Beniston and Stephenson 2004). Such events include floods, cyclones, tornadoes and droughts. Southern Africa undergoes strong interannual fluctuations in rainfall, with regular wet and dry stages (Dieppois *et al.* 2016). Variability of sea surface temperatures (SSTs) of oceans surrounding southern Africa affect rainfall fluctuations on the subcontinent (Mason and Jury 1997, Goddard and Graham 1999, Behera and Yamagata 2001, Reason 2001). For example, dry (or wet) conditions in southern Africa are often due to higher (or lower) than average SSTs in the central equatorial Indian Ocean (Jury 1995, Rocha and Simmonds 1997). These fluctuations in SST may be affected by the interaction of large-scale modes of climate variability, including the Southern Annular Mode (SAM), South Indian Ocean Dipole (SIOD) and the El Niño Southern Oscillation (ENSO) (Nash 2017). However, rainfall patterns change with how these large-scale climate modes interact over different time scales (interannual, interdecadal and quasi-decadal) (Dieppois *et al.* 2016). Accordingly, in southern Africa, ENSO predominantly influences interannual variability (2- 8 years) of summer rainfall (October to April) (Venter *et al.* 2003). Additionally, landfalling tropical cyclones may also influence interannual rainfall variability in north-eastern areas of southern Africa (Nash 2017). The ENSO phenomenon is caused by changes in atmospheric pressure conditions influenced by sea surface temperatures on the eastern Pacific Ocean (Ogutu and Owen-Smith 2003, Ogutu *et al.* 2008). ENSO has two extreme episodes; El Niño, the warm, dry phase, and La Niña, the cold, wet phase (Van Heerden *et al.* 1988, Anyamba *et al.* 1999, Kruger 1999). In southern Africa, below-average rainfall is often related to El Niño episodes, whereas above-average rainfall may be associated with La Niña and sometimes the timing of severe drought and flooding events frequently correspond with strong ENSO episodes (Ogutu *et al.* 2008, Baudoin *et al.* 2017). However, the severity of El Niño and La Niña episodes across the tropical regions may be largely dependent on the frequency and intensity of previous ENSO episodes (Ogallo 1993, Anyamba *et al.* 1999).

Droughts in southern Africa typically span from months to two or more years (Rouault and Richard 2005, Vetter 2009), and are often followed by years of above average rainfall (Vetter 2009). However, the effects of drought may not be immediate and manifest years later. These effects include the reduction in basal cover of perennial grasses and forbs, and a reduction in animal populations through decreased production of vegetation. Severe or prolonged drought can lead to reduced crop and livestock production (Richard *et al.* 2001, Rouault and Richard 2005), cause widespread mortality of vegetation (Mueller *et al.* 2005) and cause socio-economic declines from which many parties are unable to recover from once more favourable climatic conditions occur (Vetter 2009). As floods are associated with this increase in rainfall, vegetation within the entire catchment area is influenced by the increase in water availability. Apart from damage to infrastructure and loss of property, extreme floods lead to health related issues and deaths, due to the increased risk of water-borne diseases caused by inundation and the contamination of clean water supply and sanitation (Dang *et al.* 2011, Ward *et al.* 2016). Although severe flooding events are typically infrequent, the concern is that the reoccurrence frequency may be increasing due to climate change.

Table 1: Six remote sensing satellite sensors commonly used for vegetation mapping. The sensors have varying spatial and temporal resolutions and differ greatly in price.

Satellite	Spatial resolution	Temporal resolution	Details	Price	References
Advanced Very High-Resolution Radiometer (AVHRR)	Course, 1.1 x 1.1 km for local area coverage (LAC) and 5 km for global area coverage (GAC)	1 day	Capable of monitoring vegetation conditions and mapping land cover changes at regional, continental and global scales. 1980 to present.	Low cost	(Schmidt and Karnieli 2000, Xie *et al.* 2008)
Landsat TM ETM + Landsat 8	Fine, 30 x 30 m for the multispectral bands and 60 x 60 m for the thermal infrared band	16 days	Appropriate for regional scale mapping and may be applied to community level mapping. 2013 to present.	Free	Xie *et al.* 2008
Moderate Resolution Imaging Spectroradiometer (MODIS)	Medium to course, 250 x 250 m –1000 x 1000 m	16 days (composite image)	Multispectral data appropriate for mapping land cover types at regional, continental and global scales and is capable of measuring Leaf Area Index (LAI). 2000 to present.	Free	(Cleland *et al.* 2007, Xie *et al.* 2008)
SPOT (Satellite Pour l'Observation de la Terre)	Coarse resolution of 1 x 1 km at global scale and fine resolution of 2.5 x 2.5 m at the local scale	1 day	Used to map vegetation at community and species level, as well as mapping land cover types at regional and global scales. SPOT 2,4 and 5 1983,1993 and 2002 till present.	High cost	Xie *et al.* 2008
Very High Resolution (VHR)	Very fine resolution ranging from 0.41 m to 1.85 m	1 - 3 days	Category of satellites that include: QuickBird (2001 to present), Worldview-1 (2007 to present), Worldview-2 (2009 to present), GeoEye-1 (2008 to present). Can differentiate between individual trees, large shrubs and patches of grass.	High cost	(Pacifici *et al.* 2009, Rossi 2009, Immitzer *et al.* 2012), Satellite Imaging Corporation 2012
Sentinel 2	Fine resolution of 10 x 10 m	10 days	The multispectral instrument provides better multispectral data with cloud screening and improved compensation for atmospheric effects, ideal for land cover monitoring. 2013 to present.	Free	(Berger *et al.* 2012, Drusch *et al.* 2012)

Human modification and change in environmental conditions are two of the main drivers of vegetation change globally. Changes in vegetation cover not only have local implications, but global repercussions too. Land cover change due to agriculture and livestock farming often leads to changes in soil nutrients and water cycling (Friedl *et al.* 2002, DeFries and Bounoua 2004, Linderman *et al.* 2005) and carbon storage (Kamusoko and Aniya 2007). Larger changes including deforestation, land degradation due to overgrazing and changes in topography due to development, tend to lead to changes in albedo, evapotranspiration and primary productivity which could impact atmospheric fluxes of heat, alter local and global weather patterns and climate (Sellers *et al.* 1997, Friedel *et al.* 2002). Depending on the degree of land cover change and where it occurs, there may be extreme repercussions for the functioning of ecosystems by altering the total net primary productivity (DeFries and Bounoua 2004) and phenology (Gessner *et al.* 2015). Land use is often the main determinant of vegetation land cover, and in rural areas of southern Africa, small scale livestock husbandry and farming are the main land use for many communal lands (Behnke 1985, Shackleton *et al.* 2002, Dovie *et al.* 2006).

Many fence line comparison studies have been conducted in South Africa with the focus on the comparison of vegetation use by herbivores in communal lands and commercial farms or protected areas (Kiguli *et al.* 1999; Todd and Hoffman 1999; Shackleton 2000; Todd and Hoffman 2009). Fence-line contrast studies are simple natural experiments that are often linked to heavy herbivory and what the long term effect of heavy herbivory is on vegetation dynamics (Todd and Hoffman 1999). Many rural areas of South Africa continue to use older agricultural practices that often lead to excessive soil and vegetation degradation largely due to overgrazing (Beinart 2008). Although, strategies to combat degradation in former homelands were implemented in the mid 1950's, including fencing off the communal lands into multiple camps and the control of livestock densities (Benjaminsen *et al.* 2006), overgrazing is still a common occurrence. The sites on either side of the fence in fence-line studies experience the same climatic conditions and typically share the same topography and soil substrate (Illius and O'Connor 1999, Benjaminsen *et al.* 2006), thus the different land use and management may result in different equilibrial states that can be compared.

Annually, the initiation of phenological events are triggered by climatic shifts related to seasonal change such as changing temperature and rainfall (Badeck *et al.* 2004). In temperate ecosystems phenology is largely influenced by temperature and photoperiod (Reich and Borchert 1984, Hunter and Lechowicz 1992, Lu *et al.* 2006, Menzel *et al.* 2006, Polgar and Primack 2011). However in tropical ecosystems phenology is far more sensitive to the seasonal shifts in rainfall (Jolly and Running 2004, Cleland *et al.* 2007, Chambers *et* *al.* 2013, Jin *et al.* 2013). Nevertheless, temperature is still an important variable as regional rainfall changes are expected to occur concurrently with the changes in global temperature (Cubasch *et al.* 2001). Most phenological studies using remote sensing are conducted at regional (Chidumayo 2001, Heumann *et al.* 2007, Van Leeuwen *et al.* 2010, Ryan *et al.* 2014, Adole *et al.* 2018), continental (Brown *et al.* 2010, Atzberger *et al.* 2013, Ault *et al.* 2013) or global scales (Zhang *et al.* 2012, Boke-Olén *et al.* 2016), and areas in the northern hemisphere have been extensively covered (Chen *et al.* 2006, Jönsson *et al.* 2010, Van Leeuwen *et al.* 2010, Fitchett *et al.* 2015). Several studies have been conducted in southern African savannas examining the effect of multiple climatic factors on plant phenology with the use of remote sensing (Chidumayo 2001, Jolly and Running 2004, Archibald and Scholes 2007, Higgins *et al.* 2011, Jin *et al.* 2013, Whitecross *et al.* 2016, 2017a, 2017b).

It has been suggested that phenological studies can be used to characterise and understand the impacts that land use and climate related events have on vegetation (Linderman *et al.* 2005, Adole *et al.* 2016).This can be achieved by understanding how plant species respond to different land uses and changes in the regional climate conditions of southern Africa (Chmielewski and Rötzer 2001, Jolly and Running 2004, Linderman *et al.* 2005, Adole *et al.* 2016). With the aid of remote sensing an understanding of the phenology and land cover dynamics of southern African savannas can be obtained at multiple scales which allows for the monitoring of responses of different vegetation types. Thus, the influence of land use and management practice on the response of vegetation dynamics to conditions associated with extreme climatic events will be assessed.

3. Research aims and objectives

1) Quantify how land use influences vegetation phenology on either side of the north-western fence line of the Greater Kruger National Park

    i) Determine the difference in the timing of the time-related phenometrics between the protected area and the communal rangeland

    ii) Establish how the EVI related phenometrics differ on either side of the fence

2) Quantify how conditions associated with extreme flooding and drought events influence vegetation phenology at multiple sites along the north-western fence line of the Greater Kruger National Park

    iii) Determine the difference in the timing of the time-related phenometrics across the growing seasons of years of extreme climatic events

iv) Establish how the EVI related phenometrics change across growing seasons with extreme climatic events

v) Assess how the phenological dynamics relate to rainfall, temperature and photoperiod during seasons with extreme climatic events

3) Compare the differences in vegetation cover between a protected area and communal rangeland and how these change in response to years of extreme flooding and drought events, using remotely sensed images of different spatial and temporal resolutions (MODIS, Landsat, Sentinel-2)

4. Study approach

This study incorporates both spatial and temporal comparisons of vegetation response within sites along the north western fence line of the Greater Kruger National Park. The sites are located on either side of the fence line, half of which are within a communal land and half within a protected area. The communal land forms part of the Vhembe District of Venda in northern Limpopo, which borders the north western fence line of the Greater Kruger National Park. The protected area comprised of the Makuya Nature Reserve, the military owned Madimbo Corridor and the Kruger National Park. This area was selected for this study as the location of the fence provided an opportunity to conduct a fence line comparison on vegetation response to land use and climate variation, including flood and drought events, within a semi-arid savanna system that differs in many aspects to the savannas found further south in South Africa. The study area is made up of three vegetation; types, namely, Limpopo Ridge Bushveld, Makuleke Sandy Bushveld and Musina Mopane Bushveld (Mucina and Rutherford 2006). The area is dominated by *Colophospermum mopane, Combretum apiculatum, Terminalia sericea, Burkea africana* and *Kirkia apiculatum.* This study spans a six-year period from 1 July 2011 to 30 June 2017, including a flood event in January 2013 and a drought event from 2014-2016. Floods and droughts are typical disturbances experienced in semi-arid savannas, however these events often become extreme when coupled with the occurrence of the El Niño Southern Oscillation (ENSO) episodes. Phenology EVI curves, phenometrics derived from phenology and land cover change, were used to measure vegetation response to land use in the spatial comparison, and extreme climatic events in the temporal comparison. The phenological dynamics and land cover aspects were obtained through the use of remote sensing. The use of remote sensing enables one to study vegetation dynamics at various spatial and temporal scales. Chapter 2 focuses on the spatial comparison, to determine if land use- communal rangeland versus protected area- influences phenological dynamics of vegetation. Chapter 3 focuses on the temporal comparison which also uses vegetation phenological dynamics (i.e. the phenometrics), although here the impact of extreme climatic events on the response of vegetation was measured. Chapter 4 covers both the spatial and temporal aspects of land cover assessing how land cover differs with different land use and how land cover changes in response to extreme climatic events. Chapter 5 is the overall synthesis chapter, which highlights the important results of the previous chapters. And relates these findings to the ecological and environmental aspects in protected areas and communal rangelands.

The three data chapters (Chapters 2, 3 and 4) of this dissertation are written as independent papers in scientific journal formats to be submitted for publication at a later date, although there is only a single reference list at the end. As such, there will inevitably be some repetition as there are several overlapping topics shared between these chapters.

Chapter 2

Comparing the effect of land use on vegetation phenology across a fence line semi-arid savanna

Abstract

Phenology is the study of seasonal life-cycle events and the effect of environmental changes and biotic interactions on these events. Vegetation phenology focuses on the plants' annual cycle from the start of the growing season to the end of leaf senescence. Changes in land use type effects phenology and land cover of various ecosystems. Enhanced Vegetation Index (EVI) data, a measure of vegetation greenness, obtained from remotely sensed MOD13Q1 16-day composite imagery (250 m resolution), was used to extract phenological time series data and the associated phenometrics (e.g. $Start_T$ and End_T, season length of the growing season) from six consecutive growing seasons (2011-2017). Phenological responses of vegetation was assessed at multiple sites, on either side of the north-western fence line of the Greater Kruger National Park, near Pafuri, to test if land use, communal grazing lands vs. protected area, had an influence on the phenometrics. Differences in phenology and the associated phenometrics measured within the communal land and protected area were driven by land use, rather than by vegetation type. The start of greenup and the length of the growing season were significantly earlier (six days; $p<0.001$) and longer (five days; $p<0.001$) in the communal land, however, the end times did not differ notably for the two sites ($p = 0.410$). The communal land had slightly greater productivity of 1% ($p<0.05$), whereas the protected area had slightly more seasonally active vegetation of 1% ($p<0.01$). This study explores vegetation response to land use using remote sensing which adds to the long-term monitoring of the response of vegetation under different land use pressures and management practices being conducted globally.

Keywords: Communal land, EVI, fence line comparison, Greater Kruger National Park, protected area, remote sensing, vegetation response, vegetation types.

1. Introduction

Semi-arid savannas across the world provide support for subsistence farming, commercial agriculture and conservation, however the change in land use to large scale agriculture globally, has had consequences for conservation, other land uses and to an extent, climate (Brannstrom *et al.* 2008, Mwavu and Witkowski 2008; Wigley *et al.* 2010). In South Africa, savannas support commercial and private industries including wildlife farming and conservation as well as livestock farming. The wildlife and livestock industries are of key importance for tourism and livelihoods respectively (Scholes and Walker 2004, Dovie *et al.* 2006), thus understanding how vegetation phenology responds to these different land use types is essential for sufficiently maintaining and managing savanna systems. Most phenological studies which use remote sensing focus on the temporal change of phenology in response to climate change in contrast to differences between various land uses (Jolly *et al.* 2005, Brown *et al.* 2010, Richardson *et al.* 2013, Whitecross *et al.* 2017a). This study, however, provides important baseline information on the effect of land use on phenology and land cover, which can then be taken further to assess how land use affects the response of vegetation to climate change.

Fence line comparisons

Fence-line contrast studies are simple natural experiments that are often linked to heavy herbivory and its long term effect on vegetation dynamics (Kiguli *et al.* 1999, Todd and Hoffman 1999, Benjaminsen *et al.* 2006, Todd and Hoffman 2009, Fisher *et al.* 2014). The sites on either side of the fence of fence-line studies experience the same climatic conditions and typically share the same topography and soil substrate (Illius and O'Connor 1999, Benjaminsen *et al.* 2006).Thus the different land use and management may result in different equilibrial states that can be compared on sites that are otherwise similar, particularly in terms of soils and climate.

Protected areas are often bordered by areas that utilise other forms of land use and thus have habitats that have been modified in some manner by human activity (Shackleton 2000). Consequently, the people, land use practices (often livestock grazing) and conservation areas are closely linked (Todd and Hoffman 1999). These include ecological, economic and cultural links between protected areas and adjacent communities which pose opportunities, as well as constraints for the parties on both sides of the fence (Wells 1996, Shackleton 2000).

The consequences of different herbivore densities and the frequency with which an area is grazed or browsed in semi-arid regions are diverse (Mograbi *et al.* 2017). However, the effect of herbivory on vegetation depends on the frequency and intensity of herbivory or damage. Light to moderate grazing and browsing may result in increased primary production. Severe pruning may result in the production of fewer and larger shoots with larger leaves (Danell *et al.* 1994, Duncan *et al.* 1998, Bergström *et al.* 2000, Lehtilä *et al.* 2000). Depending on how much photosynthetic material is removed, it is probable that the growth performance of the plant may increase due to more water and nutrients available for the remaining photosynthetic material (Alados *et al.* 1997). Defoliation of grasses creates less self-shading and competition which permits more efficient light use (McNaughton 1979, Todd and Hoffman 1999, Fynn *et al.* 2005) and increased photosynthetic rates (McNaughton 1979, Cullen *et al.* 2006), thus increasing productivity. The growth of palatable species may be maintained and even stimulated by grazing if the species are grazing tolerant (Augustine and McNaughton 1998, Anderson *et al.* 2007), which will also increase species richness (Todd and Hoffman 1999).

Conversely, severe defoliation of trees often leads to the regrowth of smaller shoots and leaves (Gadd *et al.* 2001, Anttonen *et al.* 2002, Rooke and Bergström 2007) with increased chemical defences. Damage to the mature stems, by elephants, could cause physiological stress which may inhibit future growth, while damage caused by harvesting of wood is less severe (Botha *et al.* 2002). Herbivores can also negatively impact recruitment of woody species in areas where herbivore densities are great (Venter and Witkowski 2013). A degraded state, in many circumstances, is induced by heavy grazing where the increased grazer activity results in mortality of some plant species, often the more palatable species, and a decrease in species richness, which leads to a shift in vegetation assemblage (Todd and Hoffman 1999). Additionally, increased grazing and trampling when plants are within the early stages of growth may lead to a decrease in vegetation cover (Augustine and McNaughton 1998, van de Koppel *et al.* 2002). Added grazing pressure to an already patchily vegetated soil surface could worsen soil erosion (Wischmeier and Smith 1978). Increased erosion will lead to loss of nutrients, as a large proportion of nutrients are stored within the soil surface, and in turn affect the nutrient concentration of the remaining vegetation. Furthermore, a bare surface is disposed to compaction with decreased infiltration and more run-off (Lambin and Ehrlich 1997), which reduces the soil water available for plant production which would influence the plant phenology.

Phenology

Apart from demonstrating a heterogenous structure with the presence of prominent tree and grass layers, the woody species of semi-arid savannas have varying patterns of leaf display and phenology (Masia *et al.* 2018). These include; *Burkea africana,* *Colophospermum mopane, Combretum apiculatum, Kirkia acuminata, Terminalia prunioides* and *Terminalia sericea,* which are common species found in savannas in the north eastern parts of South Africa. *Burkea africana* and *T. sericea* are obligate deciduous species, dropping their leaves in the dry season, and greening up independently of the first rains of the growing season (Childes 1988, Whitecross *et al.* 2017a, Masia *et al.* 2018). The first leaf flush of *C. mopane* is also independent of rainfall and *C. mopane* can retain green leaves long into the dry season (Dekker and Smit 1996). *Combretum apiculatum* is dependent on rainfall for the initial spring flush and can retain leaves into the dry season (Childes 1988, Dekker and Smit 1996, Masia *et al.* 2018). *Terminalia prunioides* greens up in December. Typically leaves start to senesce in May, with no leaves present from October to November. *Kirkia acuminata* flushes in November and leaves begin to senesce in April, with no leaves by June (Dekker and Smit 1996). Phenology is driven by several environmental variables including temperature and rainfall (Badeck *et al.* 2004). Phenology in similar savannas systems will also vary depending on vegetation type, as well as land use, particularly in terms of herbivory.

Remote sensing

Spectral vegetation indices, such as Normalized Difference Vegetation Index (NDVI) and Enhanced Vegetation Index (EVI), are measures of ‘greenness’ of vegetation (Wang and Tenhunen 2004, Cleland *et al.* 2007) and may be used as a proxy for plant primary production (Beck *et al.* 2006) and for the phenological assessments of vegetation. EVI yields metrics which are used in many models and phenological studies to define phenology and characterise vegetation dynamics (Nemani *et al.* 2003, Breshears *et al.* 2005, Vintrou *et al.* 2012, Zhao *et al.* 2013, Ryan *et al.* 2017). These metrics are known as phenometrics and include the rate of greenup and senescence, amplitude of the EVI curve, the maximum and minimum EVI values and seasonal integrated greenness (small and large integrals) (Steenkamp *et al.* 2008, Wessels *et al.* 2009, Van Leeuwen *et al.* 2010, Vintrou *et al.* 2012, Wallace *et al.* 2013). Furthermore, remote sensing phenological studies derive phenometrics from satellite-based EVI time series, which aid in measuring the timing of the start, peak, length, mid period and end of the growing season (Wessels *et al.* 2007, Steenkamp *et al.* 2008, Van Leeuwen *et al.* 2010, Vintrou *et al.* 2012). Understanding how vegetation dynamics differ under different land use pressures, such as grazing pressure, provides land managers and conservation practitioners information that allows for improved management of ecosystem change.

1.1. Aim and objectives

The aim of this chapter is to quantify how land use influences vegetation phenology on either side of the north-western fence line of the Greater Kruger National Park using remote sensing. The first objective is to determine if vegetation type affects the response of vegetation to different land use types. Secondly, to determine the difference in the timing of the time-related phenometrics between the protected area and the communal rangeland, and lastly, to establish how the Enhanced Vegetation Index (EVI) related phenometrics differed on either side of the fence.

2. Methods

2.1. Study area and vegetation types

The study area is located along the north-western fence line of the Greater Kruger National Park (KNP), near Pafuri, 22°23'59.33" S, 31° 2'28.25" E (Figure 1). This area is classified as semi-arid and receives between 300-500 mm of rain annually with most the rainfall received between October and April (Venter *et al.* 2003). And the rainfall interannual coefficient of variation (CV) is > 40% for the region (Schulze 1997). This northern region falls within the northern arid bushveld zone where summers have high mean temperatures and winter is mild and typically frost free (Venter *et al.* 2003). Fire is one of the common disturbances in savannas and plays an important role in establishing and maintaining savanna systems (Du Toit *et al.* 2003, Van Langevelde *et al.* 2003). However, fire in KNP occurs at different return frequencies, with a very low return frequency of roughly 10 years in the Pafuri region (Du Toit *et al.* 2003). The most northern region of the park has two underlying geologies; Karoo basic larva- Letaba olivine-rich basalt and Soutpansberg andesite which forms rocky outcrops, hills and gorges and a lowland floodplain (Du Toit *et al.* 2003). These geologies give rise to shallow sand on hill tops, shallow clay and loam over the basalt and low lying areas and deep alluvium in the floodplain (Du Toit *et al.* 2003).

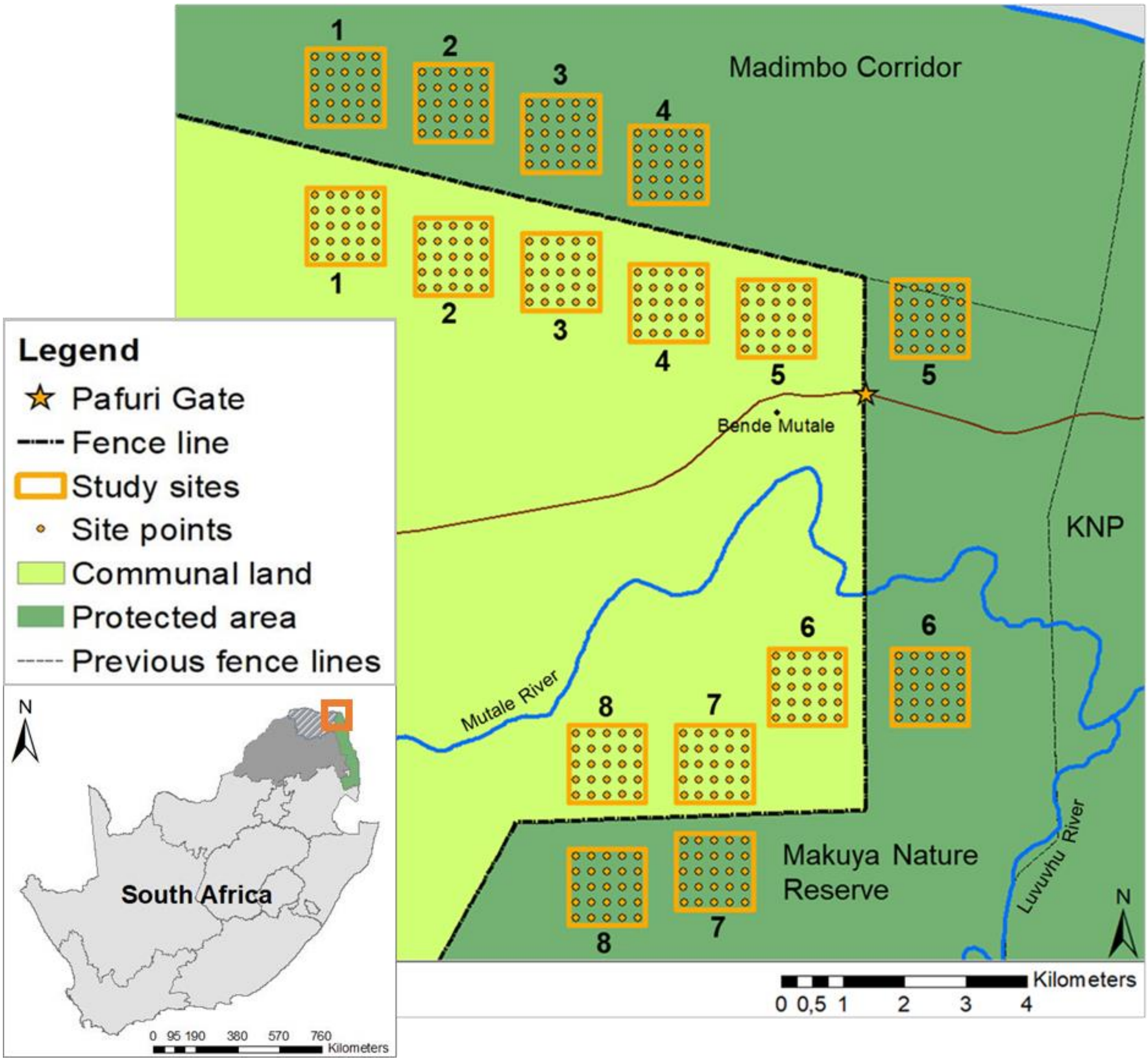

Figure 1: Location of the study area, incorporating sections of the Makuya Nature Reserve, part of the Greater Kruger National Park, the Madimbo Corridor and the adjacent communal grazing area along the north-west fence line of the Greater Kruger National Park. The study area had eight sites on either side of the fence, a site was made up of 5 x 5 pixels, where a pixel was 250 x 250 m. The study sites were placed at least one pixel (or 250m) away from other sites and from roads, rivers or human dwellings.

The northern region of the park is dominated by broad-leaved Mopane shrub and is classified more specifically as Musina Mopane Bushveld (MMB), Limpopo Ridge Bushveld (LRB), and Makuleke Sandy Bushveld (MSB) (Mucina *et al.* 2014) (Figure 2). Musina Mopane Bushveld falls within the Mopane bioregion, covers an area of 8797 km^2 and is found at altitudes between 300 m to 800 m a.s.l. Limpopo Ridge Bushveld also falls within the Mopane bioregion, covers an area of 2785 km^2 and is found at altitudes between 300 m to 1000 m a.s.l. Makuleke Sandy Bushveld falls within the Lowveld Bioregion, covers an area of 2077 km^2 and is found at altitudes between 300 m to 700 m a.s.l. (Mucina *et al.*

2014). The northern half of the sites mainly fall within the MMB vegetation type and the dominant species found in clay bottomlands within the eastern section of this vegetation type are *Colophospermum mopane* and *Terminalia prunioides. Colophospermum mopane, Terminalis sericea, Grewia flava* and *Combretum apiculatum* are dominant species in deep soils. Additionally, there is poor herbaceous cover in these *C. mopane* dominated areas. The southern half of the sites fall within MSB, where deep soils are dominated by *Terminalis sericea, Burkea africana, Guibourtia conjugata* and *Peltophorum africanum* with *Andropogon gayanus* and *Digitaria eriantha* the dominant grass species. Stoney soils are dominated by *, Croton gratissimus, Combretum apiculatum* and *Dipnorhynchus condylocarpon* as well as *Digitaria eriantha, Panicum maximum* and *Pogonarthria squarrosa* (Mucina and Rutherford 2006). More specifically, common woody vegetation found in the Pafuri region include broad-leaved species such *Burkea africana, Terminalia sericea, Pseudolachnostylis maprouneifolia, Combretum apiculatum, Kirkia acuminata, Commiphora glandulosa* and *C. mopane* present in moderately dense assemblages on slopes, and dense standings of *C. mopane* and *Euclea divinorum* in lower lying areas with dense riverine vegetation including *Hyphaene natalensis, Lonchocarpus capassa,* and *Acacia xanthoploea* (Du Toit *et al.* 2003). The Greater Kruger National Park also maintains populations of large herbivores including buffalo (*Syncerus caffer*), zebra (*Equus burchellii*), elephant (*Loxodonta africana*), and eland (*Taurotragus oryx*) (Seydack *et al.* 2012).

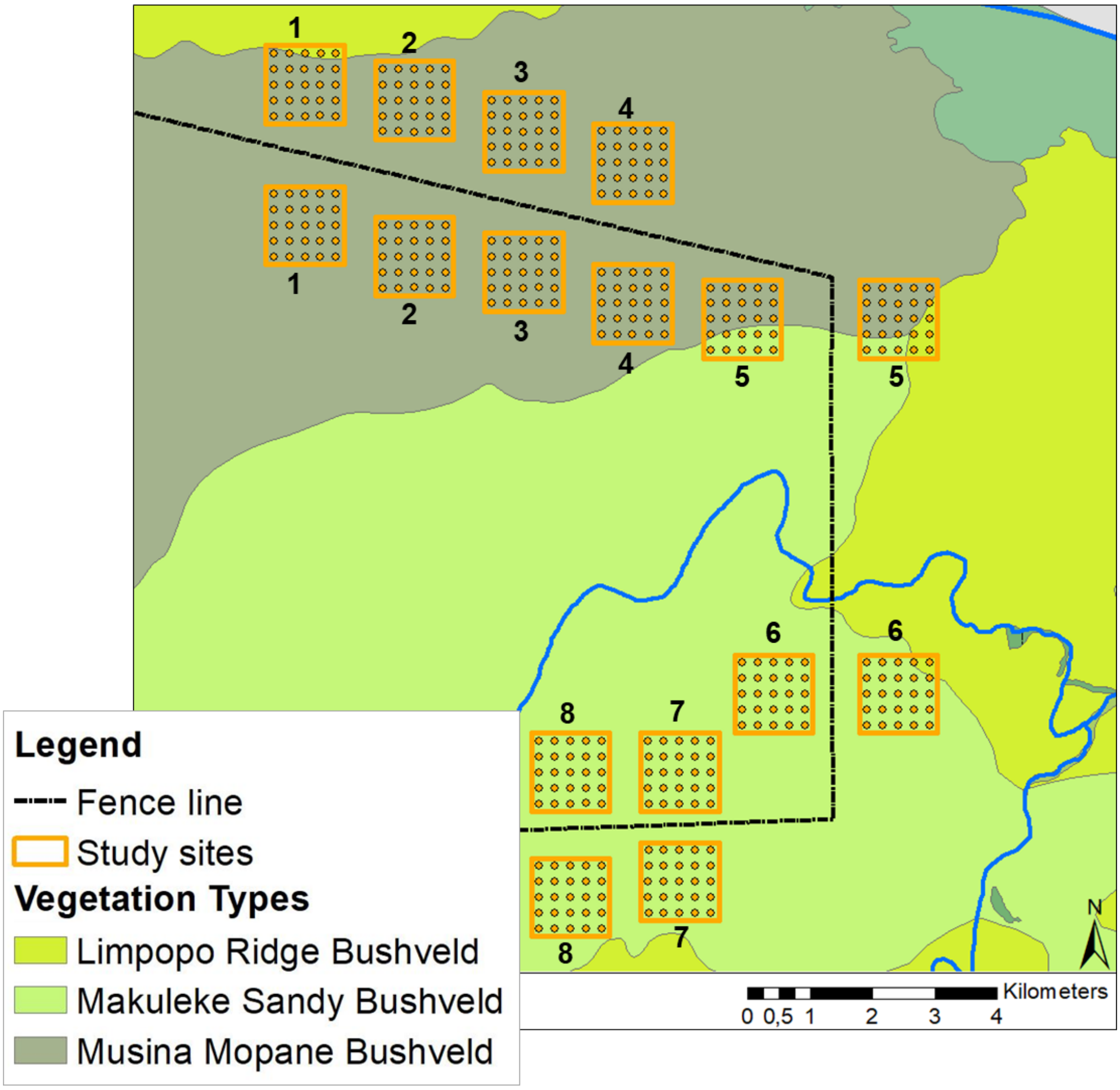

Figure 2: The three vegetation types located along the north-western fence line, near Pafuri, of the Greater Kruger National Park. These three vegetation types are Limpopo Ridge Bushveld, Makuleke Sandy Bushveld and Musina Mopane Bushveld (Mucina and Rutherford, 2006).

2.2. Experimental design

This study spanned a six-year period from 1 July 2011 to 30 June 2017 (austral years 2011/2012 to 2016/2017).The growing periods of the austral years will be referred to as the growing seasons. The study area comprised of two different land use types; communal rangelands and protected area, which were separated by the north western fence line of the Greater Kruger National Park. Sixteen study sites were selected along the fence line, eight sites within the protected area and eight matched sites in the communal land. Each site comprised of 5 x 5 MODIS pixels. A pixel was defined by the 250 x 250 m MODIS image (Figure 1). With 25 pixels per site, and eight sites on either side of the fence, a total of

200 pixels were assessed on each side of the fence. Thus, each site spanned an area of 1.25 km x 1.25 km, and the sites covered 1250 ha on either side of the fence. To prevent spectral mixing a minimum space of one pixel (or 250 m) was left between each of the selected sites. The pixels were placed in such a way as to ensure that each site is at least one pixel (or 250 m) away from any roads, rivers or human dwellings.

Within any remotely sensed image the cover types present exhibit spectral interactions or nonlinear spectral mixing. This occurs when there is a mixture of the spectral reflectance of the materials within the image which is caused by multiple reflections and transmissions between vegetation layers, soils and other objects present (Borel and Gerstl 1994, Ray and Murray 1996). Nonlinear spectral mixing may easily lead to positive spatial autocorrelation when sampling remotely sensed images. Thus, a two-pixel gap was maintained between all the sample pixels that made up each site.

2.3. Phenometrics

The Moderate Resolution Imaging Spectroradiometer (MODIS) MOD13Q1 version 6 dataset was downloaded (www.reverb.echo.nasa.gov, accessed: 22 June 2017) to obtain images from an EVI dataset- corrected for aerosols, clouds, cloud shading and water- with a 250 x 250 m resolution and a 16-day return frequency for the study area. EVI, proposed by Huete *et al.* (1994), is the refined form of NDVI (Xie *et al.* 2008) and is derived from blue, red and near infrared bands (Jin *et al.* 2013). This improved vegetation index decreases the soil and atmospheric reflectance experienced with NDVI (Bagan *et al.* 2005, Cleland *et al.* 2007), and the sensitivity for biomass estimation in dense vegetation was increased and improved. EVI aids in determining land cover types and presents information on the dynamic transformations that occur in vegetation groups (Geerken *et al.* 2005, Beck *et al.* 2006). Furthermore, time integrated EVI is effective for monitoring and expressing seasonality, as well as the spatial patterns of phenology of savannas (Chidumayo 2001, Beck *et al.* 2006, Archibald and Scholes 2007, Higgins, Delgado-Cartay, *et al.* 2011, Jin *et al.* 2013), and is thus a good tool for analysing the effect of different land use types on vegetation. Thus, EVI was selected over NDVI to reduce the chance of any changes in phenological dynamics being a result of spectral confusion due to the simple, yet often common occurrences of bare ground or dense stands of vegetation.

The EVI measurements were extracted from points which were placed in the centre of each 250m MODIS pixel, at the eight sites on either side of fence line across the six austral seasons. With the 23, 16-day MODIS composites that make up one austral year, a total of 55200 EVI replicates resulted (25 points* 16 sites* 23, 16-day* six austral years: n = 55200).

The assessment of phenological characteristics for both sides of the fence were conducted by investigating the phenometrics related to seasonal EVI patterns and the EVI time series data. The EVI related phenometrics included the small and large integrals, the rates of greenup and senescence, as well as the minimum (EVI_{min}) and maximum (EVI_{max}) EVI values. The time series related phenometrics include the start ($Start_T$), peak ($Peak_T$), mid (Mid_T) length and end (End_T) of the growing season. The small integral is an indication of the seasonally active vegetation, which is derived from the area of the section between the fitted function and the $Base_{EVI}$ (the average of the $Start_{EVI}$ and End_{EVI}), the large integral may act as a proxy for vegetation production but better indicates the standing crop of the season (Van Leeuwen *et al.* 2010). The rates of greenup (GU) and senescence (S) were calculated as follows:

$$\text{GU rate} = {(\mathrm{Midt_T} - \mathrm{Start_T})}/{\mathrm{A}}$$

$$\text{S rate} = {(\mathrm{Midt_T} - \mathrm{Endt_T})}/{\mathrm{A}}$$

where A is the amplitude, derived from the difference between the maximum and minimum EVI values, Mid_T is the mid-point of the growing season, $Start_T$ is the start of the growing season, and End_T is the end of the growing season. The amplitude of the growing season is derived from the difference between the maximum EVI and the average of the $Start_{EVI}$ and End_{EVI} values (Wessels *et al.* 2009, Van Leeuwen *et al.* 2010, Wallace *et al.* 2013) (Figure 3).

The start of the growing season is established by the onset of greenup and may be defined as the point in time where the EVI value has increased by 20% of the distance between the lowest EVI value on the left of the curve and the peak EVI value. Similarly, the end of the growing season is estimated from the peak EVI value and lowest EVI value on the right of the curve (Wessels *et al.* 2009, Van Leeuwen *et al.* 2010).

The point in time of the start of the growing season is established as follows:

$$\mathrm{Start_T} = {(\mathrm{Peak_T} - \mathrm{Min_{EVI_1}})}/{20\%}$$

$$\mathrm{End_T} = {(\mathrm{Peak_T} - \mathrm{Min_{EVI_2}})}/{20\%}$$

where $Peak_T$ is the peak time of the growing season, Min_{EVI1} is the lowest EVI value on the left of the curve while Min_{EVI2} is the lowest EVI value on the right side of the curve (Van Leeuwen *et al.* 2010) (Figure 3).

The 20% threshold is a method employed by TIMESAT (Per Jonsson and Lars Eklundh, version 3.3) which provides a simple and robust means to derive the $Start_T$ and End_T of the growing season (Wessels *et al.* 2009). Additionally, this method avoids the identification of false growing season onsets (Van Leeuwen *et al.* 2010). The peak in the growing season is established from the timing of the peak or maximum EVI value (Van Leeuwen *et al.* 2010, Wallace *et al.* 2013). While the length of the growing season is the difference in days between the $Start_T$ and End_T of the growing season (Wessels *et al.* 2009, Van Leeuwen *et al.* 2010) (Figure 3).

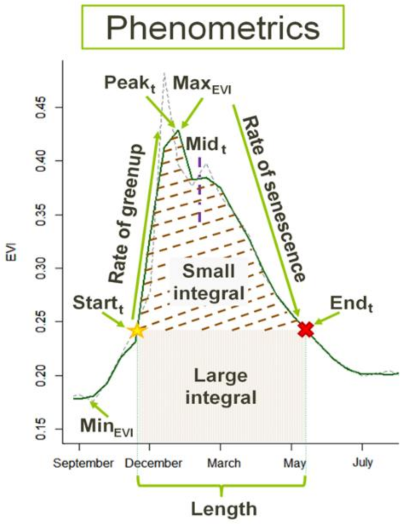

EVI Related Phenometrics	Time Related Phenometrics
Maximum EVI	Start of the growing season
Minimum EVI	End of the growing season
Small integral	Mid time of the growing season
Large integral	Peak of the growing season
Rates of green-up and senescence	Length of the growing season

Figure 3: Enhanced Vegetation Index (EVI) phenological curves demonstrating how the different phenometrics were derived and how these can be classified into temporal and EVI related metrics.

2.4. Land use comparison

Savitzky-Golay smoothed EVI time series data with standard errors were used to compare the patterns of the EVI data for the protected area and communal land. The EVI data and associated phenometrics (n = 1200) were compared between the two sites across all six growing seasons using Wilcoxon signed rank test. EVI images of the EVI across the study period and the $Start_T$, $Peak_T$, Mid_T and End_T were generated for both sides of the fence. The small and large integrals were compared using percentage change, where the greatest value was converted to 100% and the remaining values were compared based on their percentage change relative to the 100%. A fence line comparison study provides an opportunity to assess how the management and use of a protected area and adjacent communal land influence how plants respond to the same environmental factors. Amalgamated EVI images of the $Start_T$, $Peak_T$, Mid_T and End_T from all six growing seasons (2011-2017) are created for the communal land and protected area.

2.5. Vegetation type comparison

The protected area was covered by all three vegetation types; however, the communal land was only comprised of the Musina Mopane Bushveld and Makuleke Sandy Bushveld (Figure 2).Thus the effects of vegetation types on the vegetation dynamics needed to be established. This was to determine if any differences found across the fence line were a result of the different land use types or if the vegetation types simply led to the observed differences.

Linear mixed models were used to assess the EVI data and associated phenometrics of the different vegetation types between the communal land and protected area (EVI n = 55200, phenometrics n = 2400).

2.6. Analytical software

TIMESAT (version 3.3, Eklundh and Jonsson 2017) was used to derive the phenometrics from the MODIS EVI data (Figure 3). TIMESAT uses an adaptive Savitzky–Golay filtering or an asymmetrical Gaussian function method to define seasonality and the approximate timings of the growing seasons (Jönsson and Eklundh 2004, Heumann *et al.* 2007) by fitting a smooth and continuous curve to the vegetation index time series data (Heumann *et al.* 2007). This method was developed to fit mathematical functions of satellite time-series data to demonstrate how vegetation grows over a growing season (Jönsson and Eklundh 2004, Jönsson *et al.* 2010). The TIMESAT procedures analyse every time series extracted from all pixels to account for absent data, abnormalities, and “noisy” data (Boschetti *et al.* 2009). Noise may be created by atmospheric disturbances such as clouds. TIMESAT automatically captures key phenometrics such as those discussed previously (Boschetti *et al.* 2009).

3. Results

3.1. Effect of vegetation type

Makuleke Sandy Bushveld (MSB) and Musina Mopane Bushveld (MMB) were common for both sides of the fence, while Limpopo Ridge Bushveld (LRB) was only found within the sites of the protected area. The MSB in the communal land experienced the earlier $Start_T$ (four days difference), End_T (12 days difference), $Peak_T$ (two days difference) and Mid_T (three days difference) compared to the protected area. However, with MMB only the $Start_T$ (eight days difference), Mid_T (nine days difference) were earlier in the communal land as the End_T (eight days difference) and $Peak_T$ (six days difference) were earlier in the protected area (Tables 1 and 2). The length of MSB was nine days longer in the protected area, while

MMB of the communal land had a longer growing season of 15 days. The large and small integrals of both MSB and MMB were the greatest in the protected area. The rates of greenup and senescence of MSB was faster in the communal land, conversely, for MMB, these rates were faster in the protected area. The maximum EVI did not differ for MSB but was larger in the protected area for MMB. The minimum EVI and EVI from which the phenometrics were derived were greater in the protected area for MSB, and greater in the communal land for MMB (Tables 1 and 2). For the $Start_T$, Mid_T, length of the growing season, the large integral, rate of greenup and minimum EVI, land use explains the difference between the vegetation types. However, both land use and Makuleke Sandy Bushveld explain the differences between the vegetation types for the $Peak_T$, rate of senescence and maximum EVI . Musina Mopane Bushveld accounted for the difference in vegetation type of End_T, and Makuleke Sandy Bushveld explained the difference for the small integral (Figures 4.1,4.2,4.3). The number of site points (based on the Modus pixels) that fall within MMB were very similar in the protected area and the communal land, and identical for MSB, while LRB only covers six out of 200 points in the protected area (Table 3).

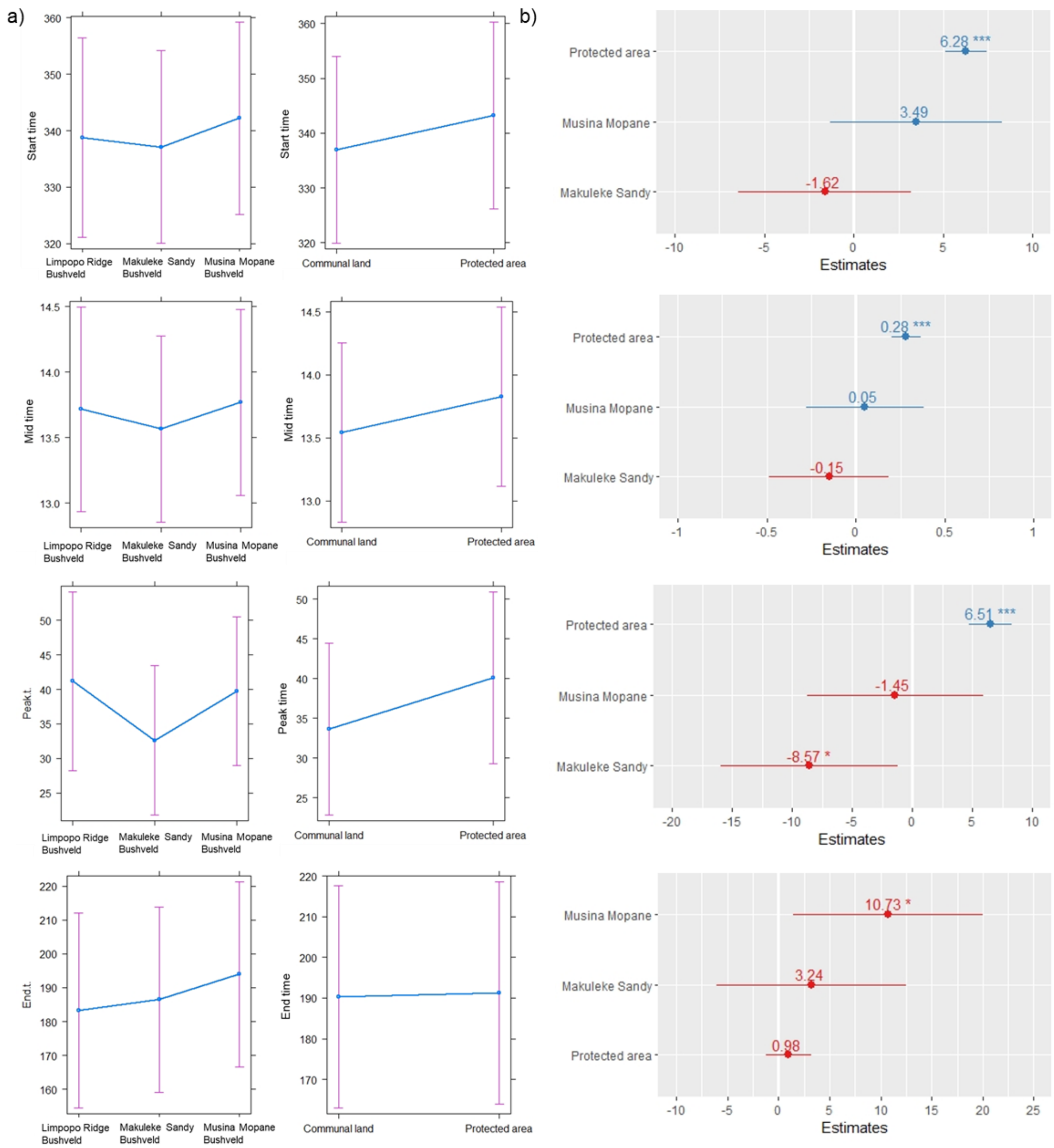

Figure 4.1: (a) Comparisons of the Start$_T$, Mid$_T$, Peak$_T$ and End$_T$ between the vegetation types and between the protected area and communal land, for the six austral years (2011-2017) as well as (b) the marginal effects of the interaction terms, with beta values and significance (<0.05 = *, <0.01 = **, <0.001 = ***) from the linear mixed models for each phenometric.

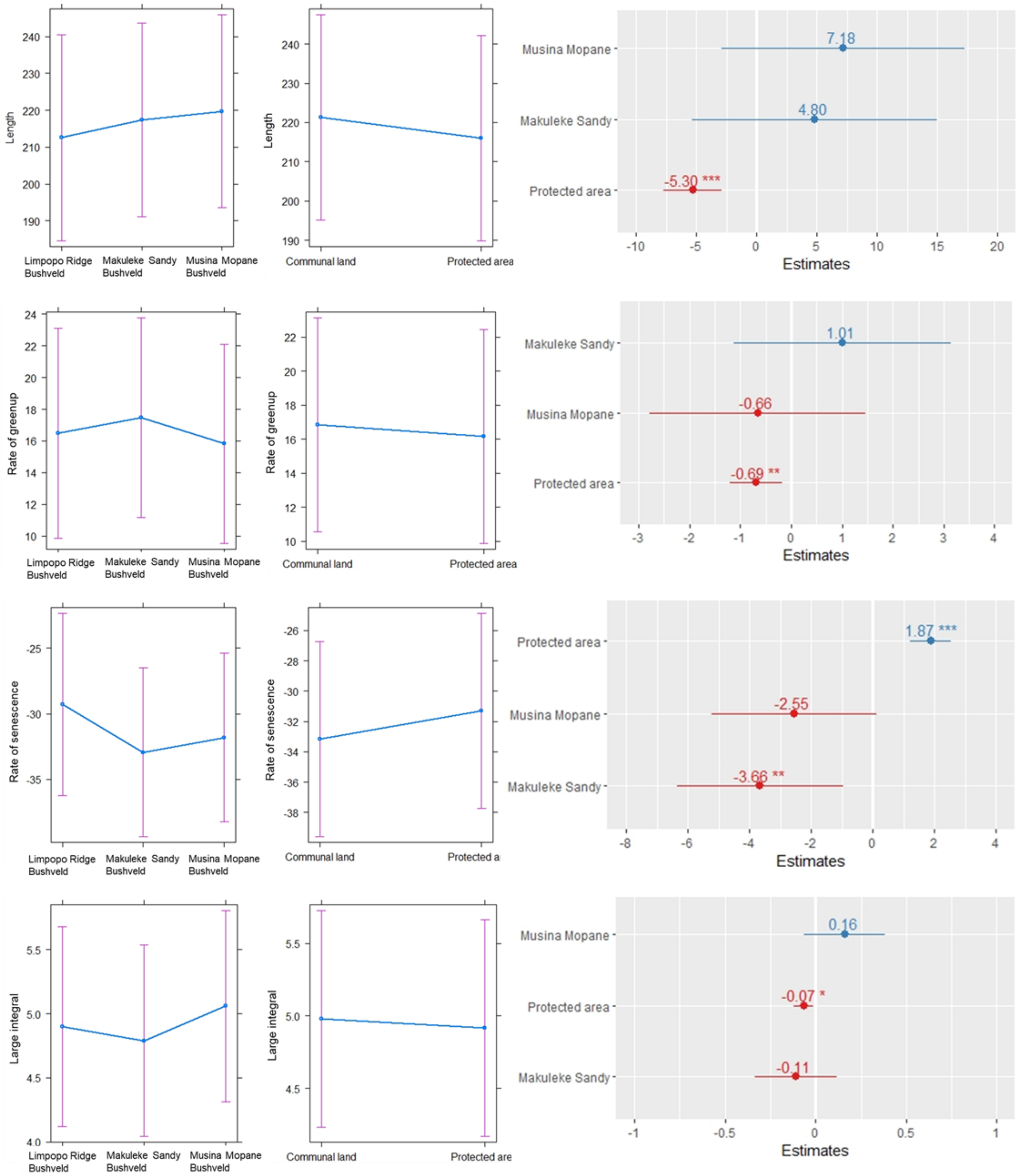

Figure 4.2: (a) Comparisons of the length of the growing seasons, rates of greenup and senescence, and large integral between the vegetation types and between the protected area and communal land, for the six austral years (2011-2017), as well as (b) the marginal effects of the interaction terms, with beta values and significance (*) from the linear mixed models for each phenometric.

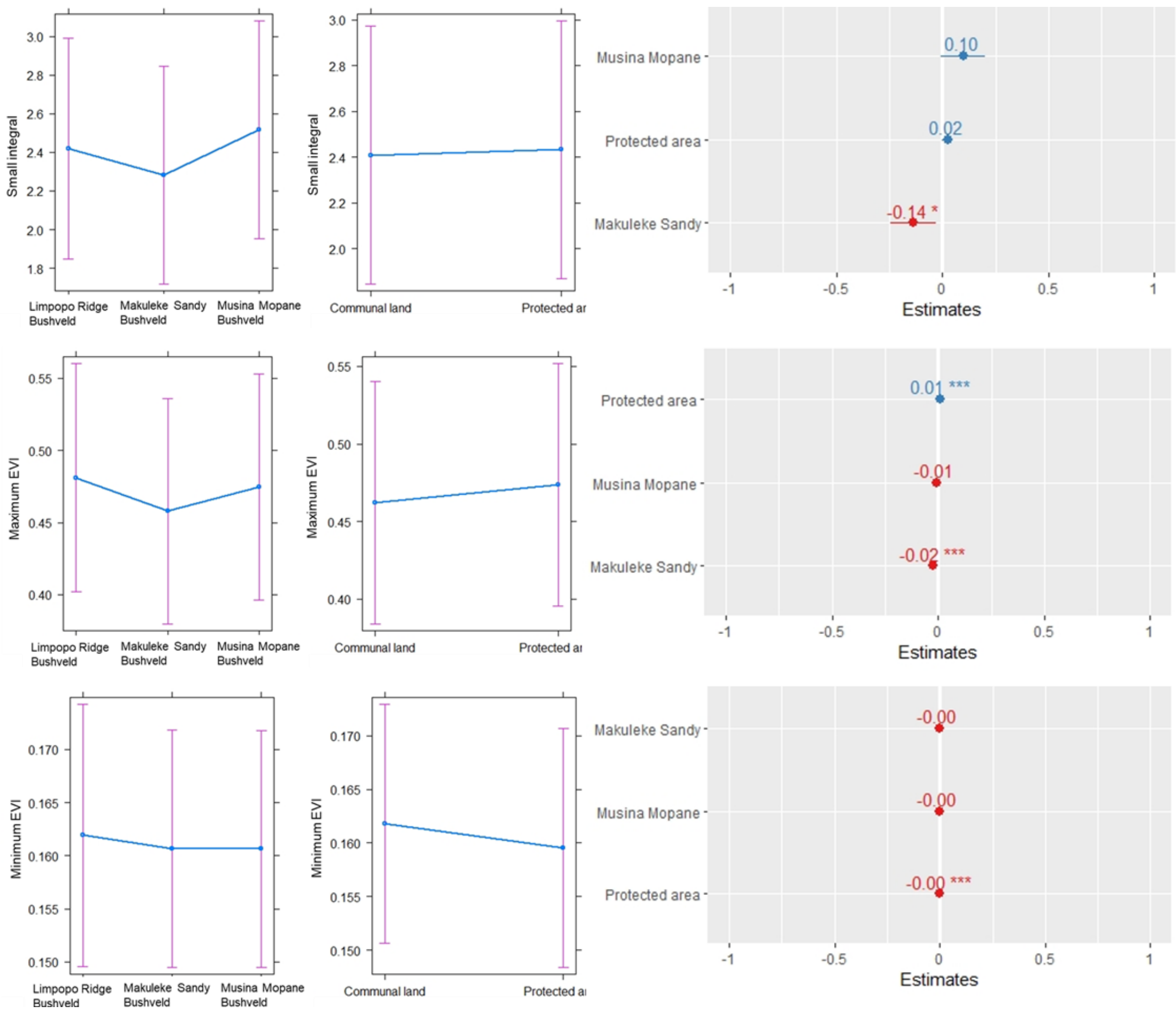

Figure 4.3: (a) Comparisons of the small integral, minimum and maximum EVI between the vegetation types, and between the protected area and communal land, for the six austral years (2011-2017) as well as (b) the marginal effects of the interaction terms, with beta values and significance (*) from the linear mixed models for each phenometric.

Table 1: Comparison of phenometrics (mean ± SE) for the vegetation types found within the sites of the protected area across all six growing seasons (2011-2017). Of the three vegetation types present across the study extent the protected area includes all three; Makuleke Sandy Bushveld (MSB), Musina Mopane Bushveld (MMB) and Limpopo Ridge Bushveld (LRB). The start time ($Start_T$), peak EVI time ($Peak_T$), mid-growing season time (Mid_T) and end time (End_T) of the growing season are shown as dates (mean Julian day ± SE), with length of the growing season as the mean day ± SE.

Vegetation Type	$Start_T$	$Peak_T$	Mid_T	End_T	Length
Limpopo Ridge Bushveld (LRB)	08 Dec (342±0.032)	15 Feb (46±0.057)	13 Feb (44±0.032)	03 Jul (184±0.059)	210 days±0.069
Makuleke Sandy Bushveld (MSB)	05 Dec (339±0.051)	11 Feb (42±0.047)	03 Feb (34±0.031)	12 Jul (192±0.070)	222 days±0.069
Musina Mopane Bushveld (MMB)	12 Dec (346±0.033)	16 Dec (47±0.049)	13 Feb (44±0.042)	09 Jul (190±0.083)	212 days±0.069

	Small integral	Large integral	Rate of greenup	Rate of senescence
Limpopo Ridge Bushveld (LRB)	2.43±0.019	4.866±0.032	16.133±0.299	-28.332±0.229
Makuleke Sandy Bushveld (MSB)	2.239±0.017	4.881±0.029	17.814±0.343	-35.041±0.361
Musina Mopane Bushveld (MMB)	2.566±0.025	4.944±0.036	15.019±0.234	-28.820±0.267

	EVI	EVI_{max}	EVI_{min}
Limpopo Ridge Bushveld (LRB)	0.268±0.001	0.487±0.003	0.161±0.0004
Makuleke Sandy Bushveld (MSB)	0.271±0.001	0.458±0.003	0.166±0.0003
Musina Mopane Bushveld (MMB)	0.270±0.001	0.484±0.003	0.155±0.001

Table 2: Comparison of phenometrics (mean ± SE) for the vegetation types found within the sites of the communal land across all six growing seasons (2011-2017). The sites of the communal land included Makuleke Sandy Bushveld (MSB) and Musina Mopane Bushveld (MMB), the Limpopo Ridge Bushveld (LRB) was only present in the protected area. The start time ($Start_T$), peak EVI time ($Peak_T$), mid-growing season time (Mid_T) and end time (End_T) of the growing season are shown as dates (mean Julian day ± SE), with length of the growing season as the mean day ± SE.

Vegetation Type	$Start_T$	$Peak_T$	Mid_T	End_T	Length
Makuleke Sandy Bushveld (MSB)	01 Dec (335±0.082)	09 Feb (40±0.053)	31 Jan (31±0.069)	29 Jun (180±0.094)	213 days±0.106
Musina Mopane Bushveld (MMB)	04 Dec (338±0.053)	10 Feb (41±0.049)	04 Feb (35±0.052)	17 Jul (198±0.104)	227 days±0.104
	Small integral	**Large integral**	**Rate of greenup**	**Rate of senescence**	
Makuleke Sandy Bushveld (MSB)	2.319±0.024	4.703±0.037	17.200±0.471	-31.013±0.402	
Musina Mopane Bushveld (MMB)	2.468±0.029	5.176±0.044	16.619±0.316	-34.814±0.437	
	EVI	**EVI_{max}**	**EVI_{min}**		
Makuleke Sandy Bushveld (MSB)	0.267±0.004	0.458±0.004	0.156±0.001		
Musina Mopane Bushveld	0.278±0.005	0.465±0.003	0.166±0.001		

Table 3: The number of site points that fall under the three vegetation types on either side of the fence. Each site had 25 points, with eight sites on either side of the fence there was a total of 200 points. The protected area was covered by all three vegetation types and the communal land were only comprised of the Musina Mopane Bushveld and Makuleke Sandy Bushveld

Vegetation type	Communal land	Protected area
Limpopo Ridge Bushveld (LRB)	0	6
Makuleke Sandy Bushveld (MSB)	116	116
Musina Mopane Bushveld (MMB)	84	78
	200	200

3.2. Effect of land use

Time-related phenometrics

The EVI seasonal growth patterns were very similar for the two land use types as the EVI values showed no overall difference. However, all the phenometrics, except the End_T of the growing seasons (Figure 8), showed significant differences across the fence line (Table 4, Figure 9). The communal lands' greenup started six days before that of the protected area (Figure 5, Table 4) resulting in a longer growing season for the communal land of five days. The $Peak_T$ occurred a week earlier in the communal land (Figure 6, Table 4), and the Mid_T of the growing seasons occurred five days earlier in the communal land compared to the protected area (Figure 7, Table 4).

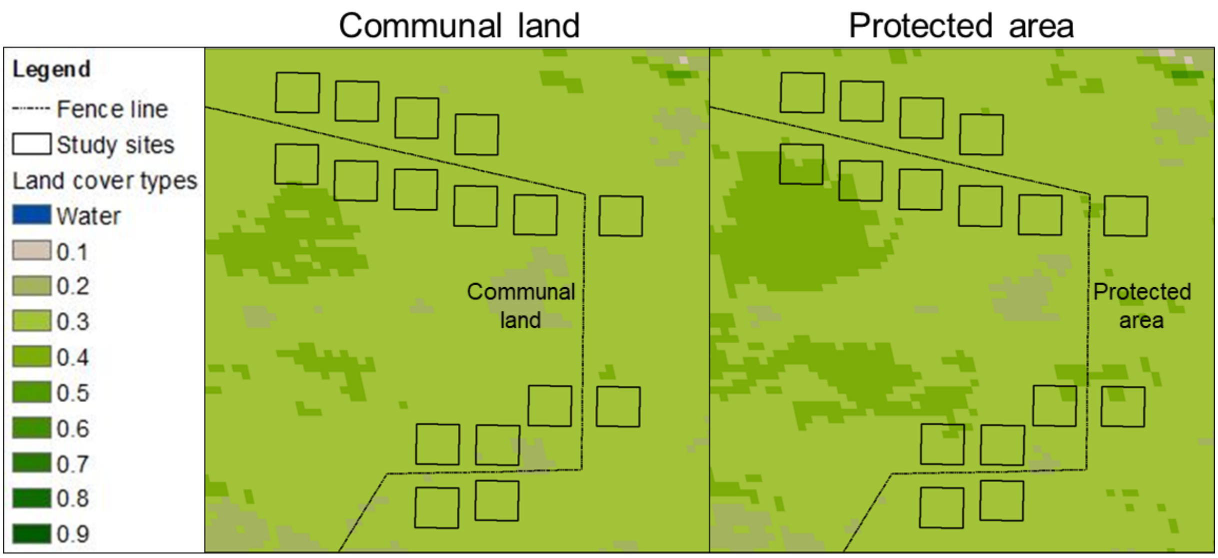

Figure 5: Enhanced Vegetation Index (EVI) image (range: 0.1-0.9) of the start time of the growing season ($Start_T$, Day of Year) for the communal land (03 Dec) and the protected area (09 December). The images are an amalgamation of the images of the six start times of the six growing seasons (2011-2017).

Table 4: Comparison of phenometrics (day ± SE) between the protected area and communal land, across all six growing seasons (2011-2017), and statistical comparisons between them (Wilcoxon signed rank test). The start time ($Start_T$), peak EVI time ($Peak_T$), mid-growing season time (Mid_T) and end time (End_T) of the growing season are shown as dates (Julian day ± SE), with length of the growing season as the day ± SE. Significant differences (p<0.05) are shown in bold.

Time-related phenometrics	**Communal land**	**Protected area**	Wilcoxon signed rank test
$Start_T$	03 Dec (337 ± 0.740)	09 Dec (343 ± 0.661)	v_{1197} = -189260, $\boldsymbol{p}$**<0.001**
$Peak_T$	02 Feb (33 ± 0.672)	09 Feb (40 ± 0.787)	v_{1197} = -51689, $\boldsymbol{p}$ **<0.001**
Mid_T	10 Feb (41 ± 0.576)	15 Feb (46 ± 0.683)	v_{1197} = 234810, $\boldsymbol{p}$ **<0.001**
End_T	09 Jul (190 ± 1.178)	11 Jul (192 ± 1.280)	v_{1197} = -350190, p = 0.8815
Length of growing season	221 days ± 1.219	216 days ± 1.231	v_{1197} = 435970, $\boldsymbol{p}$ **<0.001**
EVI related phenometrics	**Communal land**	**Protected area**	Wilcoxon signed rank test
Small integral	2.41 ± 0.020	2.44 ± 0.022	v_{1197} = 331840, $\boldsymbol{p}$ **<0.05**
Large Integral	4.98 ± 0.031	4.92 ± 0.032	v_{1197} = 388660, $\boldsymbol{p}$ **<0.05**
EVI	0.271 ± 0.0007	0.271 ± 0.0007	v_{27599} = 189260, p = 0.2442
EVI_{max}	0.462 ± 0.003	0.474 ± 0.003	v_{1197} = 268660, $\boldsymbol{p}$ **<0.001**
EVI_{min}	0.162 ± 0.001	0.160 ± 0.001	v_{1197} = 390230, $\boldsymbol{p}$ **<0.01**
Rate of greenup	16.863 ± 0.270	16.191 ± 0.289	v_{1197} = 424970, $\boldsymbol{p}$ **<0.001**
Rate of senescence	-33.219 ± 0.309	-31.229 ± 0.318	v_{1197} = -253690, $\boldsymbol{p}$ **<0.001**

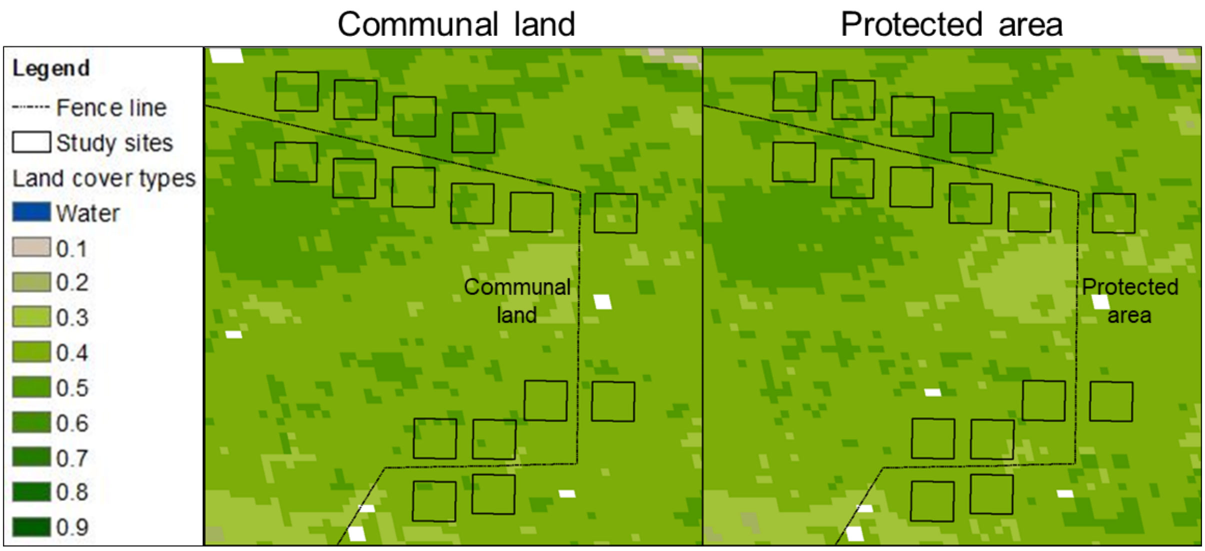

Figure 6: Enhanced Vegetation Index (EVI) image (range: 0.1-0.9) of the mean peak time of the growing season ($Peak_T$, Day of Year) for the communal land (02 February) and the protected area

(09 February). The images are an amalgamation of the images of the six peak times of the six growing seasons (2011-2017).

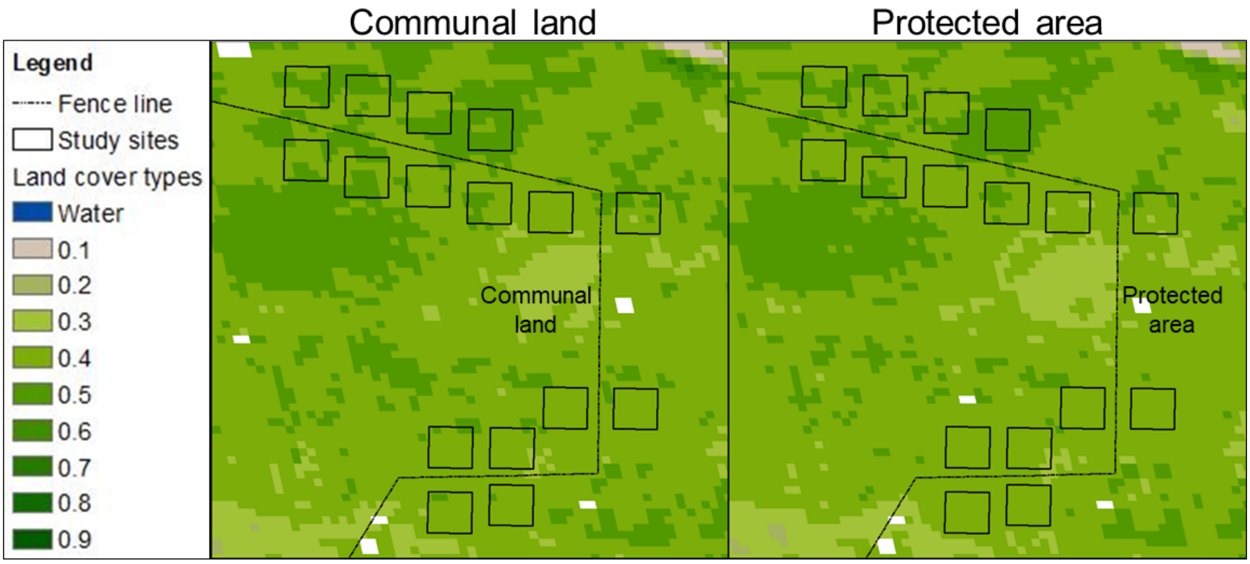

Figure 7: Enhanced Vegetation Index (EVI) image (range: 0.1-0.9) of the mean mid time of the growing season (Mid_T, Day of Year) for the communal land (10 February) and the protected area (15 February). The images are an amalgamation of the images of the six mid times of the six growing seasons (2011-2017).

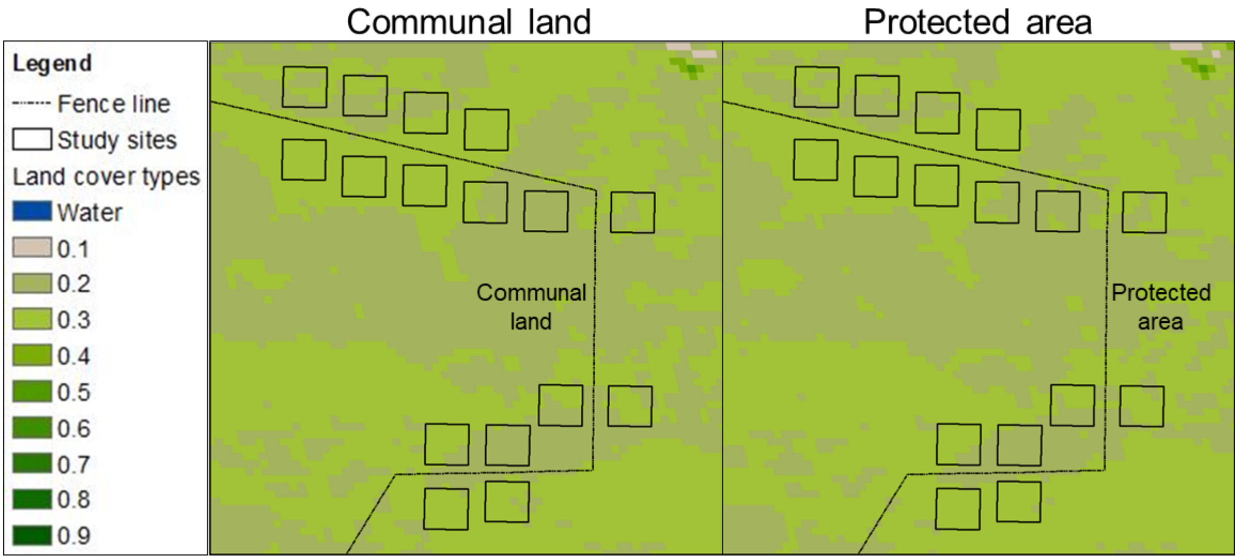

Figure 8: Enhanced Vegetation Index (EVI) image (range: 0.1-0.9) of the mean end time of the growing season (End_T, Day of Year) for the communal land (09 July) and the protected area (11 July).The images are an amalgamation of the images of the six end times of the six growing seasons (2011-2017).

EVI related phenometrics

Although the growing season was shorter in the protected area, it's maximum EVI value was higher, which led to the protected area having the greater small integral, which is indicative of 1% more seasonally active vegetation compared to the communal land. The communal land had the highest minimum EVI, as well as the greater large integral, suggesting the communal land was 1% more productive than the protected area. The rates of greenup and senescence were influenced by the $Start_T$, Mid_T and End_T, as well as the length of the growing season. With the $Start_T$ and Mid_T being earlier in the communal land, the rate of greenup was quicker in the communal land and thus the rate of senescence would also be longer as the growing seasons ended at similar times for the two sites (Table 4).

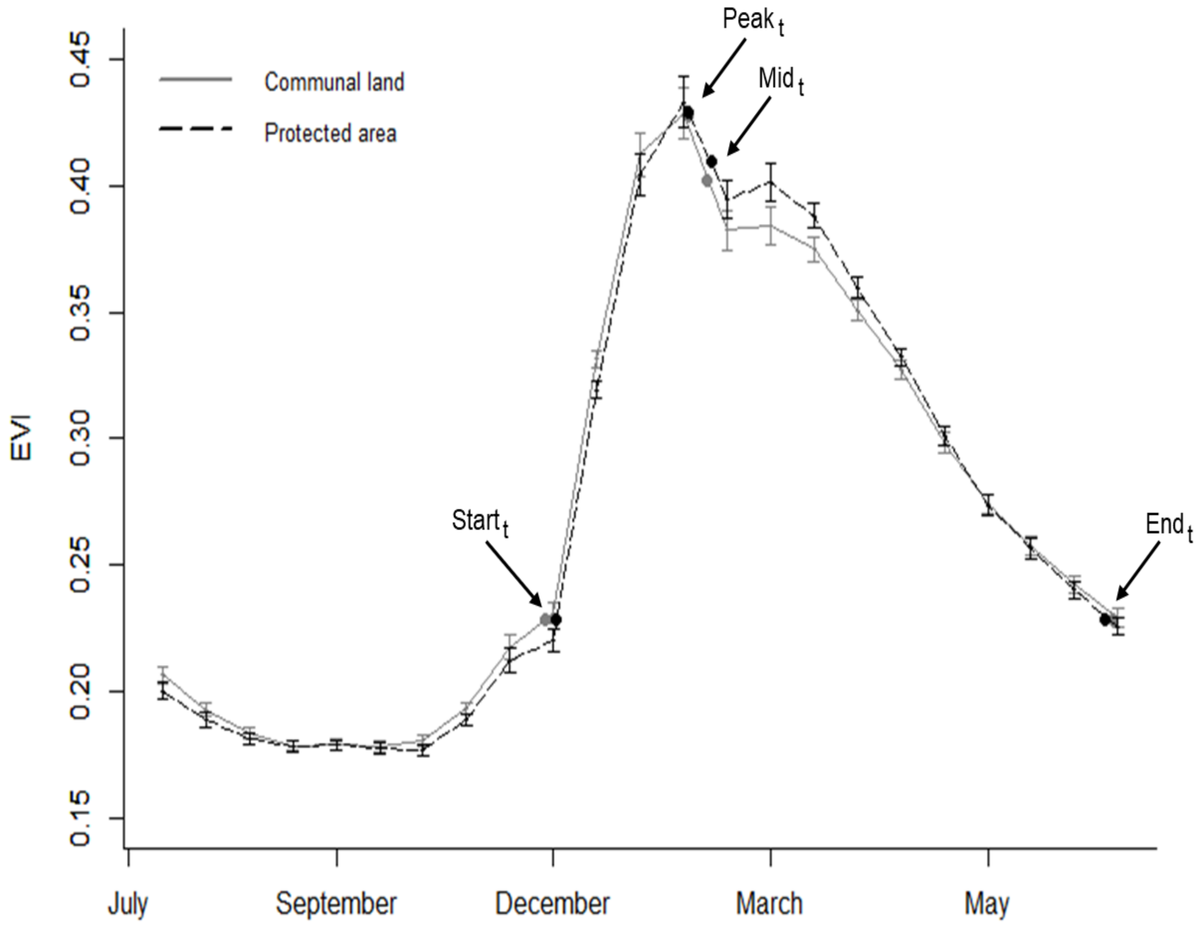

Figure 9: Savitzky–Golay smoothed Enhanced Vegetation Index (EVI) curves with standard error derived from the EVI values of all the sites within the protected and communal land over the six growing seasons (2011-2017) with the start time ($Start_T$), peak EVI time ($Peak_T$), mid-growing season time (Mid_T) and end time (End_T) of the growing seasons.

4. Discussion

4.1. Effect of vegetation type on phenological dynamics

Vegetation phenology is known to be influenced by rainfall (Jolly and Running 2004, Cleland *et al.* 2007, Chambers *et al.* 2013, Jin *et al.* 2013), temperature (Cubasch *et al.* 2001, Körner 2006, Nord and Lynch 2009) and vegetation type. As several studies have found, and as the results of this study suggest, vegetation type does influence vegetation phenology in a semi-arid mopane-dominated area (Hall-Martin and Fuller 1975, Guy *et al.* 1979, Dekker and Smit 1996). However, the near equal distribution of the MSB and MMB across the two land uses and the lack of any major difference of LRB to the other vegetation types suggests that the differences in phenology detected on either side of the fence are predominantly driven by land use.

4.2. Vegetation phenology response to land use

Time-related phenometrics

The only phenometric to show no significant difference between the protected area and communal land was the End_T. The $Start_T$, $Peak_T$, and Mid_T were significantly earlier in the communal land (six, seven and five days earlier respectively), which corresponds with previous studies that have shown the major spring leaf flush begins earlier in heavily browsed and often on coppiced savanna trees (Dekker and Smit 1996, Smallie and O'Connor 2000, Smit 2003). It is possible that coppiced trees may have a greater abundance of branches (Smallie and O'Connor 2000), which may increase the amount of photosynthetically active vegetation that would be picked up via satellite imagery. The earlier greenup and longer growing season of the communal land was likely stimulated by what was expected to be higher browsing pressure and constant harvesting of wood for the various local uses. The most common livestock kept in this region include goats, donkeys and cattle (Venter and Witkowski 2010, 2011, Paumgarten *et al.* 2018). The longer growing season of the communal land is most likely due to the earlier onset of greenup recorded. However, the northern sites are within a *C. mopane* dominated vegetation type and the density of *C. mopane* stands may also be a contributing factor to the lengths of the growing season (Dekker and Smit 1996). Denser stands tend to have lower browser densities, and lose leaves earlier in the growing seasons, and greenup later compared to low-density stands (Smit 1994). Romo-Leon *et al.* (2016) assessed the phenological response of vegetation in agricultural land and natural areas in the semi-arid region of La Costa de Hermosillo, Mexico. Where the $Start_T$ and length of the growing season were found to be earlier and longer respectively in the agricultural lands, which they concluded was likely due to a combination of irrigation, fertilisation and reduced plant competition. Depending on the size of the area used for agricultural crops within the communal land, the differences in $Start_T$ and length of the growing season between the communal land and protected area may also be influenced by the presence of agricultural crops within the communal lands.

EVI related phenometrics

The Vhembe district has previously been classified as having moderate land degradation (Wessels *et al.* 2004) and based on the initial view of the study sites originally through remote sensing (Figure 10), followed by a site visit in November 2017 (Figure 11), there was evidence of this. The striking difference between the two sites was the lack of grass cover in the communal land (Figures 10 and 11). The results, however, showed no difference in the EVI across the fence line. The images taken of the contrasting vegetation across the fence line (Figure 11) are very similar to images from a land use study conducted by Kelly and Walker (1976). The images show the contrast between “intensive utilisation” and “utilised” sites within a mopane dominated area in Zimbabwe, and the main difference between the two sites is the difference in the grassy layer as with the communal land in this study there was a lack of an herbaceous layer at the intensively utilised site.

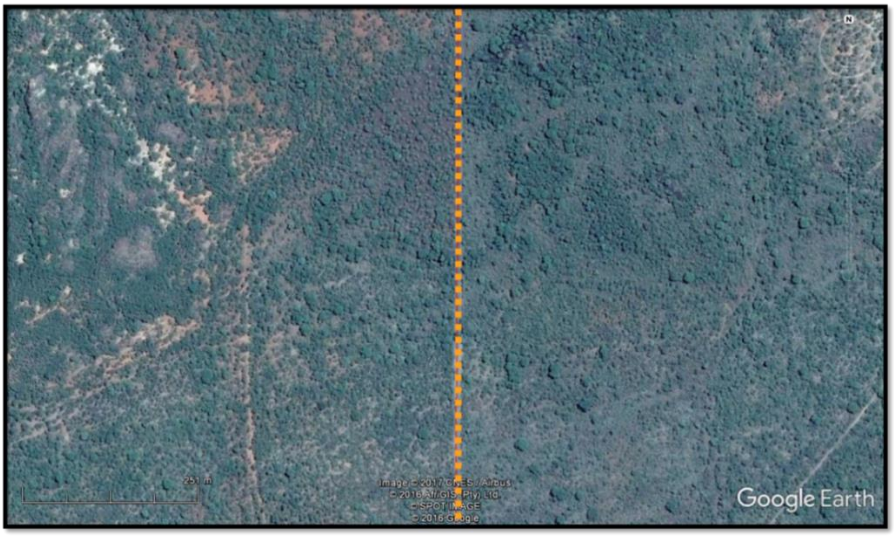

Figure 10: Google Earth image of a portion of the north western fence of the Greater Kruger National Park (early 2017) showing the difference in vegetation cover of the communal land (left) and the protected area (right). The general lack of grass cover is evident within the communal land.

Figure 11: Photographs showing the contrasting vegetation cover, both dominated by mopane, between the communal land (left) and the protected area (right). Photographs were taken on 10 November 2011 within the study location along the R525 Regional Route which becomes the H 1-9 in Kruger National Park (KNP).

The large integral provides insight into the standing crop and may be used as a proxy for vegetation production. Although there was only a 1% difference between the large integrals measured from both sides of the fence, the difference was significant, suggesting that the communal land was slightly more productive than the protected area. Smit and Rethman (1998) assessed soil water content in mopane dominated plots with varying tree densities and established that soil water content was greater in plots with a greater herbaceous cover and lower tree density. Additionally, plots where the herbaceous layer was nearly completely absent experienced high rainfall runoff. The difference in grass cover between the protected area and communal land would have influenced water infiltration and available soil moisture within these sites. As water availability is known to be one of the main drivers of vegetation productivity (Briggs and Knapp 1995, Knapp *et al.* 2001), it would be expected that the protected area would have experienced greater productivity compared to the communal land. However, this was not the case in this study. In contrast to the results of this study, Kelly and Walker (1976) found the seasonal productivity to be greater in the light to moderately utilised sites rather than in intensively utilised sites. The differences in phenological dynamics across the fence line were likely driven by different herbivore densities and the frequency at which the areas are utilised. Light to moderate grazing and browsing may result in increased primary production. Depending on how much photosynthetic material is removed, it is probable that the growth performance of the plant may increase due to more water and nutrients becoming available for the remaining photosynthetic material (Aldos et al 1997). Defoliation of grasses creates less self-shading and competition which permits more efficient light use (McNaughton 1979, Todd and Hoffman 1999, Fynn *et al.* 2005) and increases photosynthetic rates (McNaughton 1979, Cullen *et al.* 2006) thus increasing productivity. Conversely, severe defoliation of trees often leads to the regrowth of smaller shoots and leaves (Anttonen *et al.* 2002, Gadd *et al.* 2001, Piene *et al.* 2003, Rooke and Bergstrom 2007) with increased chemical defence.

Additionally, the reduced productivity in the protected area may be due to elephant damage to woody vegetation (Trollope *et al.* 1998, Fisher *et al.* 2015, Mograbi *et al.* 2017). Damage to the mature stems caused by elephants is often more severe compared to damage caused by wood harvesting (Botha *et al.* 2002). Walker (1980) quantified estimates of production of *C. mopane* dominated areas in Zimbabwe and showed that the difference in production was due to differences in management between sites of intense herbivore utilisation and sites of little to no utilisation.

Interestingly, the protected area had significantly more seasonally or photosynthetically active vegetation (based on the small integral). Although the difference in seasonally active vegetation was only 1%, the significantly greater maximum EVI of the protected area supports that the protected area is the “greener” side of the fence. This suggests that what may be heavier and constant herbivory within the communal land purely maintains the growth of the vegetation through the constant removal of accessible foliage. A common example of this is how sheep, goats and sometimes, cattle browse trees resulting in the lower branches of trees in and around villages being completely stripped of leaves and often cropped to the maximum browsing height (Van Voorthuizen 1976). And with *C. mopane* able to retain its leaves well into the dry season, it provides poor quality forage for herbivores during the dry months when forage becomes scarce (Styles and Skinner 1997). Nonetheless, this constant defoliation appears to have no detrimental effects on the trees (Kelly and Walker 1976). The lack of a grass layer within the communal land may have also been a contributing factor for the difference in seasonally active vegetation, with the grass layer present within the protected area adding to the amount of photosynthetically active vegetation during the growing season.

The 1% differences in productivity and seasonally active vegetation, although significant , between the two sites suggest that the vegetation on either side of the fence is not too dissimilar. While the parameters for selecting the sites excluded man made interruptions in the landscape as well as water sources, different substrate was not focused on. And the slight difference in substrate of sites 7 and 8 of the protected area and communal land may be contributing to the differences detected. However, the larger differences in the time related phenometrics suggest that aspects of the land use, likely herbivore distribution and forage consumption, are influencing the vegetation phenology.

The design of the study sites along the fence line may not have provided accurate information as to the vegetation-herbivore dynamics within the protected area, as the fence may have created an edge-effect, influencing animal distributions (Vanak *et al.* 2010). To further understand how the densities of herbivores influence the vegetation on both sides of the fence, and more specifically the phenology, studies on the stocking rates, mega-herbivore home ranges, as well as the number of artificial water points (as the presence of these influence herbivore distribution) for both the communal land and protected area is needed.

4.3. Vegetation dynamics and local communities

The Vhembe district is a former homeland and has a population of approximately 1.2 million people (Van Marrewijk 2011). The economy of this region is largely dependent on mining, tourism and agriculture (Van Marrewijk 2011). Although the Tshikondeni Coal Mine, which borders the Makuya Nature Reserve, is one of the largest contributors to employment opportunities, unemployment in the area is still extremely high (Medvey 2010). Most households rely on social grants and their natural environment for the harvesting of fruits, vegetables, medicinal plants, firewood and fodder (van Marrewijk 2011). The dominant woody species in this area, including *C. mopane, Terminalia sericea, Combretum apiculatum* and *Kirkia acuminata,* serve a multitude of purposes for the local people including materials for fencing posts, construction of houses and for firewood (Madzibane and Potgieter 1999, Smit 2003). *C. mopane* is a dominant species within its range and is a host for *Imbrasia belina,* the mopane worm, which is a food source for local communities (Hrabar *et al.* 2009).The main stem of smaller trees and the thin side branches of larger trees are used for fencing posts. One household can use between 1000 to 2500 posts around agricultural land and kraals. Additionally, households of around eight people can use up to 8 kg of firewood for one meal, (Madzibane and Potgieter 1999). Farming may be difficult as this region has soils that are prone to erosion (Van Marrewijk 2011). This, added to unsustainable resource use, particularly of woody plants, or overgrazing often leads to land degradation (Fisher *et al.* 2009). Alternatively, increased wood harvesting and high herbivory pressure often leads to bush encroachment. This study illustrated that the communal lands were slightly more productive than was expected, thus the area is still capable of providing sufficient forage for livestock and woody materials for fuel and local construction.

5. Conclusion

When comparing the same seasons, vegetation type was a significant predictor of phenology. However, the two dominant vegetation types, Makuleke Sandy Bushveld and Musina Mopane Bushveld, were nearly equally distributed across the communal land and protected area. This suggests that the differences in phenology the results have shown between the sites on either side of the fence was predominantly driven by different land use. The start of greenup and the length of the growing season were significantly earlier (six days; $p<0.001$) and longer (five days; $p<0.001$) respectively in the communal land, likely due to the stimulation of vegetation growth by what is assumed to be the greater herbivore pressure in the communal land. The productivity was slightly greater in the communal land (1%, $p<0.05$), while the protected area had slightly more seasonally active vegetation (1%, $p<0.05$). These minor differences in productivity and seasonally active vegetation may be a result of the sites in the communal land being constantly utilised for browsing by livestock and wood harvesting, and the general lack of a grass layer in the communal land. Savannas are important for subsistence farming, commercial agriculture and conservation in southern Africa. With the dominant tree species serving a multitude of essential purposes for the local people including materials for construction, firewood and forage for livestock, maintaining healthy savanna systems is essential. With the aid of remote sensing an understanding of the phenology of semi-arid savannas can be obtained at multiple scales which allows for the monitoring of responses of vegetation under different land use pressures and management practices. This also provides land managers and conservation officials with insights into the long-term dynamics of this system under contrasting land use practices.

Chapter 3

Assessing the response of vegetation phenology to extreme climatic events using remote sensing

Abstract

Recent changes in global climate have led to an increase in the severity and frequency of climatic events with predictions of global temperatures and regional rainfall patterns to change. Enhanced Vegetation Index (EVI) data, a measure of vegetation greenness, obtained from remotely sensed MOD13Q1 16-day composite imagery (250 m resolution), was used to extract phenological time series data and the associated phenometrics (e.g. $Start_T$ and End_T, season length) of the growing season. Six consecutive growing seasons (2011-2017) were assessed, during which two "extreme" events occurred. These included a flood in 2013 (annual rainfall = 757.8 mm) and a drought from 2014-2016, in 2014-15 (annual rainfall = 343.7 mm) and 2015-16 (annual rainfall = 307.5 mm). Interannual rainfall coefficient of variation (CV) for the six growing seasons was 45%. Phenological responses of vegetation as well as land cover change in response to these extreme events were assessed at multiple sites, on either side of the north-western fence line of the Greater Kruger National Park, near Pafuri (total area of 1250 ha on either side of the fence) to test if land management (communal grazing lands vs. protected area) had an influence on the phenometrics. EVI was not strongly influenced by rainfall (protected area: R^2 = 0.180; communal land: R^2 = 0.190) yet, the phenometrics derived from EVI were more susceptible to changes in seasonal rainfall. The flood year had the longest growing season (protected area = 229 days; communal land = 244 days; $p<0.05$) and greatest vegetation productivity (flood year to first drought year: protected area = 13% decrease; communal land = 13% decrease, $p<0.05$; flood year to second drought year-protected area = 9% decrease; communal land = 8% decrease, $p<0.05$). Due to extensive cloud cover the expected peak in EVI of the flood year did not occur, this would have affected the $Start_T$, Mid_T, $Peak_T$, length, SI (vegetation greenness) and LI (productivity). Land use type had an effect on the time-related phenological response of vegetation to the flood year and first drought year. Only the $Start_T$, $Peak_T$ and Mid_T showed significant differences in the response of the phenology between the land use types to the conditions associated with the flood and drought events. Overall the effect of the drought was not as severe on the surrounding vegetation when the vegetation dynamics were compared across the six growing seasons. Monitoring phenological changes in response to extreme climatic events using remote sensing allows one to observe and predict responses of various systems during this current period of rapid environmental change. This is important for land managers and conservation practitioners given the prediction of more frequent extreme climatic events across South Africa in the future.

Keywords: Drought, EVI, ENSO, flood, Greater Kruger National Park, semi-arid savanna, vegetation response.

1. Introduction

Recent changes in global climate have led to an increase in the severity and frequency of extreme climatic events; and current climate models predict that global temperatures, atmospheric CO_2 concentrations and regional rainfall patterns will continue changing in the future (Bloor *et al.* 2010). Floods and droughts are two severe disturbances experienced in southern African savannas and can initiate extreme shifts in vegetation dynamics such as changes in biomass production, species distribution, abundance and compositional changes in species assemblages (Stephenson 1990, Mueller *et al.* 2005). Vegetation phenology in semi-arid savannas may be sensitive to flooding and drought events, as water availability is one of the main drivers of productivity in these systems (Briggs and Knapp 1995, Knapp *et al.* 2001). Most phenological studies using remote sensing are conducted at regional (Chidumayo 2001, Heumann *et al.* 2007, Van Leeuwen *et al.* 2010, Ryan *et al.* 2014, Adole *et al.* 2018), continental (Brown *et al.* 2010, Atzberger *et al.* 2013, Ault *et al.* 2013) or global scales (Zhang *et al.* 2012, Boke-Olén *et al.* 2016), and areas within the northern hemisphere have been extensively covered (Chen *et al.* 2006, Jönsson *et al.* 2010, Van Leeuwen *et al.* 2010, Fitchett *et al.* 2015). Few studies have sought to investigate the effects of extreme climatic events and differing land use and management on the dynamics of vegetation within the diverse southern African savanna systems (Chidumayo 2001).

Floods and droughts

Severe droughts are a recurrent event in southern African savannas usually taking place once every decade (Rouault and Richard 2005, Ogutu *et al.* 2008, Dai 2011), yet extreme floods are relatively infrequent occurring only once every 50-100 years (Heritage *et al.* 2001, Ogutu *et al.* 2008). Floods can be defined as serious natural hazards caused by rainfall events (Stal 2011, Sitoe *et al.* 2015) and is typically a short event. Long durational floods, lasting several days, mostly occur in tropical regions due to unrelenting rainfall or tropical storms. These floods result in massive losses to property, health related issues and deaths, caused by inundation and the contamination of clean water supply and sanitation, increasing the risk of water-borne diseases (Dang *et al.* 2011, Ward *et al.* 2016). As floods are associated with this increase in rainfall, vegetation within the entire catchment area is influenced by the increase in water availability. Floods of varying magnitudes result in the damage or removal of riparian vegetation (Carter and Rogers 1995, Bendix *et al.* 2000, Friedman and Auble 2000, Parsons *et al.* 2005, 2006; Beater *et al.* 2008). However, vegetation in the riparian zone and surrounding flood plain respond to a flooding event with an increase in plant production and growth (Junk *et al.* 1989, Sims and Thoms 2002, Parsons *et al.* 2006).

Drought can be defined as an intricate natural hazard distinguished by below average rainfall for an extended period, which results in a water shortage that effects ecosystems and society in numerous ways (Wilhite 1993, Unganai and Kogan 1998, Dai 2011, Van Loon 2015). From this drought can be classified into four categories; meteorological drought, agricultural drought, hydrological drought and socioeconomic drought (Unganai and Kogan 1998). Drought is difficult to detect and monitor as it is a slow developing event, taking months or years to manifest (Peters *et al.* 2002, Ji and Peters 2003). Droughts in savannas result in large decreases in biomass and basal cover of grasses (Prins 1988, Baruch 1994, O'Connor 1995, Bloor *et al.* 2010) and grazing pressure further exacerbates the effects of drought by the removal of remaining grass biomass (O'Connor 1995). Although sufficient rains may follow a drought, the irreversible ecological changes will have already occurred in the form of vegetation die-off and vegetation cover change, and the decline in large herbivore numbers. Furthermore, vegetation cover can alter drastically during the transition from drought induced conditions, to average rainfall conditions and flood induced conditions (Anyamba *et al.* 1999), which influences forage availability for herbivores. Forage availability plays a large role in determining the distributions of large herbivores (McNaughton 1987), and drought and flooding related events can thus lead to changes in these distributions. The effects of drought on agriculture and livestock is a growing threat to global food security, especially in arid regions (Lin *et al.* 2013). Although extreme droughts cause economic strain globally, developing countries and more specifically self-sufficient farmers, feel the brunt of these climatic events with the loss of most, if not all, of their livestock herds and crops (Little *et al.* 2006), exacerbating poverty in already poverty stricken areas. Floods and droughts in southern Africa are often intensified by the occurrence of the El Niño Southern Oscillation (ENSO) episodes, causing these events to become extreme.

Although the southern African climate is affected by various ocean-atmospheric interactions, interannual rainfall variability is mainly influenced by El Niño Southern Oscillation (ENSO). Sea surface temperatures of the eastern Pacific Ocean cause changes in atmospheric pressure conditions that drive the ENSO phenomenon (Ogutu and Owen-Smith 2003, Ogutu *et al.* 2008). ENSO can greatly influence the climatic variability in southern Africa and these conditions can lead to great rainfall variability (Lindesay and Vogel 1990, Ogutu *et al.* 2008). ENSO has two episodes; El Niño and La Niña. El Niño, the warm, dry phase, with bellow average rainfall which often triggers extreme droughts in southern Africa. While La Niña, is the cold, wet phase, with above average rainfall where extreme flooding is more likely in the region (Van Heerden *et al.* 1988, Anyamba *et al.* 1999, Kruger 1999, Ogutu *et al.* 2008).Furthermore, the frequency and intensity of prior ENSO episodes tend to determine the severity of subsequent El Niño and La Niña episodes (Ogallo 1993).

Phenology

Several studies have been conducted in southern African savannas examining the effect of multiple climatic factors on plant phenology with the use of remote sensing (Chidumayo 2001, Jolly and Running 2004, Archibald and Scholes 2007, Higgins, Delgado-Cartay, *et al.* 2011, Jin *et al.* 2013, Whitecross *et al.* 2016, 2017a, 2017b). Phenology is the study of seasonal life-cycle events and the effect of environmental changes and biotic interactions on these events (Lieth 1974). Vegetation phenology focuses on the plants' annual cycle from the start of the growing season to the end of senescence (Adole *et al.* 2016). Depending on an organism's ability to store and access water, greenup events (initiation of the growing season) for some species occur prior to the first rainfall event of the wet season (early-greening species) (Whitecross *et al.* 2017a) while other species greenup after the first rainfall event (Archibald and Scholes 2007). Trees and grasses flush at different times and have different growing season lengths (Higgins, Delgado-Cartay, *et al.* 2011), grasses are limited by soil water availability and thus greenup after the first rains (Chidumayo 2001). Changes in temperature and photoperiod have been shown to have altered the timing of the onset of spring growth and senescence (Chmielewski and Rötzer 2001) and changed the length of the growing season in temperate regions (Nord and Lynch 2009). Phenological changes occur at different rates globally depending on the regional changes in temperature, photoperiod and rainfall (Cleland *et al.* 2007, Fitchett *et al.* 2015). With climate change, the physiological suitability of ecosystems are changing and leads to a species response of range change or shifts in phenology (Parmesan and Yohe 2003, Primack *et al.* 2009). Changes in plant phenology can have ripple effects on other ecosystem processes and services (Chmielewski *et al.* 2004, Schwartz *et al.* 2006, Archibald and Scholes 2007, Polgar and Primack 2011, Fitchett *et al.* 2015). These changes may have negative or positive effects biologically in terms of carbon and water cycling and photosynthesis which influences biomass production and forage availability, as well as economically in terms of agricultural production (Archibald and Scholes 2007, Chambers *et al.* 2013, Fitchett *et al.* 2015). Alteration in the growing seasons will change the amount of carbon sequestration, water uptake, energy exchange and resources for pollinators and herbivores, as well as reproductive cycles and crop yields.

3.1. Aim and objectives

This chapter aims to quantify how conditions associated with extreme flooding and drought events influence vegetation phenology at multiple sites along the north-western fence line of the Greater Kruger National Park using remote sensing. To do so the difference in the timing of the time-related phenometrics for all six growing seasons were determined and how the EVI related phenometrics change across growing seasons were established. Additionally, the phenological responses during the three extreme growing seasons; the 2012/2013 flood year, the 2014-2015 drought year and the 2015-2016 drought year were compared. Lastly, how the phenological dynamics relate to rainfall, temperature and photoperiod during seasons with extreme climatic events were assessed.

2. Methods

2.1. Study area

The study area is located in the northern region of the Greater Kruger National Park (KNP) (Makuya National Park), near Pafuri, and included the Madimbo Corridor and the adjacent Vhembe district of Venda outside the park along the north-western fence line (Figure 1).

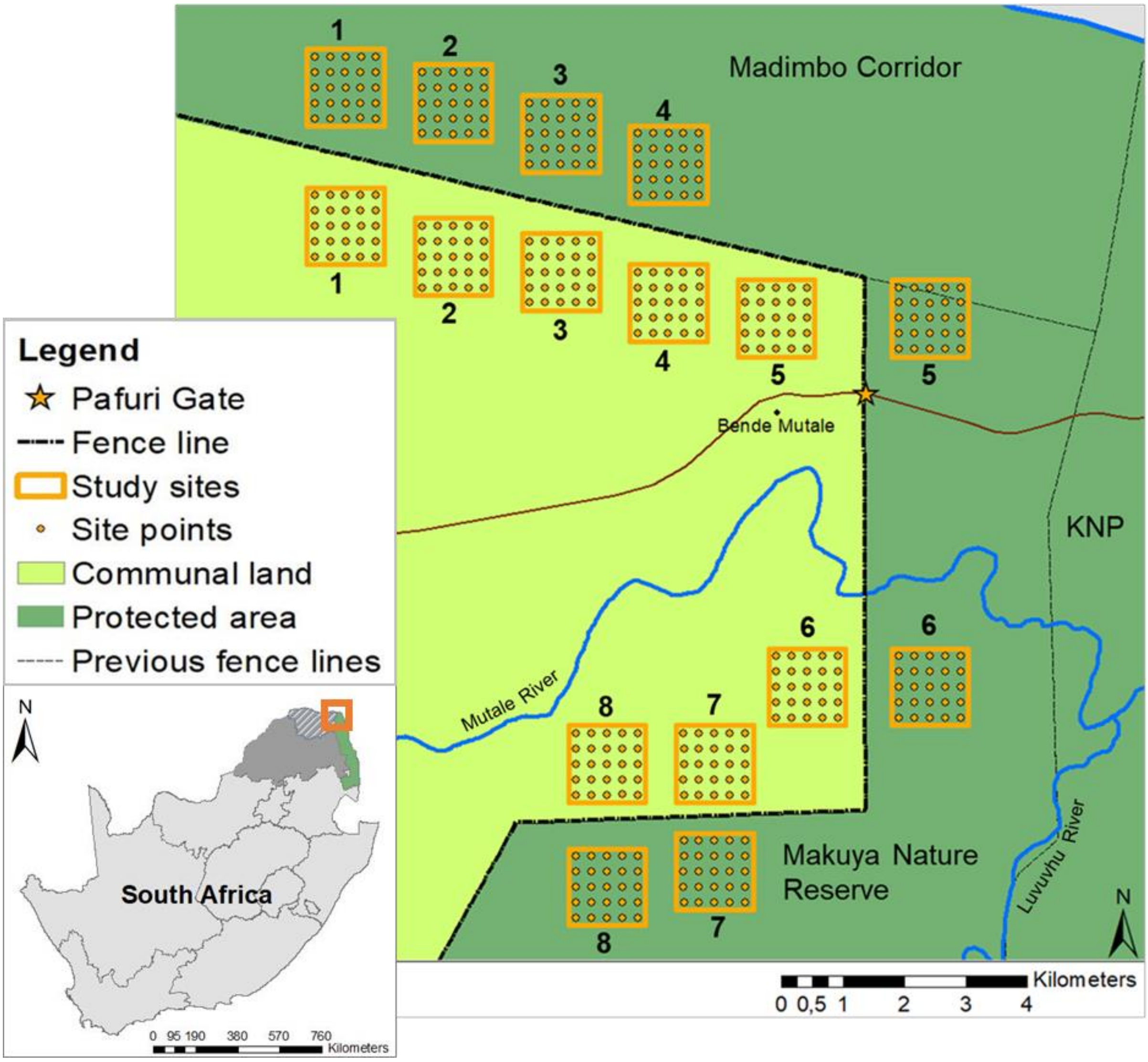

Figure 1: Location of the study area along the north western fence line of the Greater Kruger National Park, the protected area is comprised of the Makuya Nature Reserve, the Madimbo Corridor and the Kruger National Park (KNP), the communal land is predominantly used as grazing area. The eight study sites on either side of the fence, were made up of 5 x 5 pixels, where a pixel

is 250 m. The study sites were placed at least one pixel (or 250m) away from other sites and from roads, rivers or human dwellings.

2.2. Experimental design

This study spanned a six-year period from 1 July 2011 to 30 June 2017 (austral years 2011/2012 to 2016/2017), focusing on a flood event in 2013 (austral total = 772.0 mm) and a drought event that spanned two austral growing seasons, in 2014-15 (austral total = 234.5 mm) and 2015-16 (austral total = 269.5 mm), interannual rainfall coefficient of variation (CV) for the six growing seasons = 45%. This area is classified as semi-arid and in total receives between 300-500 mm of rain annually with most the rainfall received between October and April (Venter *et al.* 2003), with a rainfall interannual coefficient of variation (CV) of > 40% for the region (Schulze 1997). Sixteen study sites were selected along the north western fence line of the greater Kruger National Park, eight sites within the protected area and eight sites in the communal land. Each site comprised of 5 x 5 MODIS pixels; a pixel was defined by the 250 x 250 m MODIS image (Figure 1). For further details refer to Chapter 2, Figure 1, page 15.

2.3. Phenometrics

The EVI measurements were extracted from points which were placed in the centre of each 250m MODIS pixel, at the eight sites on either side of the fence line across the six austral seasons. With the 23, 16-day MODIS composites that make up one austral year, a total of 55200 EVI replicates resulted (25 points*16 sites*23, 16-day * six austral years: n = 55200).

The assessment of phenological characteristics for both sides of the fence were conducted by investigating the phenometrics related to seasonal EVI patterns and the EVI time series data.

2.4. Extreme environmental events

The flood event of mid-January 2013 was a result of rainfall that fell over north eastern South Africa, southern Zimbabwe and central and southern Mozambique (Manhique *et al.* 2015), which makes up the Limpopo River basin (Sitoe *et al.* 2015). Several weather stations within Mozambique recorded over 200 mm of rainfall within 24 hours. As the central to southern region of Mozambique falls in most of the Limpopo River basin, low lying areas, including several towns, experienced the detrimental impacts of this flood. Over 100 lives were lost, nearly 200 000 people were displaced, and there was great loss to economic and social infrastructure (Manhique *et al.* 2015). The effects of this flood event in the Pafuri region were, however, not as severe as experienced in Mozambique. A monthly total of 510 mm of rain fell in Pafuri during January 2013, with 290 mm of this falling over 24 hours. On average January receives 50-100 mm of rain in the

Pafuri region. Although severe flooding events are typically infrequent, occurring every 10-25 years (Sitoe *et al.* 2015), the recurrence frequency may be increasing due to climate change.

At a national scale the drought of 2014-2016 was not as severe as the droughts experienced in the early 1980s and 1990s (Swemmer *et al.* 2018). Depending on the region and severity of the drought, below-average rainfall may only have been experienced for one year or in more severe cases three years or more (Swemmer *et al.* 2018). The 1982/83 drought was preceded by a wet-year cycle of 10 years, seven of which had above average rainfall. However, the 1982/3 growing season only received 98 mm of rainfall in Pafuri, which is one of the lowest annual rainfall periods for this region. The 1991/92 drought occurred during a dry cycle that was preceded by seven years of below-average rainfall and the 1982/83 drought and a minor drought of 1986/87. The 1991/92 drought received 120.5 mm of annual rainfall in the Pafuri region (Zambatis and Biggs 1995). The 2014-2016 drought was preceded by a wet-year cycle, which included the 2012/2013 flood year (772.0 mm), whereas the 2014/2015 drought year received 234.5 mm and the 2015/2016 drought year 269.5 mm of rainfall. Although a growing season may not be experiencing drought, mid-season droughts are a common occurrence in southern Africa, where there is a break in rainfall generally in the middle of the rainy season (i.e. January) (Joubert *et al.* 1996). Mid-season droughts may also occur during periods of extreme drought, in conjunction with El Niño events (Usman and Reason 2004). The frequency of mid-season droughts may increase due to an increase in daily rainfall variability during the rainy season (Joubert *et al.* 1996).

2.4.1 Effect of flood and drought conditions

Vegetation phenology in semi-arid savannas is often sensitive to fluctuations in water availability, as it is one of the main drivers of productivity. Thus, the EVI time series data and the associated phenometrics were established for the six growing seasons. To try and provide insights on how the drier savanna systems respond to major fluctuations in environmental factors, the flood year (2012/2013) and the two drought years (2014-2016) were focused on. The seasonal EVI patterns were compared with Savitzky-Golay smoothed EVI time series data of the six growing seasons. Linear mixed effects models were used to compare the EVI data and associated phenometrics across the six growing seasons, with austral years and land use, and their interaction as fixed effects and site as a random effect. To assess how the EVI and phenometrics differed across the growing seasons, Kruskal-Wallis multiple comparison post hoc tests were conducted for the protected area and communal land separately.

2.5. Climatic data

Rainfall

Daily rainfall data for Pafuri and Punda Maria were obtained from the South African Weather service and monthly rainfall data from the Kruger National Park Meteorological Records. Unfortunately, the Pafuri daily rainfall was incomplete for 2012 and 2013. The Pafuri monthly rainfall was compared to that of Punda Maria (9.4 km to the South-East) by plotting the annual rainfall patterns and correlating the two datasets for each year to establish if Punda Maria's daily rainfall would be a viable supplement for the incomplete 2012 and 2013 daily rainfall for Pafuri, which fortunately it was. In finding alternative rainfall data, the Climate Hazards Group InfraRed Precipitation (CHIRPS) v2.0 dataset (Funk *et al.* 2015) was explored. Although this data set did provide daily rainfall estimations for the Pafuri region, the rainfall for the area was overestimated (Figures S5, S6, S7, S8).

How the onset of rainfall is defined is highly important for defining the start of the wet season and growing season, as well as the initiation of vegetation production. In West Africa, May historically marks the start of the rainy season. Sivakumar (1988) defined rainfall onset in West Africa as the first 20 mm of rainfall that fell in three consecutive days after 1 May, with no dry spell longer than a week within the following month. Dodd and Jolliffe (2001) described the onset of rainfall in East Africa as a period of six consecutive days where at least 25 mm rainfall occurs with no dry spell for ten days within a 40 day period. Hachigonta *et al.* (2008) assessed the onset of rainfall for agricultural crops in Zambia and defined onset as a period of 10 days with at least 25 mm of rainfall, followed by a 20 day period of at least 20 mm of rainfall. The onset date is then taken as the first day of the initial ten-day period (Hachigonta *et al.* 2008). Recha *et al.* (2012) adapted and modified criteria from Sivakumar (1988) such that the onset of rainfall was defined as the day after 1 March and 1 October with two days of at least 20 mm rainfall with no dry spell within the next month that exceeds seven days, for the March- May and October- December rainy growing seasons in Kenya. Whitecross *et al.* (2017a) defined the onset of rainfall in Southern Africa as at least 15 mm of rainfall within 24 hours after the dry season. The onset of the rainfall is defined differently for different regions that experience different rainfall patterns, and these patterns are largely influenced by the El Niño Southern Oscillation (ENSO). The method used for the onset of rainfall was adapted from Sivakumar (1988) and Whitecross *et al.* (2017a), where the first 15 mm of rainfall within a 24 hour period after the dry season (Whitecross *et al.* 2017a) followed by no dry spell lasting longer than seven days will establish the rainfall onset. A rainfall event of 15 mm is adequate for the onset of grass growth, as grass growth is sensitive to water availability and will commence after there is enough available soil moisture (Bate *et al.* 1982).

The seasonal variability of the rainfall was compared to the EVI time series and a regression was used to establish the relationship between rainfall and the EVI. This initial regression of rainfall and EVI was then compared to a regression between the same variables but excluding the flood year (2012/2013). The amount of rainfall that fell in the flood year may have skewed the data, masking a relationship between rainfall and EVI. The total annual rainfall error was plotted and compared across the growing seasons. A correlation analysis was undertaken between the total seasonal rainfall and each phenometric for the six growing seasons. The dates of the onset of rainfall for each season were compared to the corresponding $Start_T$ or onset of greenup.

Temperature

As no temperature records are available for Pafuri, the temperature data used was from Punda Maria (9.4 km to the South-East), although these temperature data were also incomplete for parts of 2012, 2014 and 2015. Daily maximum land surface temperature data were obtained from the MOD11A1 datasets for the area over the study site, with a daily temporal resolution, and a spatial resolution of 1 km (NASA LP DAAC 2000). The daily temperature data from Punda Maria was compared to that of the MODIS dataset by plotting the annual temperature patterns and correlating the two datasets for each year (Figures S2, S3). The seasonal variability of the maximum land surface temperature was compared to the EVI time series and a regression was run to establish the relationship between maximum temperature and EVI. The maximum land surface temperature and standard error was plotted and compared across the growing seasons.

Photoperiod

The Photoperiod data were obtained from the South African Astronomical Observatory (www.saao.ac.za), which simply provides the number of hours between sunrise and sunset. The seasonal variability of the daily photoperiod was compared to the EVI time series using linear regression. The maximum land surface temperature and standard error was plotted and compared across the growing seasons.

Cloud cover

Cloud cover data were obtained from the MOD08D3 (www.reverb.echo.nasa.gov, accessed: 06 September 2018) dataset to establish if there was any considerable cloud cover reducing the detection of EVI during the study period. This was converted to a percentage of cloud cover to compare across the growing seasons, based on the median of the 16-day composite data.

2.6. Analytical software

Refer to Chapter 2, section 2.6, page 21.

3. Results

3.1. 2012/2013 Flood year and 2014/2015 drought year

Time-related phenometrics

The EVI for the flood year (2012/2013) and the first drought year (2014/2015) for both the communal land and protected area showed no overall differences (Table 3). However, the patterns of seasonal growth curves were different, with the first drought year experiencing a peak in EVI before slowly senescing, while the flood year had no peak and maintained plateaued growth before senescing (Figure 2). All time-related phenometrics for the protected area were significantly different between the flood year and first drought year. For the communal land, however, the $Start_T$ was the only time-related phenometric to show no significant difference between the two growing seasons (Tables 1, 2 and 3). In the protected area the $Start_T$ of the first drought year occurred five days before the $Start_T$ of the flood year, however the End_T of the first drought year was nearly a month and a half earlier than that of the flood year, which led to the length of the flood year's growing season being 41 days longer than the first drought year (Table 1, Figures 3 & 4). The communal land exhibited similar patterns as in the protected area with regards to the $Start_T$ and lengths of the growing seasons, with the $Start_T$ only occurring one day before that of the flood year and the length of the growing season being 44 days longer during the flood year. Although, the End_T of the flood year and first drought year were earlier in the communal land, the growing season of the flood year in the communal land still ended nearly 50 days after that of the first drought year (Table 1, Figures 3 & 4). The $Peak_T$ of the first drought year was 33 days before the peak of the flood year in the protected area and 35 days before in the communal land (Table 1, Figures 3 & 4). Similarly, the Mid_T of the first drought year occurred 39 days before that of the flood year in the protected area and 41 days before in the communal land (Table 1, Figures 3 & 4).

Enhanced Vegetation Index (EVI) related phenometrics

The maximum EVI of the communal land showed no significant difference between the flood year and second drought year, however the maximum EVI for the protected area as well as the minimum EVI for both sides of the fence were significantly different between the flood year and second drought year (Table 2). Maximum and minimum EVI were greater during the first drought year for both the protected area and communal land. The rates of greenup were faster in the protected area for the flood year, as well as the first drought year. For both sites the first drought year greened up more than twice as fast as the flood year due to the earlier Mid_T of the drought year. The rates of senescence were slower during the flood year as the growing season lengths were longer during this growing season (Table 3). Both the large and small integrals were larger for the flood year for both sides of the fence, indicating a 15% (protected area) and 18% (communal land) decrease in vegetation greenness and a 13% (communal land and protected area combined) decrease in vegetation production from the flood year to the first drought year (Table 3).

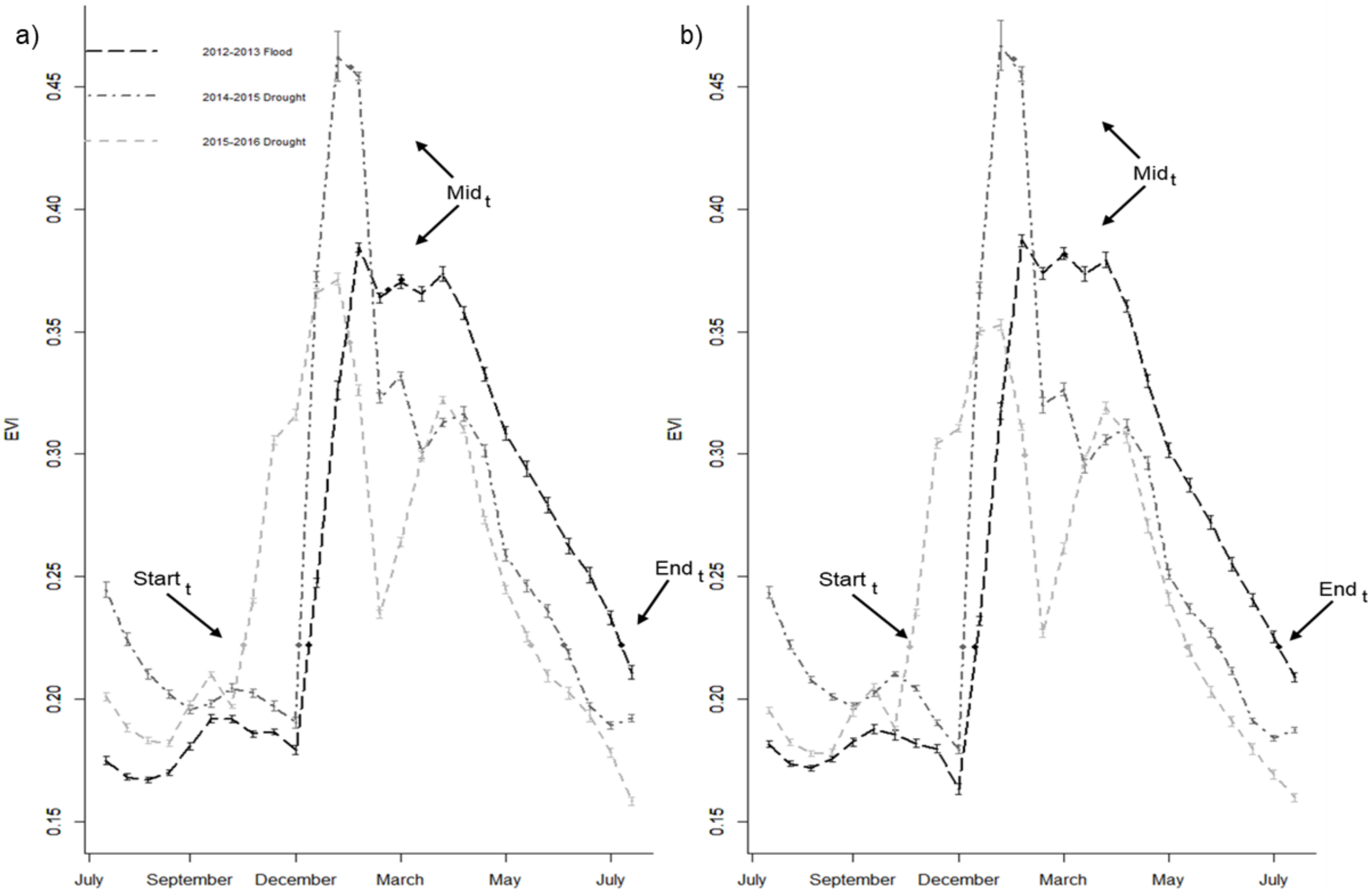

Figure 2: Smoothed Enhanced Vegetation Index (EVI) curves of a) protected area and b) communal land along the fence line of the Greater Kruger National Park during the flood year (2012/2013), the first drought year (2014/2015) and the second drought year (2015/2016) with the start time ($Start_T$), peak EVI time ($Peak_T$), mid-growing season time (Mid_T) and end time (End_T) of the growing seasons.

Table 1: Comparison of time-related phenometrics (mean day ± SE) of the six austral years (2011-2017) for the two sites across the fence line, the protected area and the communal land. The time-related phenometrics are: start time (Start$_T$), peak Enhanced Vegetation Index (EVI) time (Peak$_T$), mid-growing season time (Mid$_T$) and end time (End$_T$) of the growing season are shown as dates (mean Julian day ± SE), with length of the growing season as the mean day ± SE. Different superscript letters within each column between austral years (a) communal land and (b) protected area, indicate significant differences between vegetation types (Kruskal-Wallis multiple comparison post hoc test, p<0.05). The flood occurred during the 2012/2013 growing season, and the drought spanned the 2014/2015 and 2015/2016 growing seasons.

Communal land	**Start$_T$**	**Peak$_T$**	**Mid$_T$**	**End$_T$**	**Length**
2011/2012	30 Nov (334 ± 0.011)^{c}	31 Jan (31 ± 0.052)^{d}	05 Feb (36 ± 0.023)^{c}	15 May (136 ± 0.050)^{e}	170 days ± 0.054^{e}
2012/2013	17 Dec (352 ± 0.052)^{b}	25 Feb (56 ± 0.048)^{a}	08 Mar (67 ± 0.029)^{a}	16 Aug (228 ± 0.052)^{a}	244 days ± 0.049^{b}
2013/2014	21 Nov (325 ± 0.015)^{d}	06 Feb (37 ± 0.028)^{c}	13 Feb (44 ± 0.022)^{b}	13 Aug (225 ± 0.060)^{a}	268 days ± 0.059^{a}
2014/2015	16 Dec (350 ± 0.031)^{b}	21 Jan (21 ± 0.015)^{e}	26 Jan (26 ± 0.025)^{d}	01 Jul (182 ± 0.039)^{c}	200 days ±0.056^{d}
2015/2016	28 Oct (301 ± 0.035)^{e}	13 Jan (13 ± 0.016)^{f}	26 Jan (26 ± 0.037)^{d}	20 Jun (172 ± 0.041)^{d}	238 days ± 0.040^{b}
2016/2017	24 Dec (359 ± 0.005)^{a}	12 Feb (43 ± 0.019)^{b}	14 Feb (45 ± 0.011)^{b}	18 Jul (199 ± 0.030)^{b}	208 days ± 0.030^{c}
Protected area	**Start$_T$**	**Peak$_T$**	**Mid$_T$**	**End$_T$**	**Length**
2011/2012	02 Dec (336 ± 0.01)^{c}	17 Feb (48 ± 0.055)^{ab}	16 Feb (47 ± 0.032)^{b}	31 May (152 ± 0.085)^{e}	184 days ± 0.088^{d}
2012/2013	27 Dec (362 ± 0.029)^{a}	24 Feb (55 ± 0.044)^{a}	06 Mar (65 ± 0.029)^{a}	11 Aug (223 ± 0.043)^{b}	229 days ± 0.050^{b}
2013/2014	04 Dec (338 ± 0.021)^{c}	10 Feb (41 ± 0.027)^{b}	20 Feb (51 ± 0.021)^{b}	25 Aug (237 ± 0.068)^{a}	267 days ± 0.074^{a}
2014/2015	23 Dec (357 ± 0.013)^{b}	22 Jan (22 ± 0.028)^{d}	26 Jan (26 ± 0.027)^{d}	27 Jun (178 ± 0.034)^{d}	188 days ± 0034^{d}
2015/2016	02 Nov (306 ± 0.033)^{d}	30 Jan (30 ± 0.074)^{c}	04 Feb (35 ± 0.051)^{c}	08 Jun (160 ± 0.037)^{e}	221 days ± 0.051^{b}
2016/2017	25 Dec (360 ± 0.014)^{ab}	15 Feb (46 ± 0.016)^{b}	17 Feb (48 ± 0.013)^{b}	17 Jul (198 ± 0.026)^{c}	206 days ± 0.025^{c}

Table 2: Enhanced Vegetation Index (EVI) related phenometrics (mean ± SE) of the six growing seasons (2011-2017) along the fence line of the Greater Kruger National Park between the protected area and the adjacent communal land. For (a) protected area and (b) communal land separately, different superscript letters within each column indicate significant differences between growing seasons (Kruskal-Wallis multiple comparison post hoc test, p<0.05). The flood occurred during the 2012/2013 growing season, and the drought spanned the 2014/2015 and 2015/2016 growing seasons.

Communal land	**EVI**	**EVI_{max}**	**EVI_{min}**
2011/2012	0.240 ± 0.0006^{d}	0.391 ± 0.001^{d}	0.159 ± 0.0005^{cd}
2012/2013	0.264 ± 0.0005^{b}	0.399 ± 0.001^{c}	0.163 ± 0.0005^{c}
2013/2014	0.313 ± 0.0008^{a}	0.556 ± 0.001^{b}	0.175 ± 0.0006^{b}
2014/2015	0.270 ± 0.0007^{b}	0.472 ± 0.002^{c}	0.180 ± 0.0005^{a}
2015/2016	0.255 ± 0.0005^{c}	0.373 ± 0.001^{e}	0.157 ± 0.0004^{d}
2016/2017	0.221 ± 0.0013^{e}	0.580 ± 0.001^{a}	0.137 ± 0.0004^{e}
Protected area	**EVI**	**EVI_{max}**	**EVI_{min}**
2011/2012	0.240 ± 0.0005^{e}	0.399 ± 0.001^{d}	0.154 ± 0.0005^{c}
2012/2013	0.263 ± 0.0006^{c}	0.407 ± 0.001^{d}	0.162 ± 0.0005^{b}
2013/2014	0.309 ± 0.0005^{a}	0.572 ± 0.001^{b}	0.171 ± 0.0004^{a}
2014/2015	0.267 ± 0.0006^{c}	0.477 ± 0.002^{c}	0.174 ± 0.0004^{a}
2015/2016	0.249 ± 0.0005^{d}	0.361 ± 0.001^{e}	0.156 ± 0.0004^{c}
2016/2017	0.294 ± 0.0006^{b}	0.629 ± 0.001^{a}	0.140 ± 0.0004^{d}

3.2. 2012/2013 Flood year and 2014/2015 drought year

Time-related phenometrics

Length of the growing season and rate of senescence were the only phenometrics to not differ significantly between the flood year (2012/2013) and second drought year (2015/2016) for both the communal land and protected area (Tables 1, 2, & 3). Although the difference in the $Start_T$ for the two growing seasons in the protected area was 56 days, with the second drought year greening up first, the difference between the End_T was even greater at 63 days, as the second drought year reached senescence before the flood year. This resulted in the lengths of the growing seasons only differing by eight days, with the flood year experiencing the longer growing season. The communal land showed the same pattern with the second drought year initiating growth 51 days before the flood year and the season ending 56 days before the flood year, leading to the lengths of the season differing by only six days. Again, the second drought year showed earlier timing with the $Peak_T$ and Mid_T being 25 days and 30 days earlier respectively compared to the flood year. The $Start_T$ and

$Peak_T$ occurred earlier in the communal land for both growing seasons, while the End_T occurred later, leading to both growing seasons being, longer in the communal land. Furthermore, the mid $Peak_T$ of the flood year was earlier in the protected area but earlier in the communal land for the second drought year (Table 1, Figures 3 & 4).

Table 3: Enhanced Vegetation Index (EVI) related phenometrics (mean ± SE) of the six growing seasons (2011-2017) along the fence line of the Greater Kruger National Park between the protected area and the adjacent communal land. For (a) protected area and (b) communal land separately, different superscript letters within each column indicate significant differences between growing seasons (Kruskal-Wallis multiple comparison post hoc test, $p<0.05$). The flood occurred during the 2012/2013 growing season, and the drought spanned the 2014/2015 and 2015/2016 growing seasons.

Communal land	**Small integral**	**Large integral**	**Rate of greenup**	**Rate of senescence**
2011/2012	1.731 ± 0.006^{e}	3.745 ± 0.016^{e}	19.213 ± 0.153^{c}	-27.123 ± 0.222^{b}
2012/2013	2.400 ± 0.010^{c}	5.228 ± 0.020^{b}	22.304 ± 0.207^{c}	-43.249 ± 0.186^{e}
2013/2014	3.117 ± 0.010^{b}	6.420 ± 0.026^{a}	14.620 ± 0.097^{d}	-29.911 ± 0.159^{c}
2014/2015	1.805 ± 0.007^{e}	4.387 ± 0.019^{d}	10.248 ± 0.188^{e}	-34.501 ± 0.226^{d}
2015/2016	2.076 ± 0.005^{d}	4.732 ± 0.014^{c}	27.061 ± 0.312^{a}	-42.458 ± 0.322^{e}
2016/2017	3.309 ± 0.010^{a}	5.36 ± 0.016^{b}	7.721 ± 0.041^{f}	-22.057 ± 0.102^{a}
Protected area	**Small integral**	**Large integral**	**Rate of greenup**	**Rate of senescence**
2011/2012	1.843 ± 0.006^{de}	3.94 ± 0.023^{f}	20.374 ± 0.121^{b}	-27.459 ± 0.463^{b}
2012/2013	2.331 ± 0.011^{c}	4.983 ± 0.022^{c}	18.174 ± 0.152^{c}	-40.395 ± 0.163^{d}
2013/2014	3.254 ± 0.011^{b}	6.465 ± 0.026^{a}	12.882 ± 0.193^{d}	-29.299 ± 0.173^{b}
2014/2015	1.796 ± 0.007^{e}	4.150 ± 0.015^{e}	8.357 ± 0.161^{e}	-32.309 ± 0.219^{c}
2015/2016	1.923 ± 0.005^{de}	4.413 ± 0.016^{d}	29.831 ± 0.341^{a}	-38.364 ± 0.202^{d}
2016/2017	3.460 ± 0.017^{a}	5.549 ± 0.017^{b}	7.239 ± 0.037^{e}	-19.592 ± 0.091^{a}

Enhanced Vegetation Index (EVI) related phenometrics

The flood year had higher overall maximum EVI, as well as minimum EVI for both the communal land and protected area (Table 2). The rate of greenup during the flood year was roughly 1.5 times faster than the second drought year in the protected area, the two rates only differed slightly in the communal land with the flood year greening up faster. The rates of senescence for both sides of the fence were slightly slower during the flood year for both communal land and protected area (Table 3). The small and large integrals were both larger during the flood year for both sites, indicating a 12% (protected area) and 10% (communal land) decrease in vegetation greenness and a 9% (communal land) and 8% (protected area) decrease in vegetation production from the flood year to the second drought year (Table 3).

3.3. 2012/2013 Flood year and 2014/2015 drought year

Time-related phenometrics

The protected area showed significant differences in all the phenometrics between the two drought years. The communal showed significant differences between the two drought years for all phenometrics apart from the Mid_T (Tables 1, 2, & 3). In the protected area the $Start_T$ of the second drought year was 51 days earlier than the first drought year, however, the End_T of the second drought year was only 18 days before the end of the first drought season, thus the second drought year had the longer growing season by 33 days. Likewise, in the communal land the second drought year started greening up 49 days before the first drought year. The first drought year ended ten days earlier compared to the second drought year, resulting in the second drought year experiencing a longer growing season by 38 days. Although the first drought year started later than the second drought year in the protected area, the $Peak_T$ was eight days earlier in the first drought year and the Mid_T was nine days earlier than in the second drought year. In the communal land the $Peak_T$ was also eight days earlier in the first drought year, yet the Mid_T were the same for the two growing seasons (Table 1, Figures 3 & 4).

Enhanced Vegetation Index (EVI) related phenometrics

The first drought year showed higher overall EVI, maximum, as well as minimum EVI for both the communal land and protected area (Table 2). In the protected area the rate of greenup of the first drought year was over 3.5 times faster than the rate of greenup of the second drought year, while in the communal land the first drought year greenup was 2.5 times quicker. The rates of senescence were slightly faster during the first drought year than the second drought year in both sites. The small integrals were very similar for the two drought years in the protected area, yet the second drought year showed a slightly greater value. The large integral for the protected area and the small and large integrals for the communal land were all larger in the second drought year, indicating a 4% (protected area) and 8% (communal land) increase in vegetation greenness and a 4% (communal land) and 5% (protected area) increase In vegetation production from the first drought year to the second drought year (Table 3).

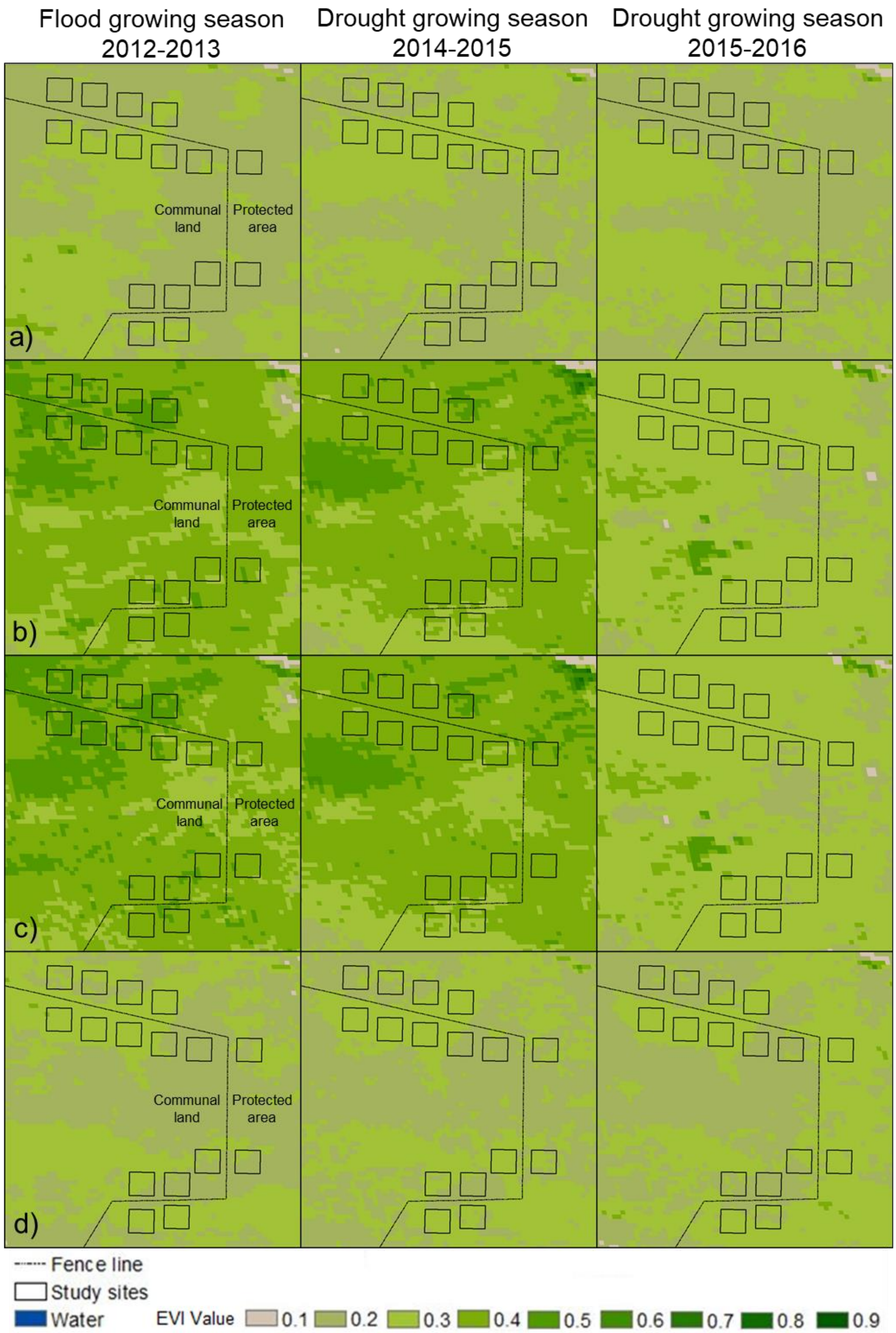

Figure 3: Enhanced Vegetation Index (EVI) images of (a) the start of the growing season ($Start_T$, Day of Year), (b) the peak time of the growing season ($Peak_T$, Day of Year), (c) the mid time of the growing season (Mid_T, Day of Year) and (d) the End_T of the growing season (End_T, Day of Year) for the flood year (2013) and the drought years (2014/2015 and 2015/2016) for both the communal land and protected area.

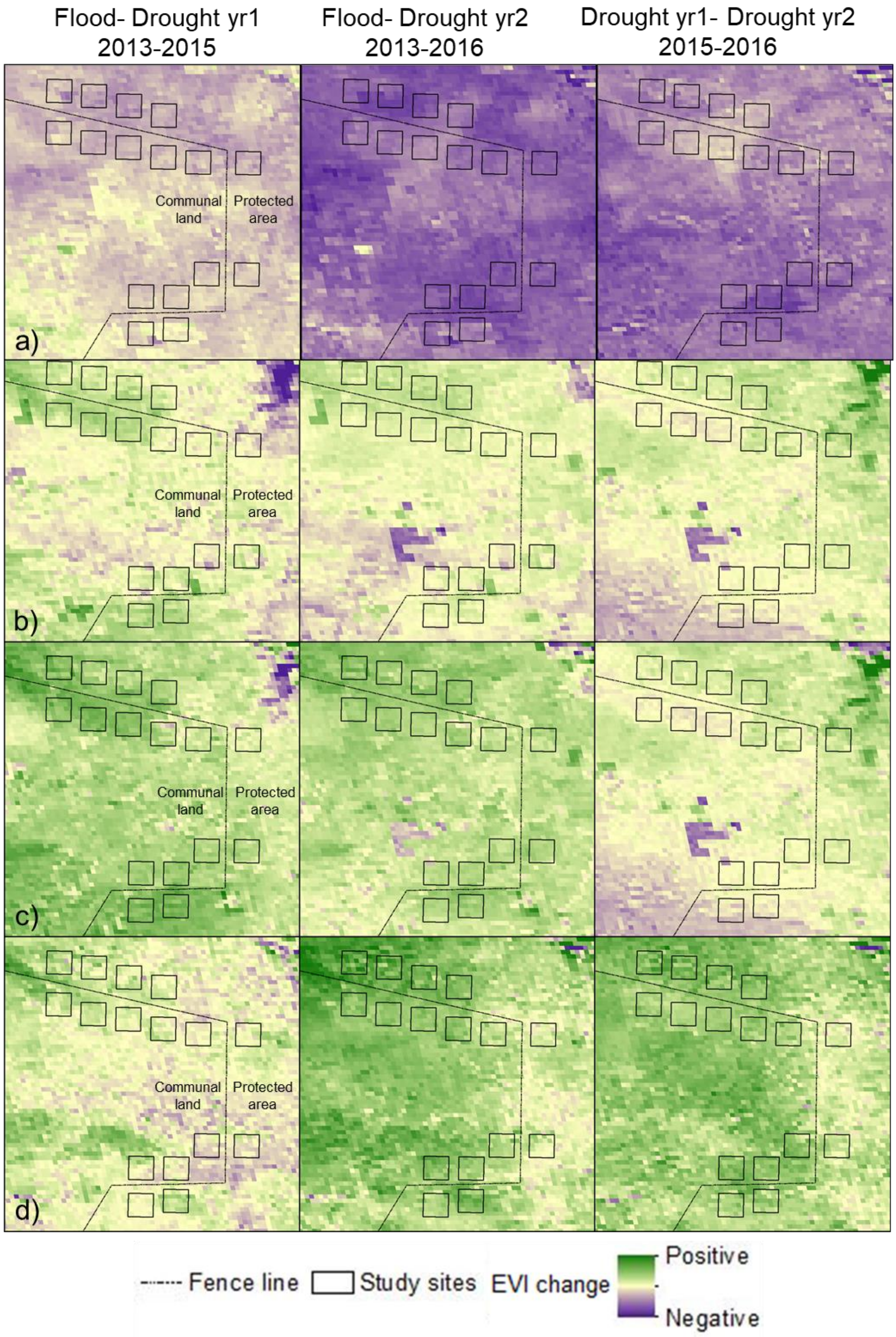

Figure 4: Enhanced Vegetation Index (EVI) images of the changes in EVI of (a) the start of the growing season ($Start_T$, Day of Year), (b) the peak time of the growing season ($Peak_T$, Day of Year), (c) the mid time of the growing season (Mid_T, Day of Year) and (d) the End_T of the growing season (End_T, Day of Year) between the flood year (2013) and both the drought

years (2014/2015 and 2015/2016) and between the two drought years (2014/2015 and 2015/2016) for both the communal land and protected area.

3.4 Response of vegetation to land use across six austral seasons

The various phenometrics were affected differently by land use, temporal change and the interaction between land use and temporal change. The differences in $Start_T$ and rate of greenup from the protected area and communal land across the six austral growing seasons were explained by temporal change and the interaction of the first four growing seasons with land use (Figures 5.1 and 5.3). The End_T differences between the two land use types across the six growing seasons was explained by land use, temporal change and the interations between land use and the 2011/2012, 2013/2014, 2014/2015, 2015/2016 and 2016/2017 growing seasons (Figure 5.1). The length of the growing seasons of both land use types across the six austral growing seasons was the only phenometric to be explained by all the independent variables. These are land use, temporal change and the interaction between the two (Figure 5.2). The differences in Mid_T and $Peak_T$ were explained by land use, temporal change and the interaction between the 2011/2012, 2012/2013, 2013/2014, 2014/2015, and 2016/2017 growing seasons and land use (Figures 5.1 and 5.2). For the small and large integrals land use, temporal change and the interactions between growing seasons 2012/2013, 2014/2015 and 2015/2016 with land use accounted for the differences between the communal land and protected area over the six growing seasons (Figure 5.2 and 5.3). The differences in the rate of senescence is explained by temporal change and the interaction of land use with growing seasons 2012/2013, 2014/2015 and 2015/2016 2016/2017 (Figure 5.3). Differences in maximum EVI were accounted for by temporal change, and the interaction between growing seasons 2014/2015 and 2015/2016 2016/2017 with land use. Lastly, the differences between the communal land and protected area over the six growing seasons for minimum EVI were explained by the 2015/2016 growing season and the interaction between land use and growing season two to five (Figure 5.4).

Response of vegetation to land use during seasons of extreme climatic events

The mixed effects models suggest that land use had a significant effect on the response of vegetation phenology during the flood year and the first drought year (Figures 5.1- 5.4). Only half of the phenometrics showed evidence of a difference in response between the communal land and protected area to the conditions of the second drought year. The minimum and maximum EVI generally showed no significant difference between the communal land and protected area over the three extreme growing seasons.

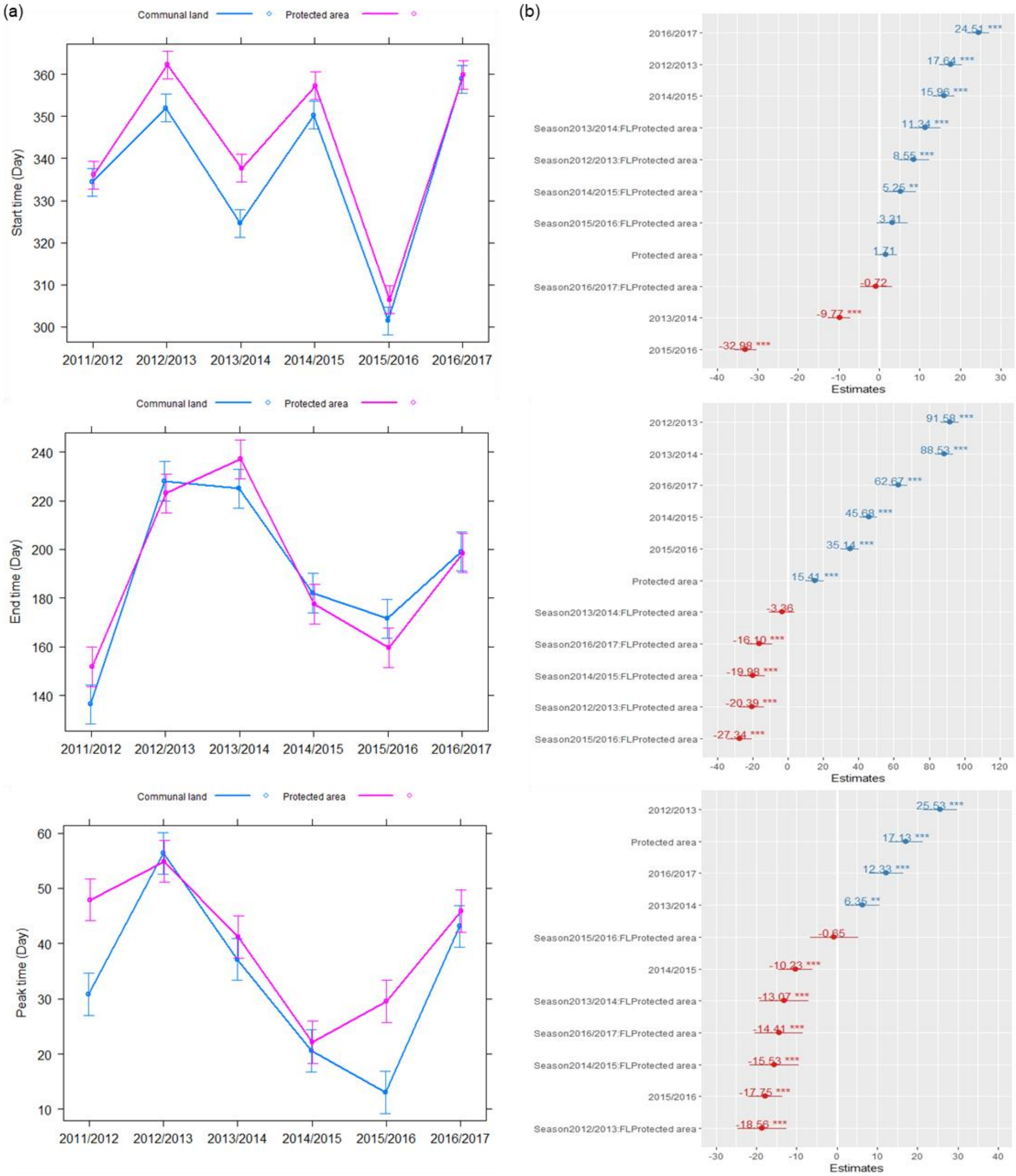

Figure 5.1: (a) Comparisons of the $Start_T$, End_T and $Peak_T$ between the protected area (pink) and communal lands (blue), for the six austral years (2011-2017), as well as (b) the marginal effects of the interaction terms from the linear mixed effects models for each of the phenometrics.

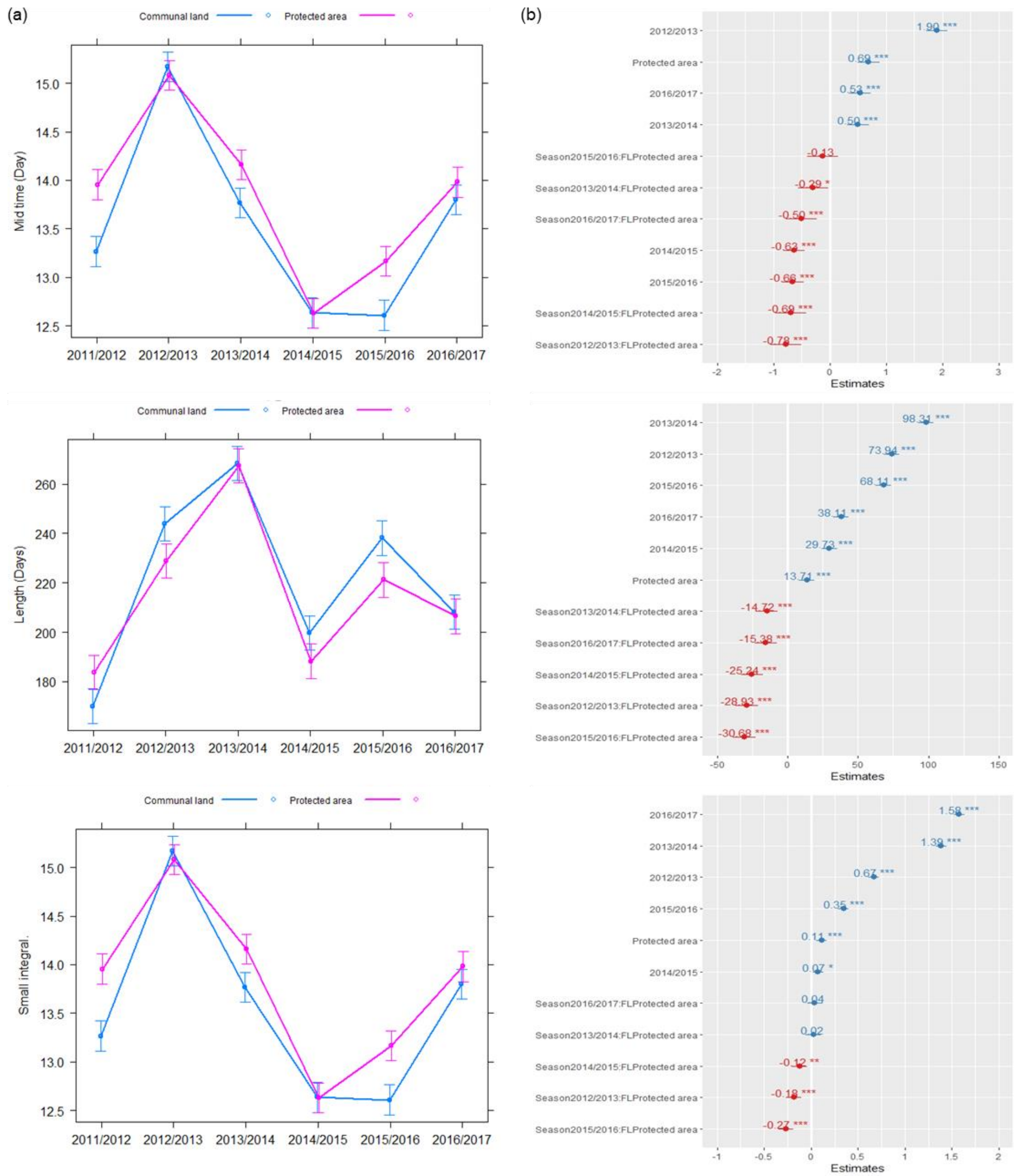

Figure 5.2: (a) Comparisons of the Mid_T, length and small integral between the protected area (pink) and communal lands (blue), for the six austral years (2011-2017), as well as (b) the marginal effects of the interaction terms from the linear mixed effects models for each of the phenometrics.

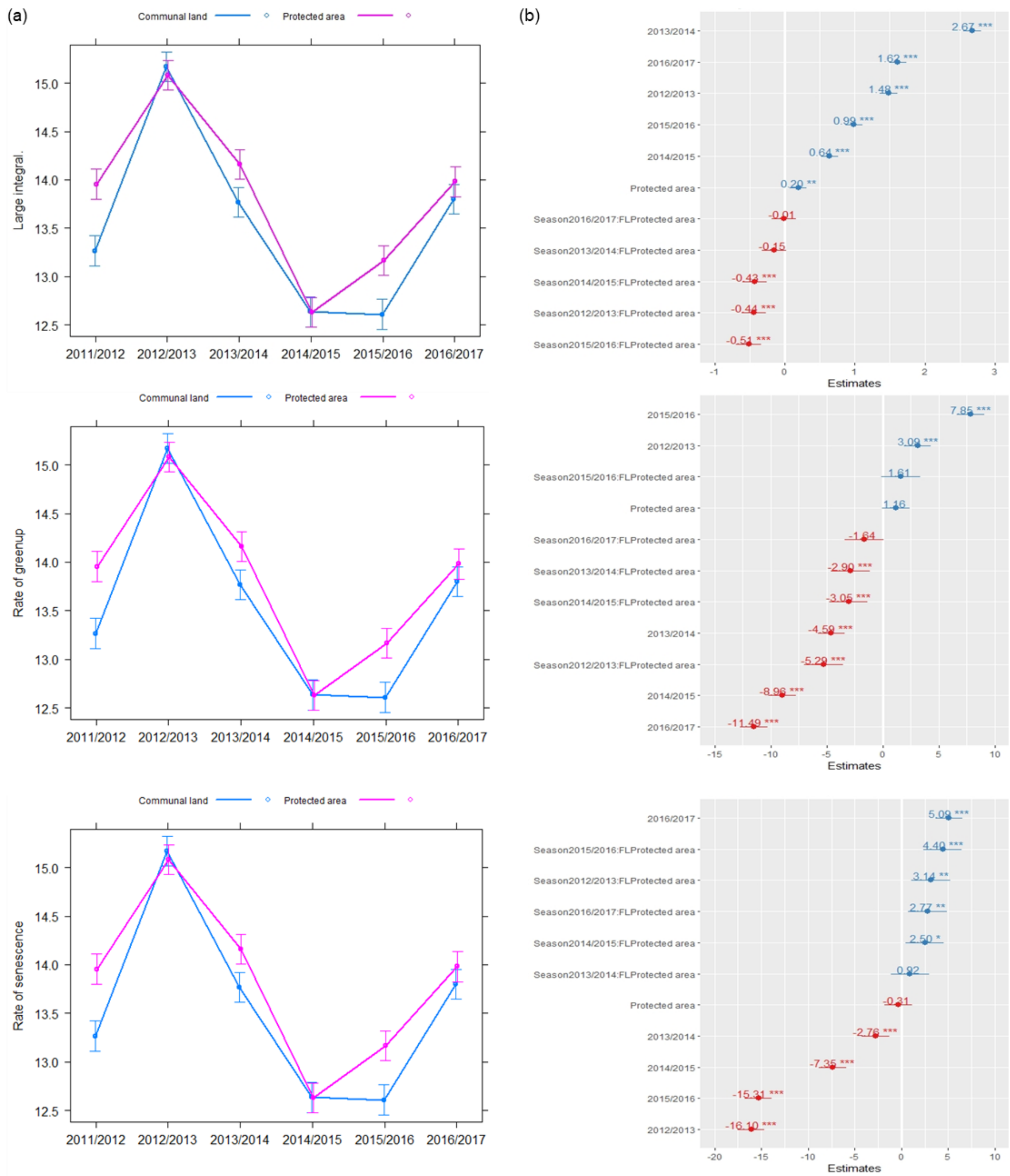

Figure 5.3: (a) Comparisons of the large integral, and rates of greenup and senescence between the protected area (pink) and communal lands (blue), for the six austral years (2011-2017), as well as (b) the marginal effects of the interaction terms from the linear mixed effects models for each of the phenometrics.

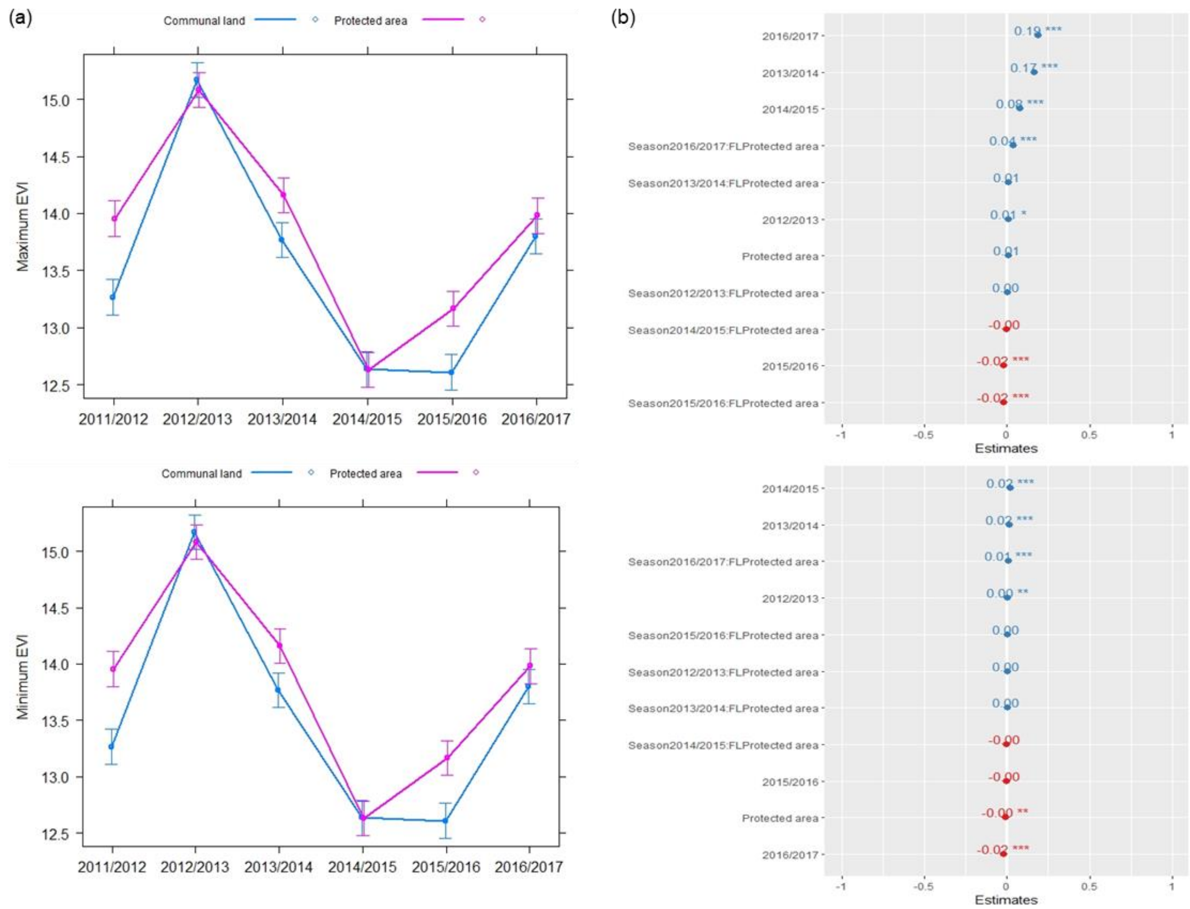

Figure 5.4: (a) Comparisons of the maximum and minimum EVI between the protected area (pink) and communal lands (blue), for the six austral years (2011-2017), as well as (b) the marginal effects of the interaction terms from the linear mixed effects models for each of the phenometrics.

3.5. Climatic effect

Rainfall

The seasonal rainfall patterns were highly variable across the growing seasons, even during years of lower rainfall (Figures 6 and 7). The flood year (2012/2013) experienced a seasonal total of over 750 mm, being nearly 200 mm greater than all the other years, more than 400 mm more than the first drought year (2014/2015) and roughly 450 mm more than the second drought year (2015/2016). The region normally receives between 300 – 500 mm of rain annually therefore the first drought year falls within the lower range for the area, while the second drought year barely falls within the total rainfall window for the area. The flood year is well above the average rainfall of the area (Figure 7).

The EVI values for both the protected area (R^2 = 0.180, P = 0.004,) and the communal land (R^2 = 0.190, P = 0.002) generally increased as the total seasonal rainfall increased (Figure 8). Although the relationship is weak, the EVI time series data had a lagged response to several of the rainfall peaks throughout the growing seasons (Figure 11). The 2011/2012, 2014/2015 (first drought year) and 2015/2016 (second drought year) growing seasons seem to have mid-season droughts, where there is a large drop in rainfall or in these cases there is no rainfall for one or two of the 23, 16-day composites on which the time series data is based. The flood year exhibited plateaued growth after the initial growing season increase, with the EVI showing no peak in growth which is not expected for a flood year. The rainfall from the flood event fell over roughly ten days, which should have allowed the vegetation in the area to greenup quickly proceeding this event. However, this growing season is the only growing season that was not apparently influenced by the peak in rainfall during the rainy season (Figure 9). Furthermore, the temperature and photoperiod data of this growing season exhibited no considerable difference to the data of the other growing seasons to explain the lack of a peak in EVI compared to the other growing seasons (Figure 9). When comparing the effect of rainfall on EVI outside of the flood season, a stronger relationship was observed (R^2 = 0.206, P = 0.002) (Figure S1).

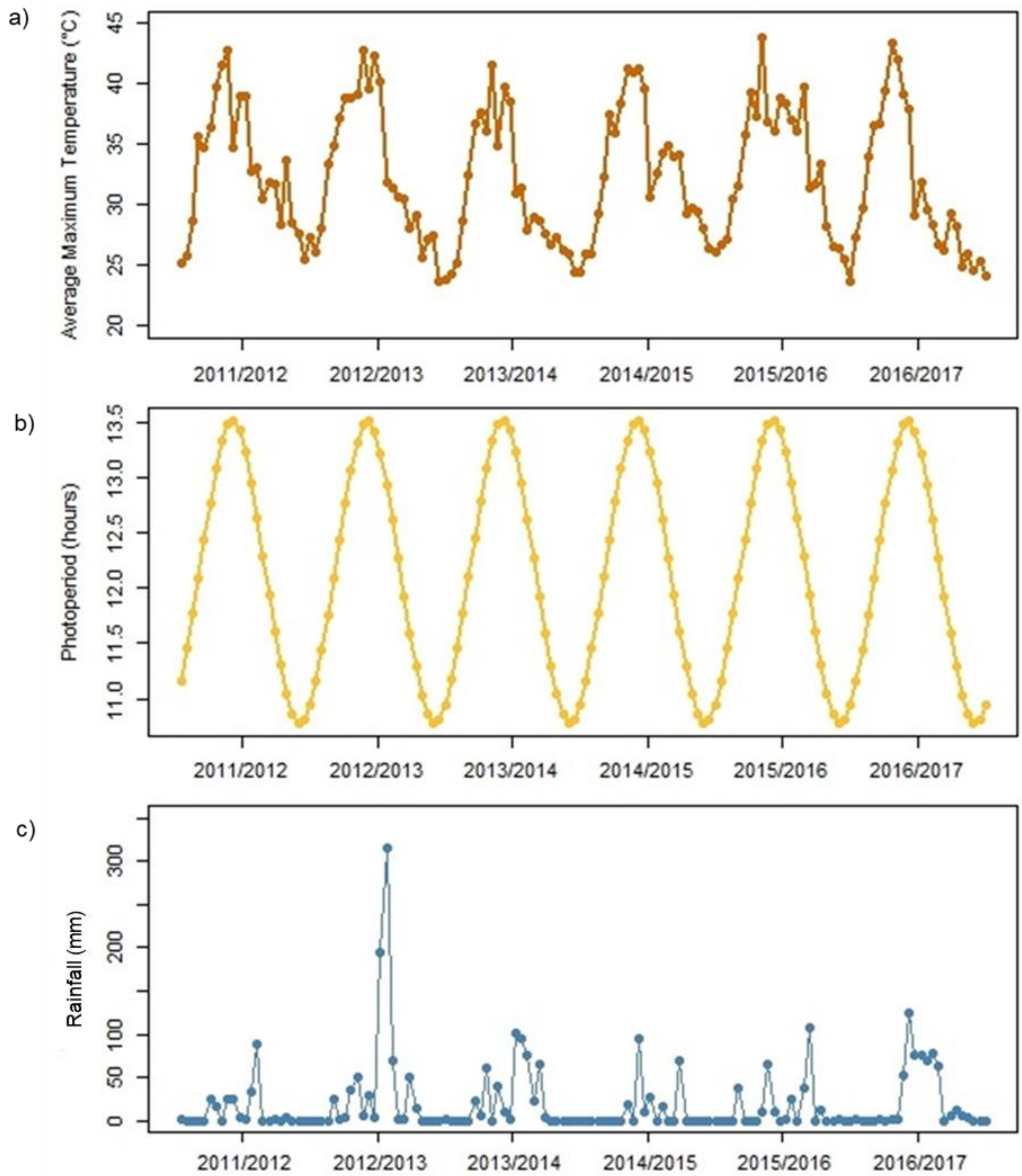

Figure 6: Seasonal curves of the 16-day average a) maximum surface temperature, b) photoperiod, and c) rainfall for the six growing seasons, based on the 23, 16-day composites. Each growing season is comprised of 23, 16-day composite days which correspond to those of the Enhanced Vegetation Index (EVI) datasets.

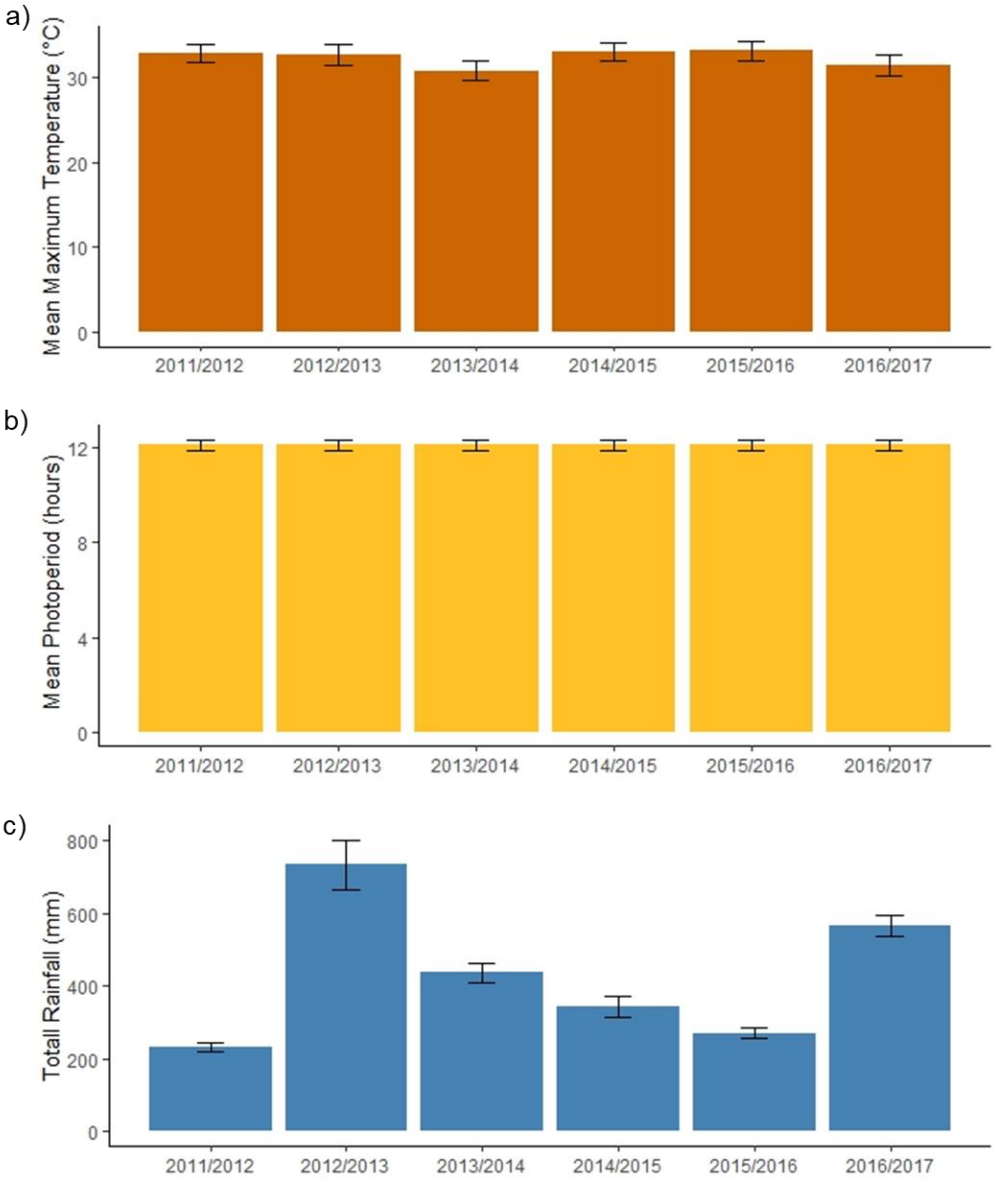

Figure 7: a) Mean ± SE maximum surface temperature, b) mean ± SE photoperiod, and c) total ± SE rainfall for the six growing seasons based on the 23, 16-day composites.

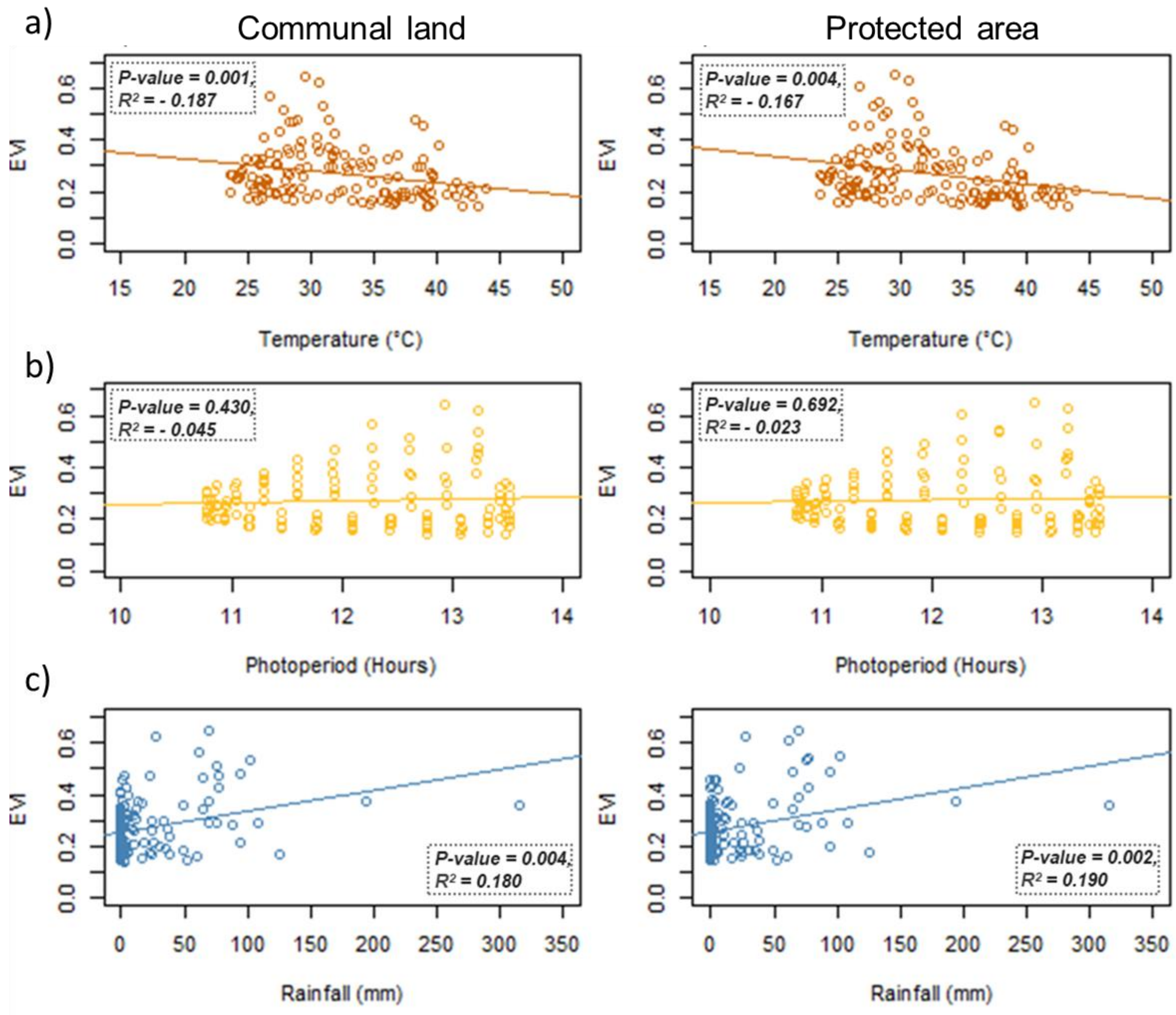

Figure 8: The relationship between Enhanced Vegetation Index (EVI) and a) average temperature; b) photoperiod; and c) rainfall for the six growing seasons based on the 16-day composites.

All the time-related phenometrics of the protected area showed strong positive relationships with the total seasonal rainfall (Figure 11). Generally, time-related phenometrics of the communal land also showed strong positive relationships with the total seasonal rainfall. The $Start_T$ in the communal land, however, showed a moderate positive relationship (Figure 12). Generally, the greater the seasonal rainfall the later the $Start_T$, End_T, $Peak_T$ and Mid_T and longer the growing season. The small and large integrals of both sites also showed a strong positive relationship with total rainfall, indicating that there is greater seasonally active vegetation and more standing biomass with more rainfall. The EVI values in the protected area showed a moderate relationship with total rainfall, and the remaining phenometrics exhibited weak relationships with total rainfall, with the minimum EVI and rates of senescence showing a negative relationship. The remaining EVI related phenometrics in the communal land had similar relationships with the total rainfall, however, all the relationships were weak. The majority of the phenometrics on both sides of the fence were not significantly correlated with total rainfall, but this is likely due to the small number of replicates being compared (Figures 11 and 12).

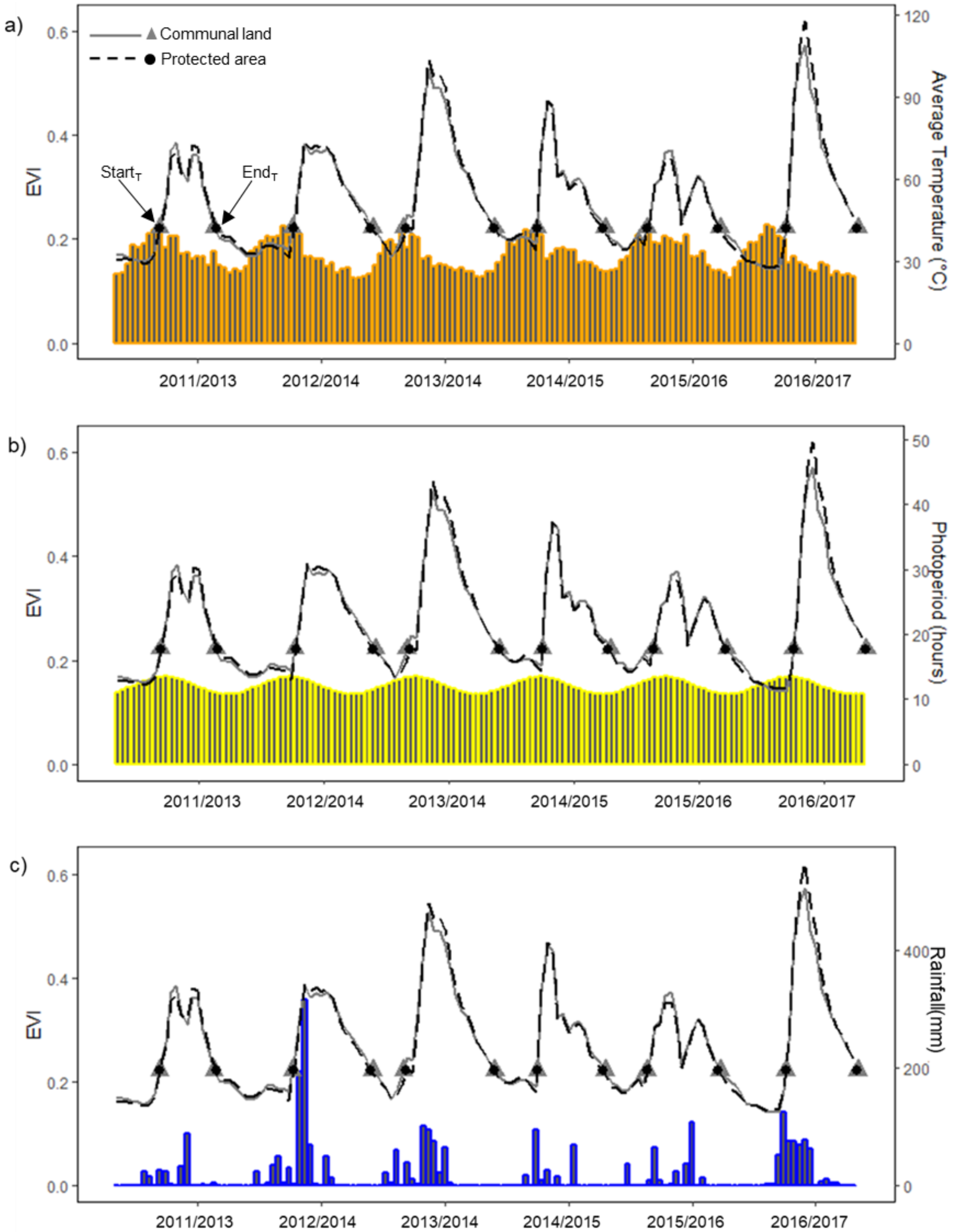

Figure 9: Smoothed Enhanced Vegetation Index (EVI) (line curves) and $Start_T$ and End_T of the growing seasons with the a) average temperature; b) photoperiod; and c) rainfall for the six growing seasons. Each growing season is comprised of 23, 16-day composite days which correspond to those of the EVI datasets.

The flood year only started greenup 65 days and 55 days after the onset of rainfall in the protected area and communal land respectively. The first drought year commenced greenup 12 days after the onset of rainfall in the protected area and 5 days after in the communal land. The second drought year was the only growing season to exhibit early greenup, prior to the rains. This growing season started 23 days prior in the protected area and 18 days prior in the communal land (Table 2). Neither the protected area (R^2 = - 0.006, P = 0.991) or communal land (R^2 = - 0.146, P = 0.783) $Start_T$ was correlated with the onset of rainfall times (Figure 10).

Table 4: Comparison of total seasonal rainfall for each austral year from 2011-2017 and the dates of rainfall onset with the start of greenup ($Start_T$), between the protected area (PA) and the communal land (CL), with the difference in days between $Start_T$ and rainfall onset. A negative difference is indicative of the $Start_T$ occurring before the onset of rainfall.

Growing season	**Communal land $Start_T$**	**Protected area $Start_T$**	**Rainfall onset**	**Onset-$Start_T$ (PA)**	**Onset-$Start_T$ (CL)**	**Total seasonal rainfall (mm)**
2011/2012	30 Nov (334)	02 Dec (336)	23 Nov (327)	-9	-7	221.1
2012/2013	17 Dec (352)	27 Dec (362)	23 Oct (297)	-65	-55	772.0
2013/2014	21 Nov (325)	04 Dec (338)	22 Oct (295)	-43	-30	481.5
2014/2015	16 Dec (350)	23 Dec (357)	11 Dec (345)	-12	-5	234.5
2015/2016	28 Oct (301)	02 Nov (306)	20 Nov (324)	18	23	269.5
2016/2017	24 Dec (359)	25 Dec (360)	24 Nov (329)	-31	-30	566.0

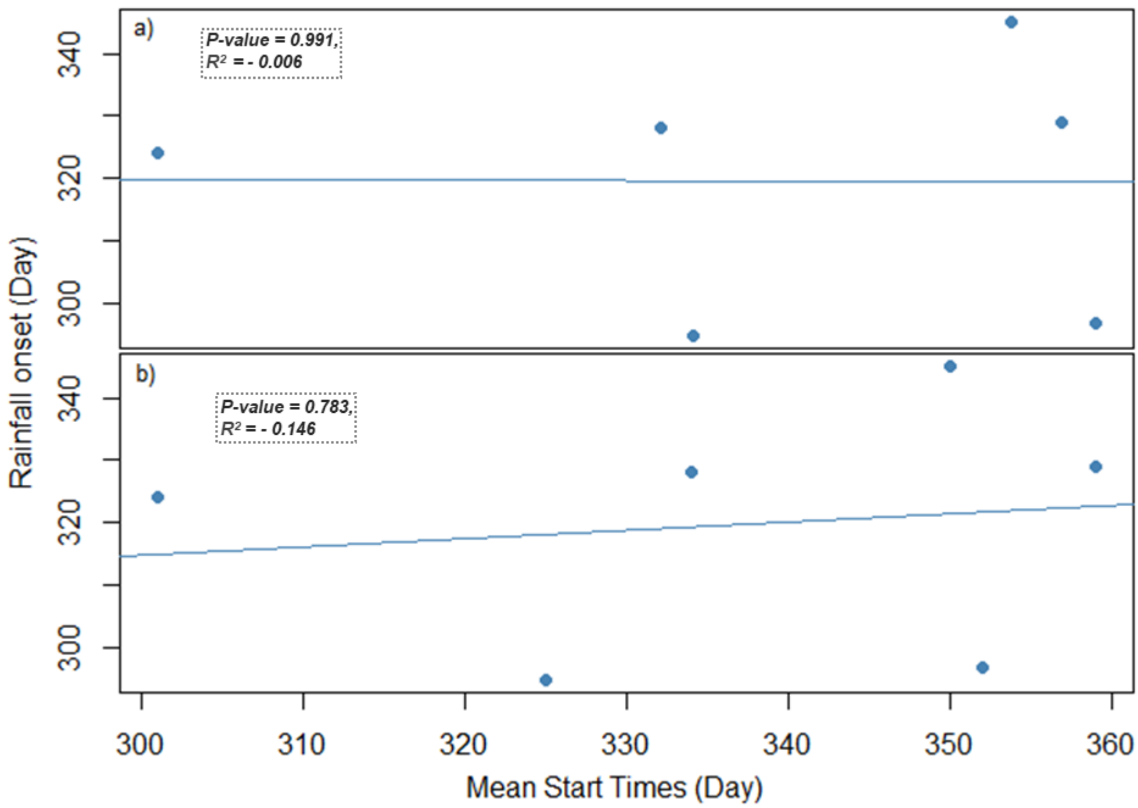

Figure 10: The relationships between the timing of the onset of rainfall and the start of greenup for a) the protected area and b) the communal land.

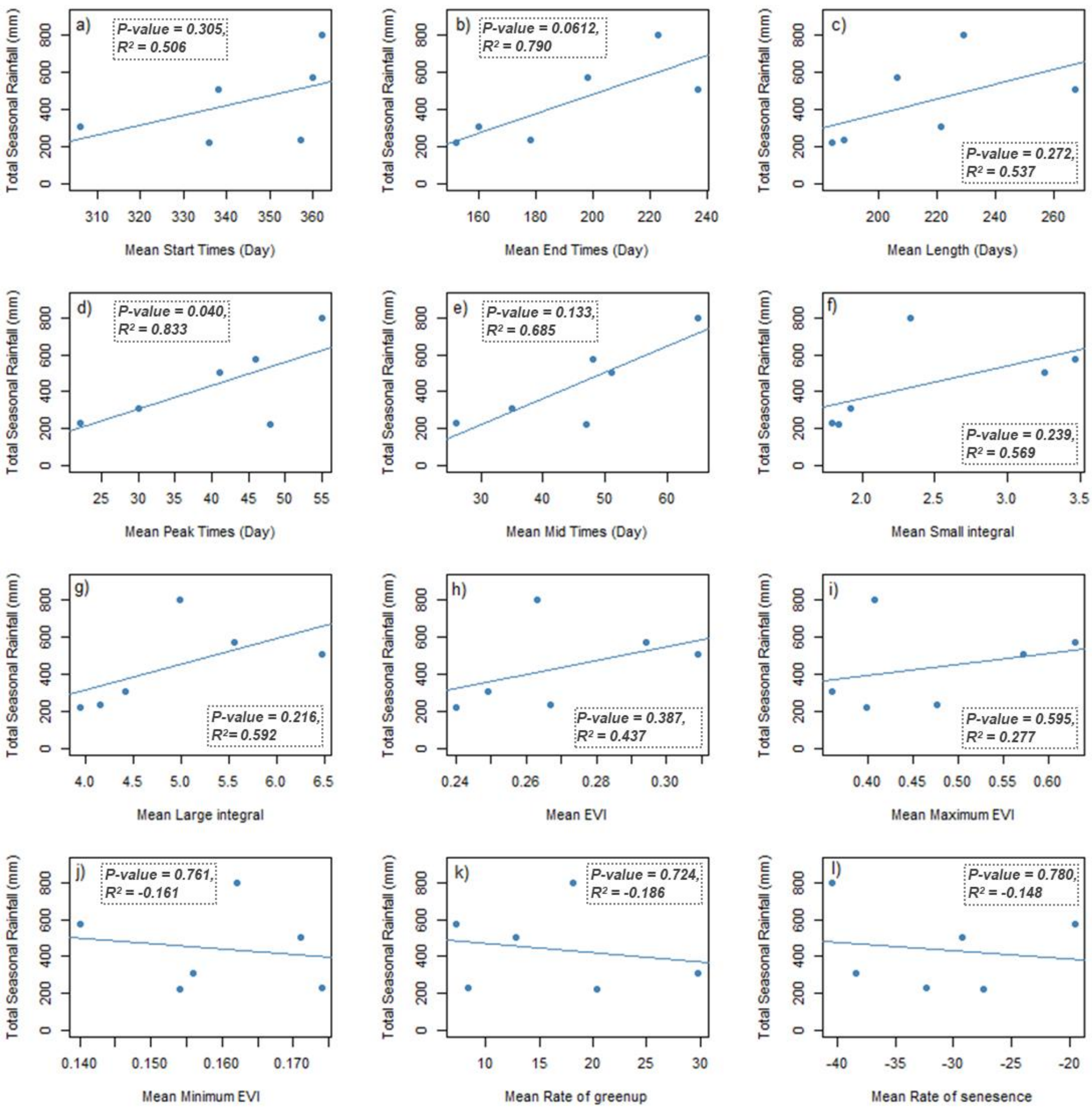

Figure 11: For the protected area: The relationships between the total seasonal rainfall and a) start time ($Start_T$) of the growing seasons, b) end time (End_T) of the growing seasons, c) length of the growing seasons, d) peak time ($Peak_T$) of the growing seasons, e) mid time (Mid_T) of the growing seasons, f) small integral (seasonally active vegetation), g) large integral (standing crop or proxy for vegetation production), h) EVI, i) maximum EVI ,j) minimum EVI, k) rate of greenup, and l) rate of senescence.

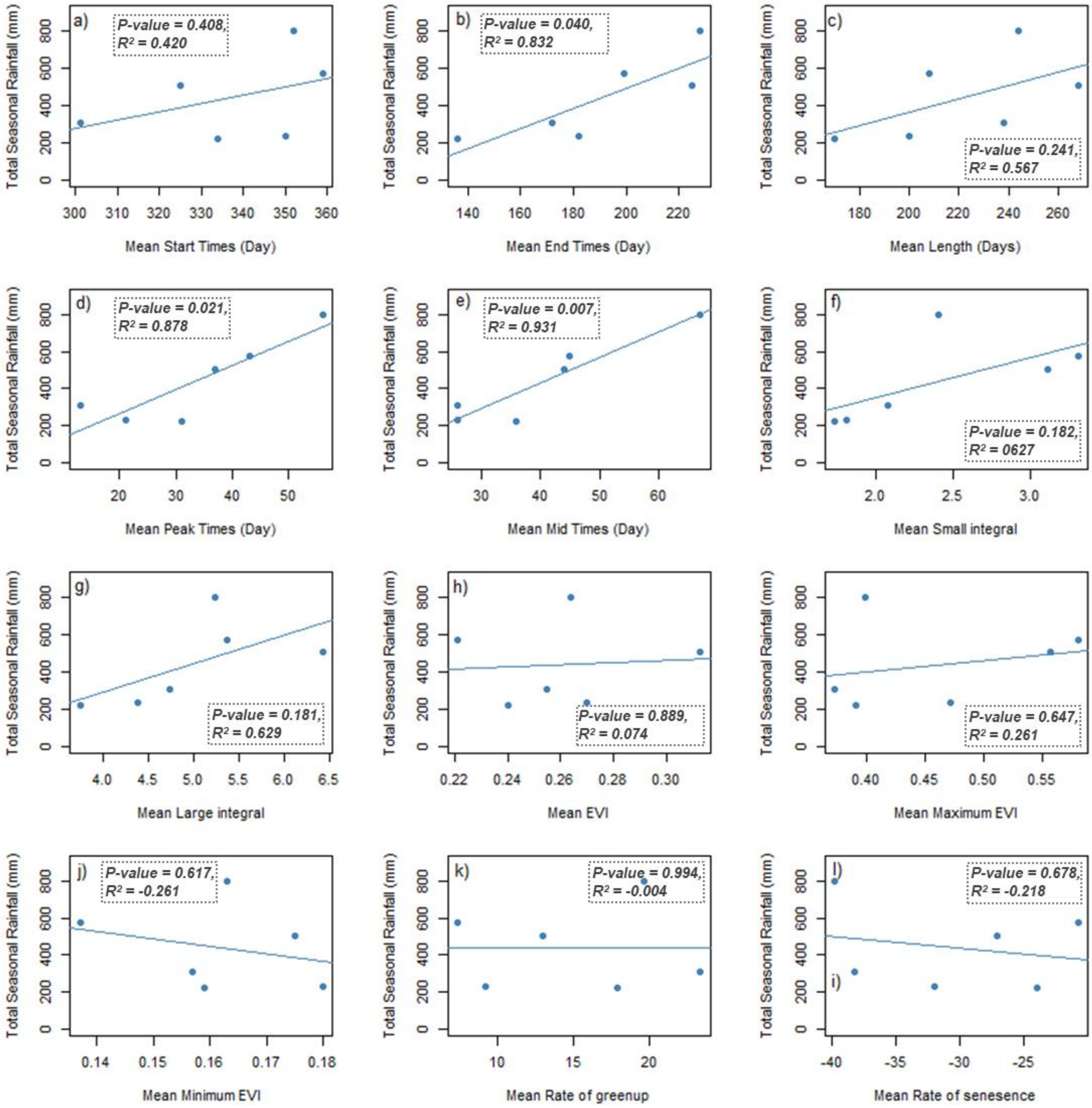

Figure 12: For the communal land: The relationships between the total seasonal rainfall and a) start time ($Start_T$) of the growing seasons, b) end time (End_T) of the growing seasons, c) length of the growing seasons, d) peak time ($Peak_T$) of the growing seasons, e) mid time (Mid_T) of the growing seasons, f) small integral (seasonally active vegetation), g) large integral (standing crop or proxy for vegetation production), h) EVI, i) maximum EVI ,j) minimum EVI, k) rate of greenup, and l) rate of senescence.

Cloud cover

The lack of a peak in EVI for the 2012/2013 flood year is very likely due to the cloud cover that brought the high rainfall over the time during which the peak should have occurred, while the remaining five growing seasons had minimal cloud cover during the time that the peak EVI was detected (Figure 13, Figure S4).

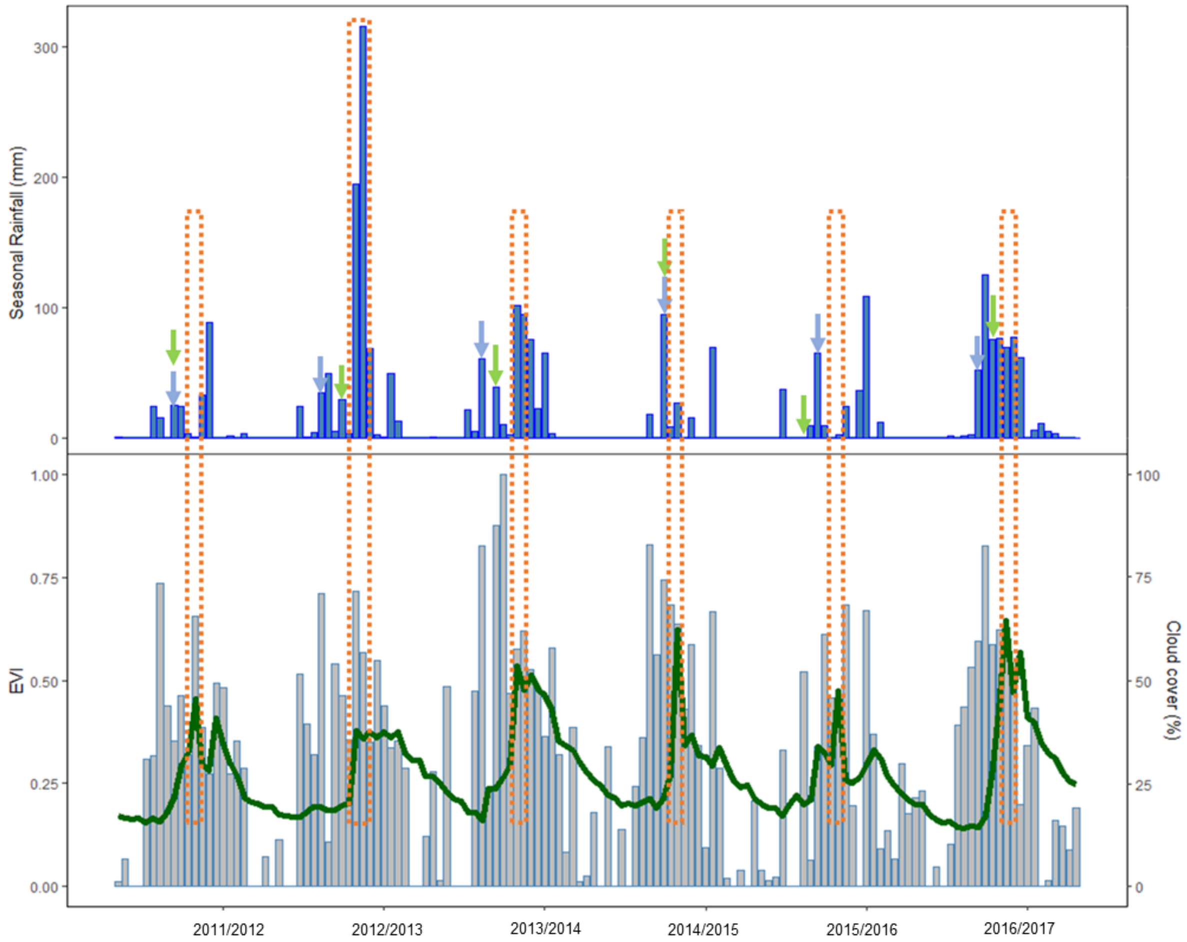

Figure 13: Median cloud cover (grey bars), Enhanced Vegetation Index (EVI) (green line) and rainfall (blue bars) across the six growing seasons (2011-2017) highlighting the correspondence of EVI peaks with low cloud cover for seasons one and three to six, while the flood year (2012/2013) shows high cloud cover over the time of the expected peak in EVI. Blue arrows indicate the onset of rainfall and green arrows indicate the start of the growing season.

Temperature

Although the maximum land surface temperatures deviate from the trends of the maximum temperatures obtained from Punda Maria by between 5°C - 10°C from about September, all the estimated temperatures have a strong correlation to the original temperatures (S2 and S3). The maximum land surface temperature and Punda Maria maximum temperatures follow a very similar trend, until September when the two trends deviate slightly (Figure 14). The maximum temperature and EVI had very weak relationships for the protected area (R^2 = -0.187, p = 0.001) and the communal land (R^2 = -0.167, p = 0.004) (Figure 8).The average maximum temperature was greatest during the second drought year, this growing season was half a degree warmer than the flood year. The first drought year had the second highest temperature and was 0.35°C warmer than the flood year.

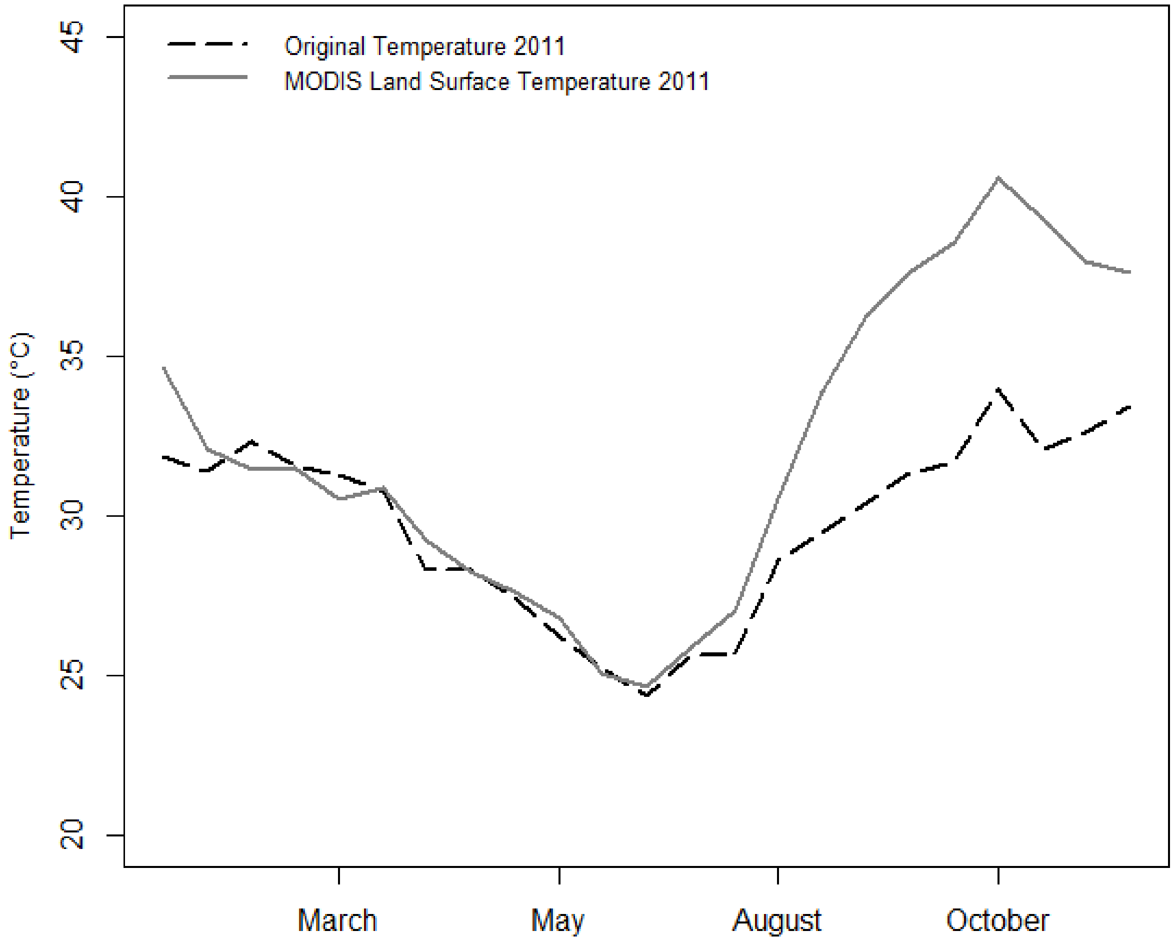

Figure 14: The mean seasonal trends of the maximum temperature obtained from Punda Maria (original temperature) and the maximum land surface temperature of the study extent in 2011.

Photoperiod

The photoperiod exhibits the typical seasonal fluctuations (Figure 9), with the means only differing by a few minutes between the growing seasons, consequently photoperiod has a negligible effect on EVI for both sites (protected area (R^2 = - 0.045, p = 0.430) and communal land (R^2 = - 0.023, p = 0.692)) (Figure 8).

4. Discussion

4.1. Vegetation response to extreme climatic events

Time-related phenometrics

The timing of the onset of the growing seasons occurred after the onset of rainfall for five out of the six growing seasons. However, this study showed no relationship between the $Start_T$ and the rainfall onset, with the $Start_T$ dates ranging from late October to late December in the communal land and early November to late December in the protected area. *Colophospermum mopane, Combretum apiculatum* and *Terminalia sericea* are prominent woody species in the northern sites while *T. sericea, C. apiculatum, Burkea. africana* and *Kirkia acuminata* are dominant woody species in the southern sites. *Combretum apiculatum* and *T. sericea* are common dominant species for both the northern and southern sites. Of these five dominant species across the study sites, *C. mopane, T. sericea* and *B. africana* have the potential to green-up independently of rainfall (Childes 1988, Dekker and Smit 1996, Whitecross *et al.* 2017a, Masia *et al.* 2018), whereas, *C. apiculatum* and *K. acuminata* are reliant on rainfall before the initial leaf flush (Dekker and Smit 1996, Masia *et al.* 2018). The varying phenologies between these prominent species are likely why there was no obvious pattern in green-up and rainfall. However, the amount and distribution of rainfall experienced during the previous growing season influence the timing of the spring flush.

The length of the growing season is central in determining the primary productivity (Eamus 1999, Higgins *et al.* 2011) and as this study found, is largely influenced by rainfall (Odekunle 2004, Mugalavai *et al.* 2008, Oguntunde *et al.* 2014). The 2014/2015 drought year had the second lowest mean seasonal rainfall of the extreme years and the shortest growing season. There would have been less water and nutrients available which would have been depleted sooner (Augustine and McNaughton 2006), especially after the season experienced a rapid greenup rate and high peak in EVI shortly after the onset of greenup. The growing season of the 2015/2016 drought year was only a few days shorter than that of the flood year, due to the rainfall in March 2016 which would have allowed the growing season to extend slightly. Typically, trees respond to an increase in water availability by either flushing earlier or maintaining leaves longer into the dry season (Myers *et al.* 1998, Lobo *et al.* 2008, Stevens *et al.* 2016).

EVI related phenometrics

Stevens *et al.* (2016) conducted a study on facultative deciduousness of *C.mopane*, and found that watered and unwatered plants aged differently. Watered trees continued to photosynthesise at a high rate well into the dry season, while the unwatered trees photosynthesised until the leaves were dropped in the dry season. Additionally, Childes (1988) found leaf drop of many semi-arid savanna trees, including *B. africana* and *T. sericea,* to depend on available soil moisture. Delayed leaf drop would increase the length of the growing season as well as productivity. This was evident from the results of the small and large integrals for which the flood year showed the greatest values, indicating more seasonally or photosynthetically active vegetation and greater vegetation productivity.

Interestingly, the flood year's growing season did not exhibit the expected peak in EVI. This lack of a major EVI peak is more likely because of the peak not being detected by the MODIS satellite due to the high cloud cover rather than the event not occurring. There is evidence of missing or degraded MODIS time series data caused by atmospheric conditions (Poggio *et al.* 2012). An important difference to note when comparing the flood year to the remaining seasons is that the peaks in EVI for the remaining growing seasons coincide with low cloud cover. This would have also affected the estimation of the start of the flood year's growing season as well as the rate of greenup. Even though the $Start_T$ of the flood year may not be a true representation of the actual initiation and the rate of greenup, the flood year still experienced the longest growing season as the End_T of the flood year's growing season was considerably later than those of the drought years, providing a slower rate of senescence. The above average rainfall would have resulted in this increase in vegetation growth and delay in leaf drop for this season.

4.2. Climatic drivers of EVI

Typically, the phenology of southern African savannas is determined by rainfall and temperature (Cubasch *et al.* 2001, Jolly and Running 2004, Cleland *et al.* 2007, Chambers *et al.* 2013, Jin *et al.* 2013). As expected, photoperiod had no notable effect on EVI, however, significant, but weak relationships between EVI and rainfall and EVI and maximum temperature were not expected. Chidumayo (2001) assessed phenology of mopane dominated savannas and woodlands in response to rainfall and minimum and maximum temperature at multiple sites in Zambia and Botswana. Some of the sites within Zambia showed insignificant relationships between rainfall and EVI, while the remaining sites as well as the mopane sites in Botswana showed significant, but mostly weak interactions. However, the relationships between EVI and maximum temperature for all but one of the mopane dominated sites in both countries showed similar weak, R^2 trends, as was found in this study. A clearly important aspect which was not conducted for this study, was to assess what the effect of the interaction of the climatic variables had on the EVI, as the Chidumayo (2001) study found the interaction of rainfall, minimum and maximum temperature to significantly and strongly affect EVI across all of the mopane dominated sites for both Zambia and Botswana.

4.3. Vegetation phenology response to land use under conditions associated with flooding and drought events

Although the phenometrics suggested that land use had a significant effect on the response of vegetation phenology during the flood year and the first drought year (Figures 5.1- 5.4), most of the phenometrics had similar magnitudes of response in the communal land and protected area, overall indicating similar responses to the extreme events (Tables 1,2 and 3). The $Start_T$, $Peak_T$ and Mid_T were the only phenometrics to show differences in magnitude between the communal land and protected area, suggesting significantly different responses in the communal land and protected area of these phenometrics to the flood year and first drought year. Similar responses were found by Romo-Leon *et al.* (2016) and Kariyeva *et al.* (2012), where both studies found the time-related phenometrics, as well as the small integral to show different magnitudes of response by the different land use types to environmental conditions.

4.4. Overall impacts of the 2013 flood and 2014-2016 drought

The semi-arid regions of South Africa are naturally drought prone (Gibberd 1996). Extreme droughts that persist over several years occur due to the co-occurrence of an El Niño event (Baudoin *et al.* 2017). El Niños return at least once within a ten-year period globally (Rouault and Richard 2005). In South Africa, the severe droughts of 1982-1983, 1991-1993 and 2014-2016 were due to the combined effects of a typical drought and a strong El Niño event (Baudoin *et al.* 2017). When the EVI and phenometrics were compared across all six growing seasons, the short-term effects of the 2014-2016 drought was not as severe as was expected. Even at a national scale the drought of 2014-2016 was not as severe as the droughts experienced in the early 1980s and 1990s (Swemmer *et al.* 2018). However, for some regions of South Africa the 2014-2016 drought was as severe as the 1992-1995 drought (Baudoin *et al.* 2017) and was classified as one of the worst droughts in 23 years (Vogel and van Zyl 2016). The regions of South Africa that were classified as experiencing “extreme drought” included the western part of the Western Cape (WC), northern Eastern Cape (EC), northern Kwa-Zulu Natal (KZN), northern Free State (FS) and northern Mpumalanga (MP) (Swemmer *et al.* 2018). Many of these regions are still grappling with the effects of this drought, and as most of these regions are agricultural regions that specialise in grain (WC and FS), cattle (FS and KZN) and subsistence farming (EC), the detrimental economic knock-on effect has been noted (Waldner *et al.* 2017). One of the worst hit regions in South Africa was northern Mpumalanga. This area does not consist of agricultural land, but incorporates the southern half of the Kruger National Park as well as supporting 7.8% of the South African population (Statistics South Africa 2016). The management approaches in Kruger were altered after the 1991-1993 drought. This included the closing of artificial waterholes, removal of fences between KNP and neighbouring protected areas and ending of culling of buffalo, hippo, and elephants. This would have resulted in a different distribution of animals and forage resources, particularly in areas far from water sources (Swemmer *et al.* 2018), such as areas in the northern section of the park. Buffalo tended to migrate to the northern section of the park, where the drought was less severe. Thus, the population only declined by 26% in the latest drought compared to the 48% during the 1991-93 drought. Conversely, hippo populations in the Kruger National Park suffered a 45% mortality as they were restricted by water sources (Swemmer *et al.* 2018).

Although the 2013 flood caused minimal loss in South Africa, it was devastating in central and southern Mozambique. The study area of this study falls within the Limpopo river basin (Sitoe *et al.* 2015), and within this catchment area two extreme flood events have occurred in the last 20 years. These floods occurred in February- March 2000 and mid-January 2013, the flood on which this study is focused (Sitoe *et al.* 2015). Both floods occurred during La Niña episodes, however, the 2000 flood was caused by an anomalous lower tropospheric cyclone, called Eline, which resulted in the increased rainfall (Sitoe *et al.* 2015, Hoell and Cheng 2018). The 2013 flood however, was as a result of the combination of various atmospheric systems including the La Niña episode along with tropical temperate troughs (TTT), which strengthened the South Indian Converge Zone (SICZ) leading to the increased rainfall (Manhique *et al.* 2015). These extreme floods have resulted in a strain on food and livestock production in the areas affected, and threaten food security as the people living within these regions are still predominantly reliant on agriculture and livestock farming (Brida *et al.* 2013). Although flooding of the Luvuvhu river (the river running through the study area) would have occurred, there is no evidence of great loss within the focus area and overall the 2013 flood only led to a positive vegetation response due to the high rainfall that fell across the ten days in January.

4.5. Looking ahead

Colophospermum mopane is known to be a drought resilient species (Dekker and Smit 1996, Styles and Skinner 1997, Veenendaal *et al.* 2004) and recruitment and growth of larger trees during droughts have been documented (O’Connor 1998). Thus, the high EVI yielded by the drought years is understandable. Furthermore, *C. mopane* will take advantage of sufficient rainfall events to capitalise on growth (February *et al.* 2013). This is evident in the lagged response of the seasonal peaks in EVI to the larger rainfall events within the growing seasons, particularly in the EVI peak shortly after the rainfall experienced in March 2016. However, many of the other dominant trees in the study area are not as drought resilient, particularly *T. sericea* and *B. africana,* and large stands of trees are prone to die-off during severe drought (Parry 1989).

The resilience of *C. mopane* to drought conditions may lead to the distribution of the species spreading south with the increase in global temperatures and frequency of severe droughts. At high densities *C. mopane* can suppress the herbaceous layer (Smit and Rethman 1998, Smit 2005) and can outcompete many other woody species as it is a mono-dominant species, often leading to low species diversity (Mapaure 1994). Areas where *C. mopane* have outcompeted the herbaceous layer may be susceptible to soil erosion and have the potential to become less fertile (Thompson 1960). Although the decrease in soil fertility is not always the case within a mopane-dominated savanna, the spread of this species into areas focused on agriculture may become an issue in future.

5. Conclusion

EVI was not as strongly influenced by rainfall as originally expected (protected area: R^2 = 0.180; communal land: R^2 = 0.190), however, the phenometrics derived from EVI were far more sensitive to changes in water availability. As expected, the flood year had the longest growing season (protected area: 229 days; communal land: 244 days), with the greatest vegetation productivity (flood year to first drought year: protected area =13% decrease; communal land= 13% decrease, p<0.05; flood year to second drought year: protected area= 9% decrease; communal land= 8% decrease, p<0.05) even though the $Start_T$ and peak EVI were most likely inaccurate due to the presence of high cloud cover during the flood year's growing season. Overall the drought was not as severe when the vegetation dynamics were compared across the six growing seasons. Land use only had a significant effect on the response of $Start_T$, $Peak_T$ and Mid_T to the climatic conditions of the flood year and the first drought year.

Monitoring phenological changes in response to extreme climatic events allows one to observe and predict responses of various systems during this period of rapid environmental change. Using remote sensing platforms to assess and monitor the effect of climate change on vegetation on small scale and localised studies, such as this one, provide more detailed insight on how rural communities and conservation areas respond to extreme events and may help to further predict the occurrences of extreme flooding and drought events in the future (Cleland *et al.* 2007, Chambers *et al.* 2013, Fitchett *et al.* 2015) and aid in the establishment of better strategies to combat the negative effects of climate change. These strategies may be in the form of adaptive farming or management practices or plans to alleviate the resultant ecological and sociological issues. Assessing how extreme climatic events affect phenological patterns will also add to the understanding of how changes in phenological patterns may influence the greater ecosystem of not only semi-arid savannas in southern Africa, but similar systems globally.

6. Appendix

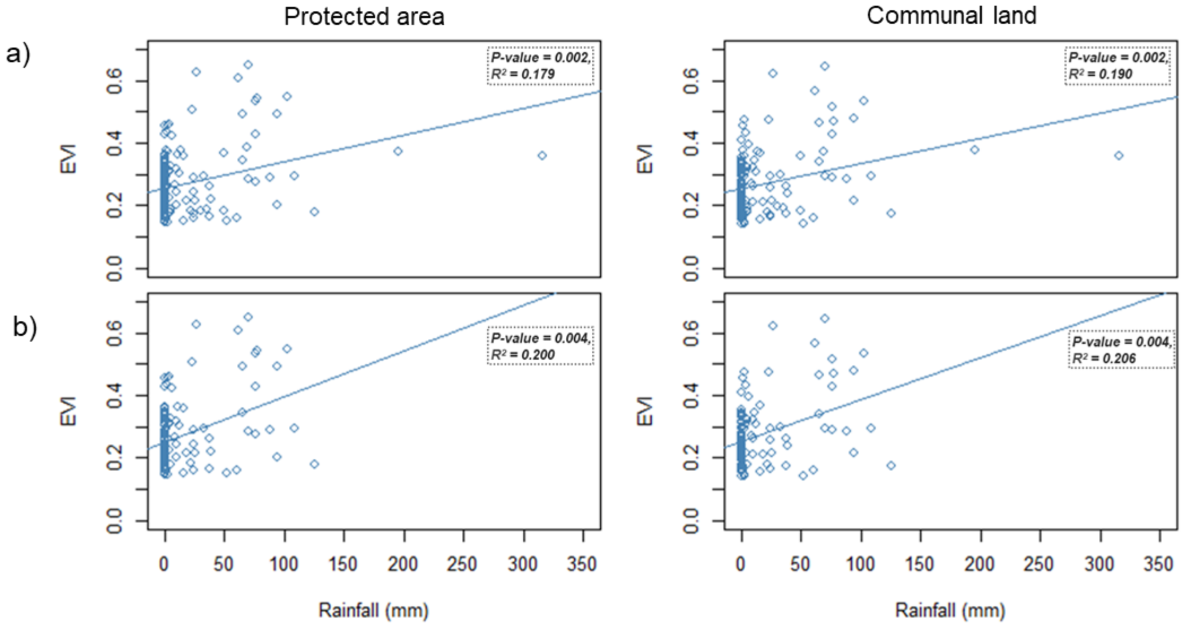

Figure S1: A comparison of the relationship between Enhanced Vegetation Index (EVI) and the 16-day total rainfall a) with all the growing seasons and b) without the flood year growing season (2012/2013).

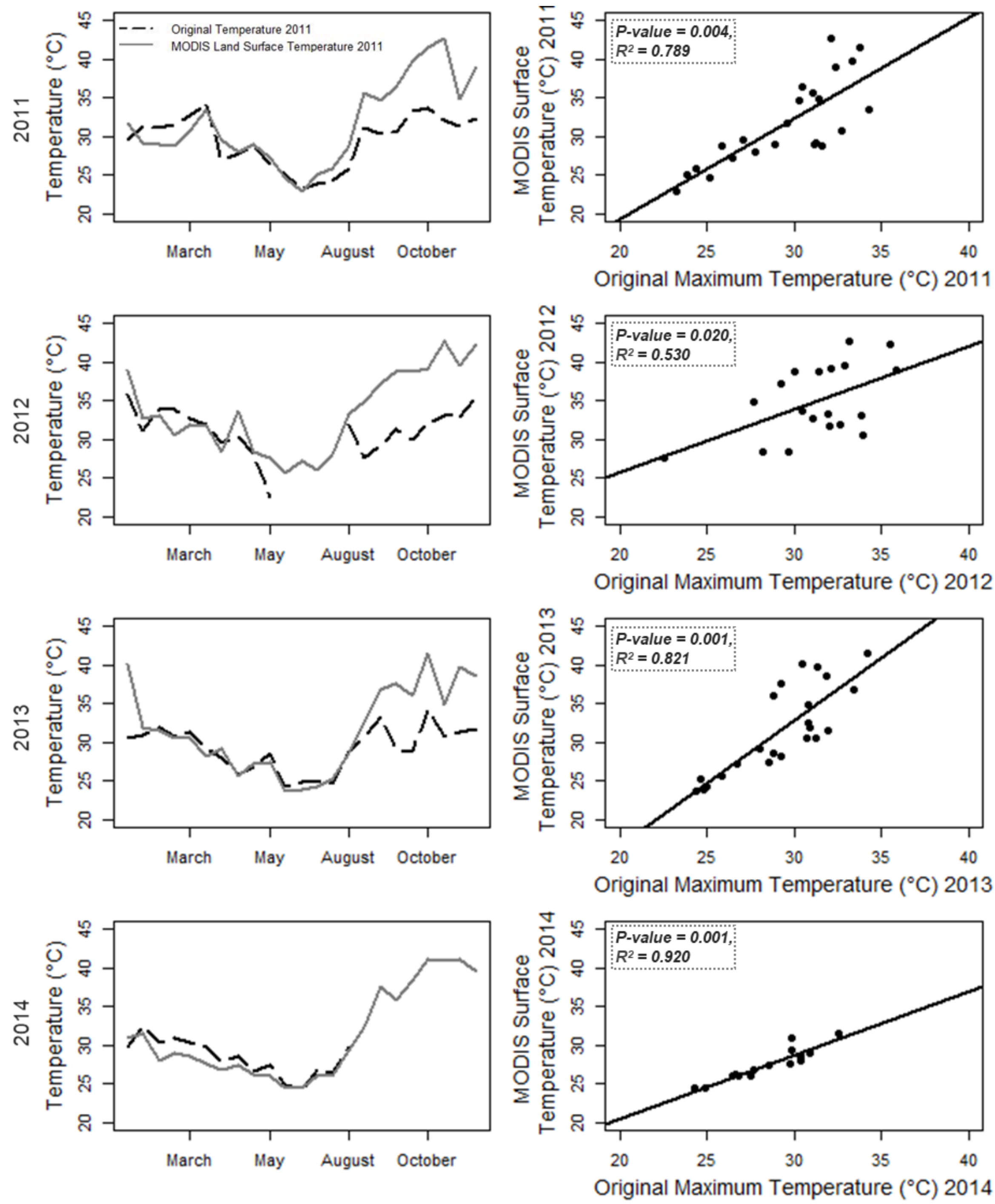

Figure S2: Seasonal trends of the maximum temperature obtained from Punda Maria (original temperature) and the maximum land surface temperature of the study extent and correlation of the two temperature datasets for 2011-2014

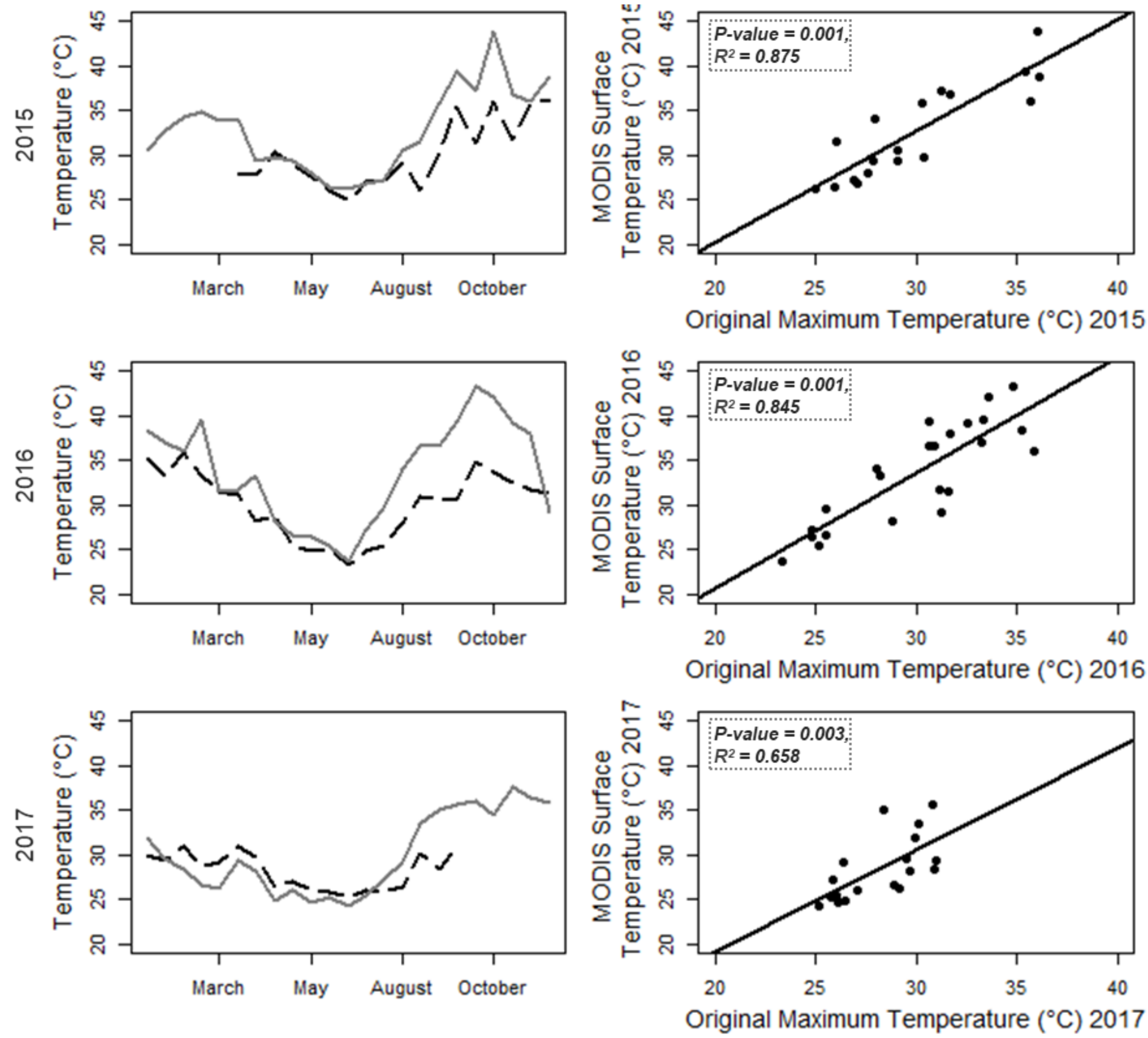

Figure S3: Seasonal trends of the maximum temperature obtained from Punda Maria (original temperature) and the maximum land surface temperature of the study extent and correlation of the two temperature datasets for 2015-2017

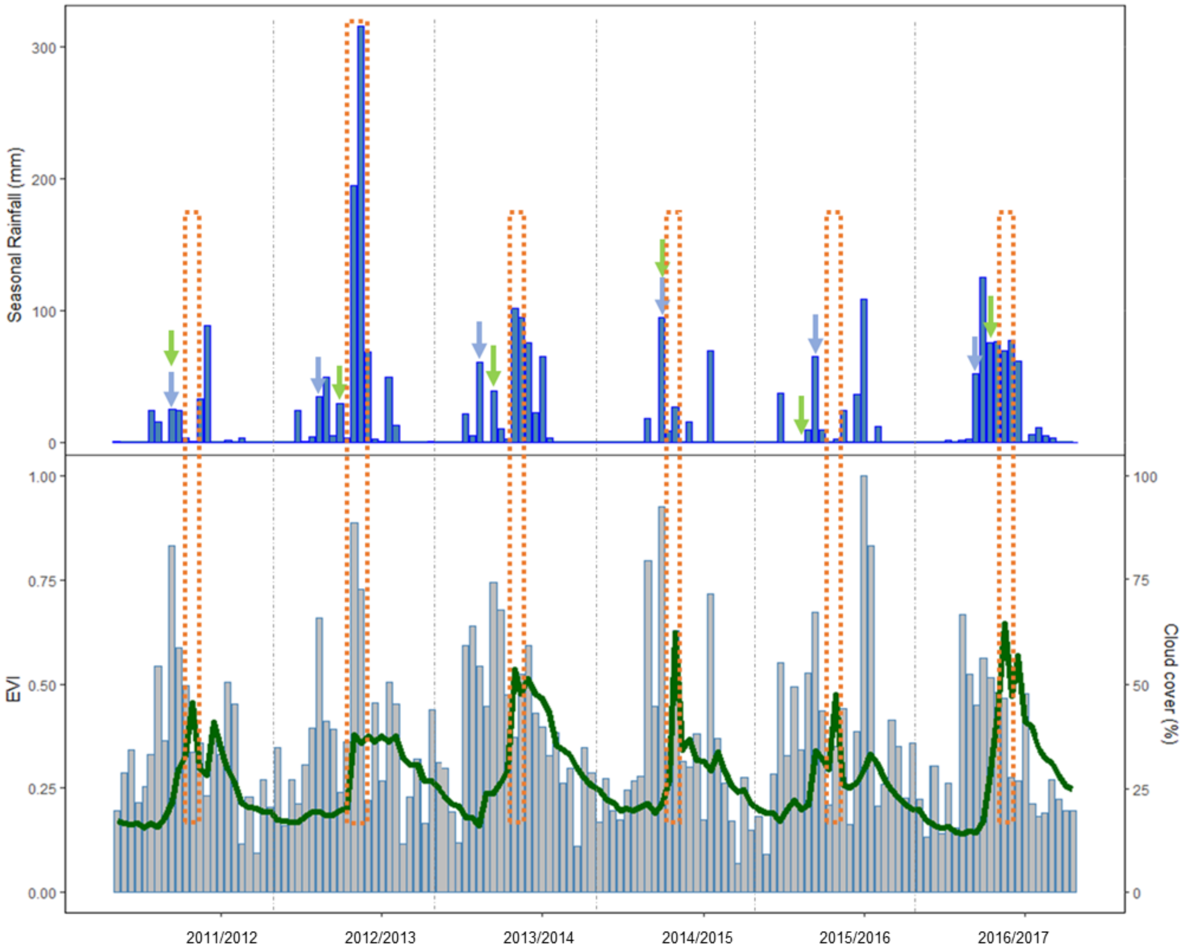

Figure S4: Maximum cloud cover, Enhanced Vegetation Index (EVI) and rainfall across the six growing seasons (2011-2017) highlighting the correspondence of EVI peaks with low cloud cover for seasons one and three to six, the flood year (season two) shows high cloud cover over the time of the expected peak in EVI. Blue arrows indicate the onset of rainfall and green arrows indicate the start of the growing season

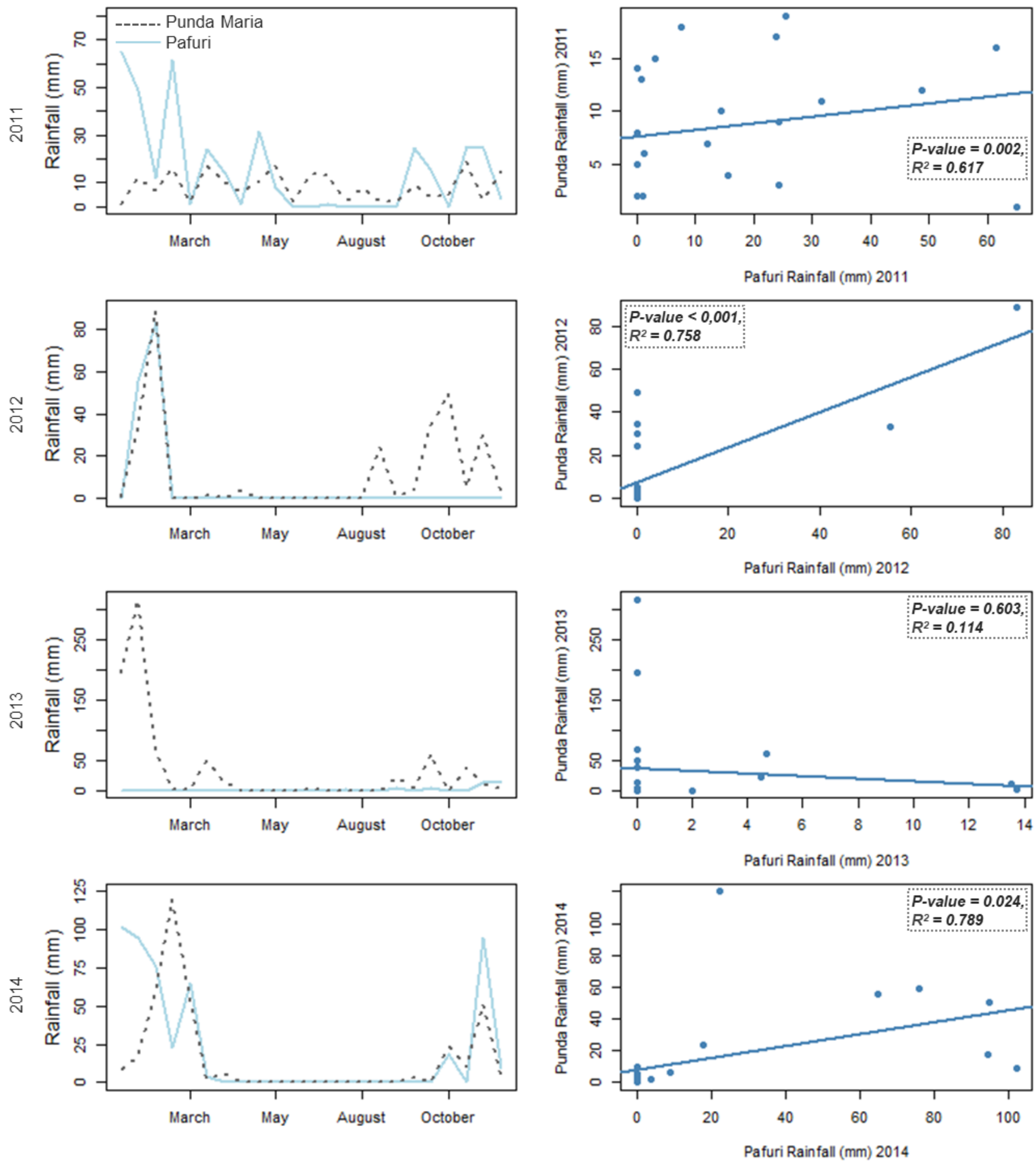

Figure S5: Seasonal trends of rainfall obtained for Pafuri (original data) and Punda Maria for the study extent and correlation of the two rainfall datasets for 2011-2014 to determine if Punda Maria's daily rainfall would be a viable supplement for the incomplete 2012 and 2013 daily rainfall for Pafuri.

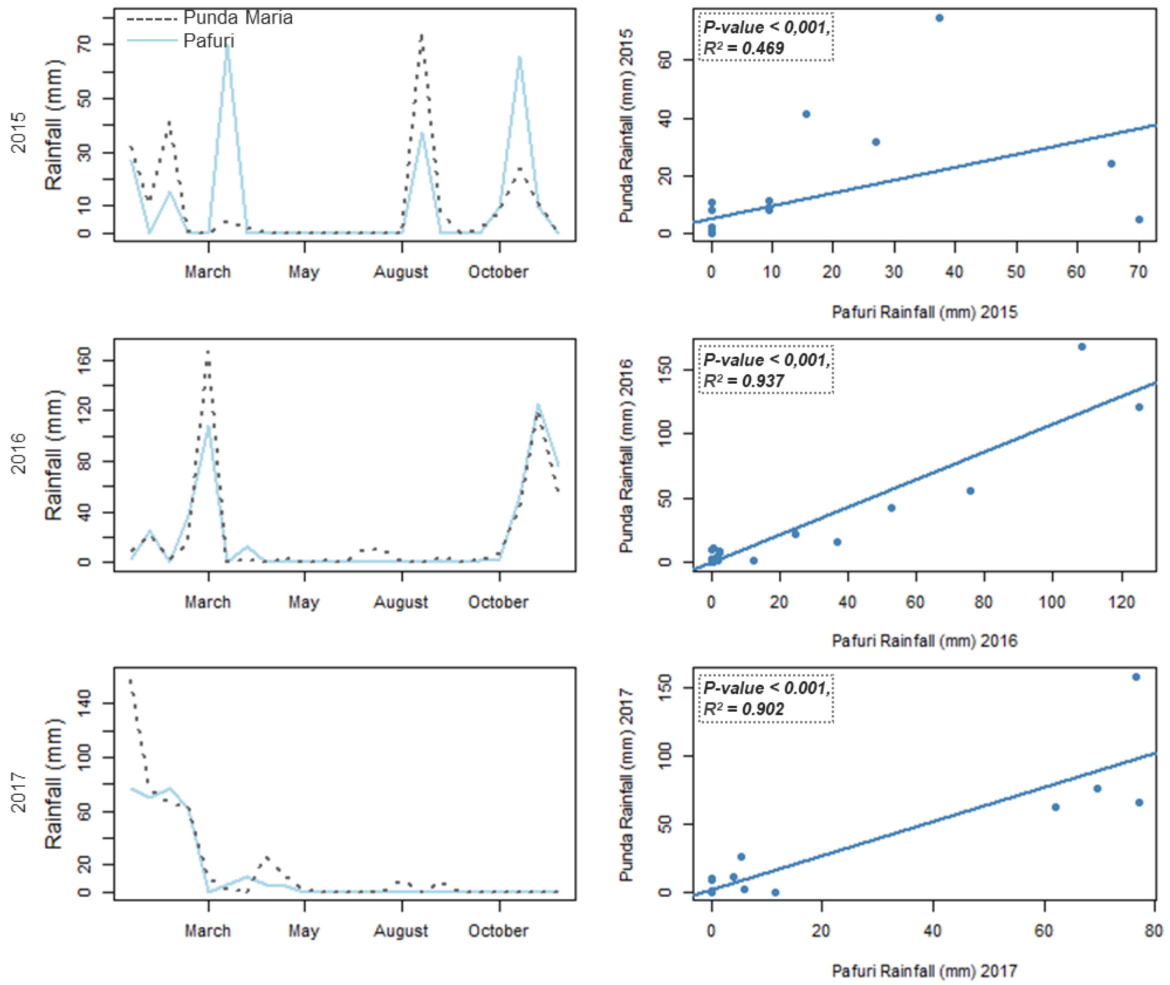

Figure S6: Seasonal trends of rainfall obtained for Pafuri (original data) and Punda Maria for the study extent and correlation of the two rainfall datasets for 2015-2017 to determine if Punda Maria's daily rainfall would be a viable supplement for the incomplete 2012 and 2013 daily rainfall for Pafuri.

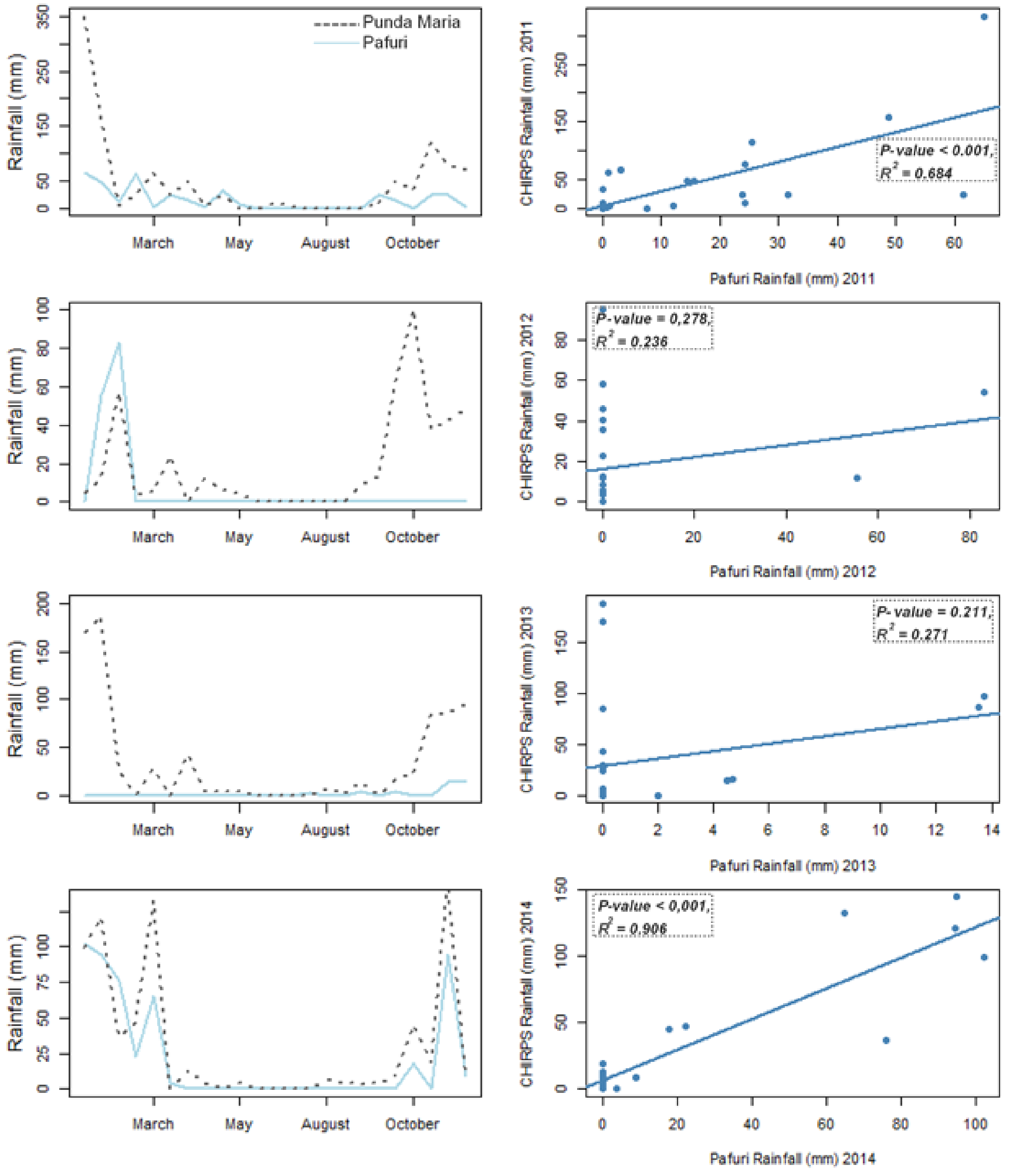

Figure S7: Seasonal trends of rainfall obtained from Pafuri (original data) and CHIRPS for the study extent and correlation of the two rainfall datasets for 2011-2014 to determine if the CHIRPS daily rainfall would be a viable supplement for the incomplete 2012 and 2013 daily rainfall for Pafuri.

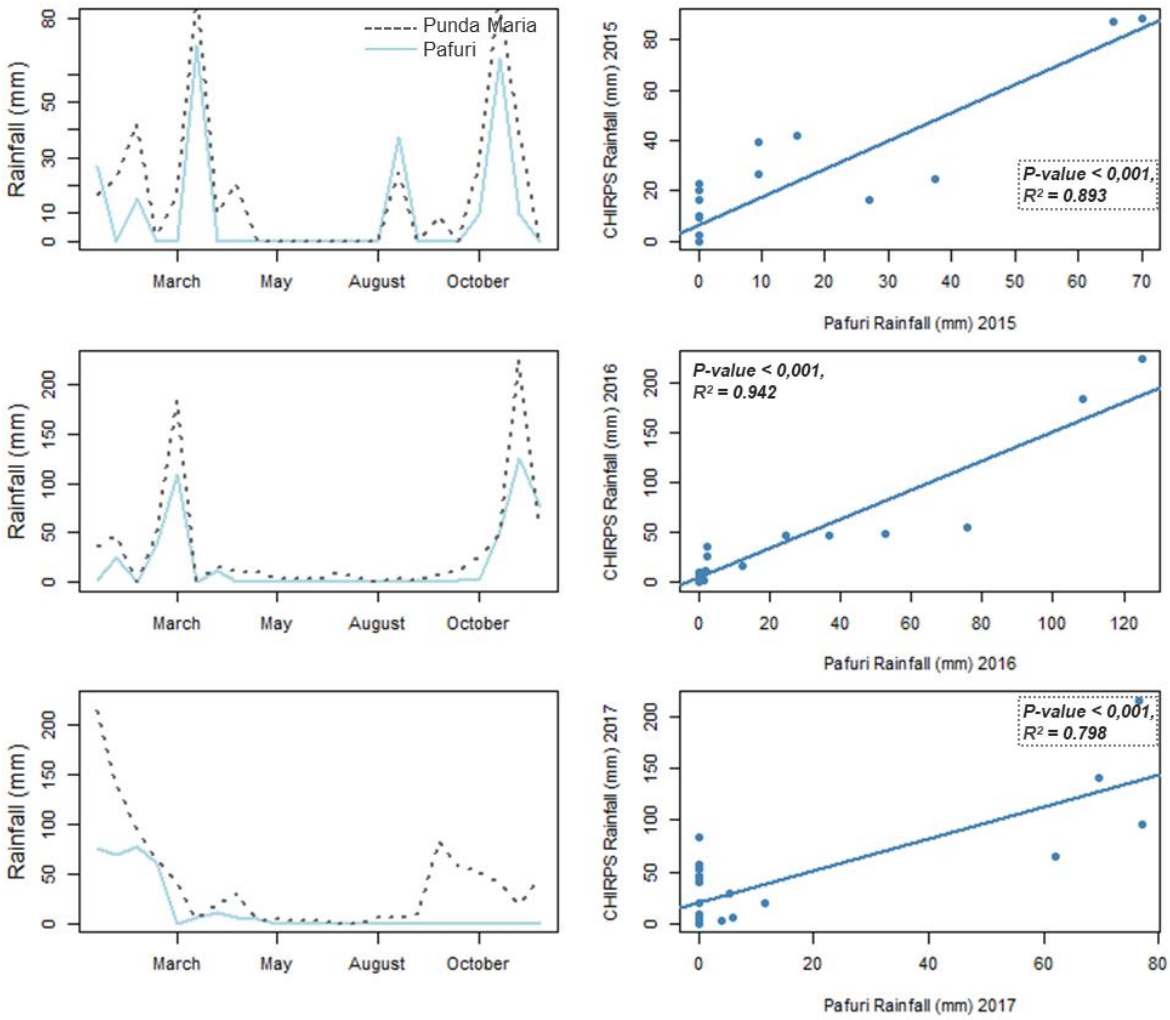

Figure S8: Seasonal trends of rainfall obtained from Pafuri (original data) and CHIRPS for the study extent and correlation of the two rainfall datasets for 2015-2017 to determine if the CHIRPS daily rainfall would be a viable supplement for the incomplete 2012 and 2013 daily rainfall for Pafuri.

Chapter 4

Assessing the effects of land use and extreme climatic events on land cover change using remote sensing

Abstract

Land cover represents the ecological state of an area's abiotic and biotic components and can be mapped over time to illustrate changes within the ecosystem. Land cover was assessed using remotely sensed imagery at multiple sites, on either side of the north-western fence line of the Greater Kruger National Park, near Pafuri. Land cover was obtained from three land cover platforms, with different temporal and pixel resolutions; 500 m MODIS MCD12Q1 (all seven years), 30 m Landsat 8 OLI and TIRS (five years) and 10 m Sentinel-2A (two years), to assess differences between the protected area and communal rangeland, over six consecutive austral growing seasons (2011-2017). Two "extreme" events occurred during this time - a flood in 2013 and a drought from 2014-2016. Five land cover classes were identified from each platform. The MODIS classes were broad-leaf crops, cereal crops, deciduous broadleaf trees, grass and shrub. While the Landsat and Sentinel classes were dense shrub, shrub, open shrub, sparse vegetation, and bare ground. There was little difference in land cover across the fence line based on the five land cover classes identified with the finer resolutions of Landsat 8 and Sentinel-2 datasets. However, dense shrub was the most dominant land cover class for both sides of the fence as detected by Landsat 8 (communal land = 50%, protected area = 42%) and Sentinel-2 (communal land = 43%, protected area = 28%). MODIS, however, showed that grass was by far the most dominant land cover class, followed by deciduous broadleaf trees, with grass cover significantly higher in the protected area (communal land = 83%, protected area = 95%, $p<0.01$), while deciduous broadleaf trees were significantly higher in the communal lands (communal land = 12%, protected area = 6%, $p<0.05$). All three methods showed change in land cover across most of the austral growing seasons, and more importantly, after the flood and drought events. Landsat 8 and MODIS showed considerable land cover change after the flood year, with a decrease in woody vegetation the year after the flood. Landsat 8 and Sentinel-2 detected an increase in woody vegetation cover the year after the drought event. Understanding how land cover changes at local scales in response to inter-annual variation, as well as extreme climatic events, will help to develop mitigation strategies to deal with any negative changes in vegetation or land cover that will affect the livelihoods of local communities and landscape level biodiversity and conservation efforts.

Keywords: Drought, flood, Greater Kruger National Park, land cover change, land use, remote sensing, savanna, vegetation response.

1. Introduction

Humans have altered the earth's surface for centuries in order to make land suitable for agricultural activities (Reid *et al.* 2000). Over the decades, land altered for agricultural purposes as well as for urban development has steadily increased in order to support the fast-growing human population. This increasing shift in land use has also led to a shift in landscape patterns. Liu *et al.* (2010) describe landscape pattern as the "spatial arrangement of various landscape elements in different sizes and shapes". Human activities as well as natural processes can drive change in landscape patterns, and these changes affect not only the structure of an ecosystem but the function too (Dadashpoor *et al.* 2019).

Land cover mapping

Land cover mapping provides insight into the biotic and abiotic components that are closely linked to the ecological state of the areas they represent (Friedl *et al.* 2010). This allows for an important platform for environmental change and sustainability research (Yang *et al.* 2017). Remote sensing platforms, particularly satellite imagery, provide easily available, impartial data at varying temporal and spatial scales, which has made the use of remote sensing an effective and essential method for monitoring and mapping land cover change (Gong *et al.* 2013, Jia *et al.* 2014, Hoffman *et al.* 2018). Land cover change has been extensively mapped at the global scale (Hansen *et al.* 2000, Loveland *et al.* 2000, Friedl *et al.* 2002, Bartholomé and Belward 2005, Defourny *et al.* 2012, Gong *et al.* 2013, Yu *et al.* 2013, Chen *et al.* 2015, Grekousis *et al.* 2015, 2015, Yang *et al.* 2017), and although land cover change has been mapped at regional scales (Giri and Long 2014, Grekousis *et al.* 2015, Latifovic *et al.* 2016), there are very few datasets for Africa, with East Africa mostly being mapped (Di Georgio and Jansen 1996). However, mapping land cover can be challenging for heterogenous systems such as savannas, as land cover is typically a combination of trees, shrubs and grasses with varying densities. This results in the occurrence of indistinct land cover class boundaries with patches which transition between open and closed forms of savanna (Gessner *et al.* 2013).

Most temporal land cover studies have focused on the impacts of direct anthrophonic change (Hulme *et al.* 1999, Petit *et al.* 2001, Jarnagin 2004, Seki *et al.* 2018, Ren *et al.* 2019). Very few studies have focused on land cover change as a result of flood and drought events (Sharma *et al.* 2011), and to my knowledge no study has been conducted on the response of land cover to land use and extreme climatic events (excluding high anthropogenic effects) at a local scale in the semi-arid savannas of southern Africa using remote sensing.

Drivers of land cover change

Several ecological processes at various scales interact and influence the heterogeneity of a landscape (Csillag and Kabos 2002, Liu *et al.* 2010), which in turn affects biodiversity and social and economic functions (Lausch *et al.* 2015). Thus, land cover in savannas is determined by several factors at different scales. At a regional scale, precipitation largely drives vegetation cover, particularly woody vegetation cover (Sankaran *et al.* 2005, Wessels *et al.* 2011). At a continental scale, vegetation cover and structure is predominantly driven by topography, substrate, fire and large herbivores, particularly elephants (Witkowski and O'Connor 1996, Venter *et al.* 2003). However, human land use plays a role in altering savanna vegetation structure and land cover at the local scale (Higgins *et al.* 1999, Wessels *et al.* 2011). Biodiversity and ecosystem function at these different scales are at risk due to changes in the tree-grass balance as a result of land use pressures and changing climate. Changes in vegetation cover in savanna regions could result in large feedbacks into the earth-atmosphere system (Archer *et al.* 2001). Changes in land use and land cover provides a measure for changes in landscape patterns. Changes in land cover have local and global implications as land cover is an essential aspect of ecosystem and biogeochemical processes. Land cover change due to agriculture and livestock farming often leads to changes in nutrient and water cycling (Friedl *et al.* 2002, DeFries and Bounoua 2004, Linderman *et al.* 2005) and carbon storage (Kamusoko and Aniya 2007). Larger changes, including deforestation and woodland loss (Mwavu and Witkowski 2008, Coetzer *et al.* 2010), land degradation due to fuelwood harvesting, particularly for fuelwood and charcoal production (Luoga *et al.* 2000, Kalema *et al.* 2015), as well as overgrazing and changes in topography due to development (Jewitt *et al.* 2015). These tend to lead to changes in albedo, evapotranspiration and primary productivity which could impact atmospheric fluxes of heat alter local and global weather patterns and climate (Friedl *et al.* 2002, Matthews *et al.* 2004, Clark 2017).

As land cover change is one of the contributors to climate change, the shifts in climatic variables as a result of climate change may in turn affect the remaining vegetation land cover. However, the current distribution and dominance of many plant species has been influenced by changing climatic conditions over centuries. Additionally, local and regional climate is known to influence land cover with short term interannual variability, particularly in rainfall, and this variability is often intensified by ENSO episodes (Ward *et al.* 2014). Thus, it is important not to confuse any short term fluctuations in vegetation response to common short term changes in climatic variables with those caused by climate change (DeFries and Bounoua 2004, Wessels *et al.* 2004). However, there are still some uncertainties as to how climatic conditions that are being altered by climate change will influence vegetation response at both regional and local scales within heterogenous ecosystems across the globe. The occurrence of flood and drought events that coincide with ENSO episodes provide opportunities to assess the response of vegetation during more extreme climatic conditions. Monitoring at local scales, especially in rural areas, highlights the impact of vegetation and land cover change on local communities. Depending on the degree of land cover change and where it occurs, there may be extreme repercussions for the functioning of ecosystems by altering ecosystem services such as water quality, total net primary productivity (Lambin *et al.* 2001, DeFries and Bounoua 2004) and forage availability for subsistence, private and commercial livestock (Hao *et al.* 2018). This in turn affects an ecosystem's ability to support human needs (Lambin *et al.* 2001). Thus, the extent of land cover change has led to increased concerns over the quality of water and air, general ecosystem health and sustainable land management as well as human well-being which is reliant on ecosystem services (Reid *et al.* 2000, Friedl *et al.* 2010).

Land use is often the main determinant of vegetation land cover, with small scale livestock farming and crop farming being the main land use for many communal lands throughout southern Africa (Behnke 1985, Cousins 1994, Shackleton *et al.* 2002, Dovie *et al.* 2003, 2006). Protected areas and the surrounding regions, often communal rangelands, are managed differently depending on the role the environment plays (Anthony 2006). Protected areas are in place to conserve and maintain biological diversity and natural resources (Bruner *et al.* 2001, Anthony 2006), as well as to aid in the reduction of poverty in surrounding areas by providing various employment opportunities and by contributing to national development (Naughton-Treves *et al.* 2005). One such protected area is the Kruger National Park (KNP), and along the north western fence line the Makuya Nature Reserve now forms part of the Greater Kruger National Park. The Makuya Nature Reserve boarders the Vhembe district, of northern Venda, Limpopo (Van Marrewijk 2011). Conversely, communal lands serve as a source of natural resources for people within the community that do not own land (Shackleton *et al.* 2005). Communal land is seen as common property with the ownership and management rights falling to a social unit within the community and is treated as 'open access' (Ainslie 1999). This land is mostly used for propagation of staple crops, a source for fuelwood and medicinal plants and to support livestock (Ainslie 1999, Shackleton *et al.* 2001). As a result of the greater number of people utilizing communal lands for livestock and unsustainable resource use, the area is frequently overgrazed and degraded (Todd and Hoffman 1999). In the Vhembe district, the main land use within the densely populated villages is subsistence agriculture and animal husbandry. The subsistence crops are cultivated in the wet season and the grazing of livestock (i.e. donkeys, goats and cattle) occurs in wooded plains (Venter and Witkowski 2010). However, the semi-arid nature of this area makes subsistence farming a challenge and often results in low yields. Additionally, overgrazing and general environmental degradation has occurred around many villages due to overstocking of livestock (Venter and Witkowski 2013). This area has high levels of poverty, few job opportunities, and limited service provision and development due to very few industries in the area (Venter and Witkowski 2013, Paumgarten *et al.* 2018). Thus, there is still a great reliance on natural vegetation and ecosystem services in the surrounding area.

1.1. Aims and objectives

This final chapter aims to compare the differences in land cover between the protected area and communal land, and to assess how land cover changed after years of extreme flooding and drought events using three land cover datasets of various temporal and spatial resolutions; 500 m resolution MCD12Q1 MODIS (2011-2017) imagery, 30 m Landsat 8 OLI and TRS (2013-2017) imagery and 10 m Sentinel-2 (2016-2017) imagery.

2. Methods

2.1. Study area and vegetation types

Refer to chapter 2

2.2. Experimental design

This study spanned a six-year period from 1 July 2011 to 30 June 2017 (austral years 2011/2012 to 2016/2017), focusing on a flood event in 2013 and a drought event that spanned two austral growing seasons, in 2014/2015 and 2015/2016.

Land cover was determined from three platforms; the MODIS Terra + Aqua Land Cover Type MCD12Q1 dataset; the Landsat 8 Operational Land Imager (OLI) and Thermal Infrared Sensor (TIRS) dataset and the Sentinel-2A Level 1C dataset. The three satellite platforms used for land cover assessment have quite different spatial resolutions, however, the size of the study sites was maintained from the phenological assessment. Thus, rather than extracting the data to points within the sites, the analyses were based on how many pixels fell within the sites.

2.3. Land cover comparison

MODIS- MCD12Q1

The MODIS Terra + Aqua Land Cover Type MCD12Q1 global land cover dataset has an annual, 500 m resolution (https://search.earthdata.nasa.gov, accessed 8 July 2018), from which land cover images for all seven years, 2011-2017 was obtained. This dataset was used as it has a predefined land cover map for Africa, of which there are very few. Simply, this dataset was selected in order to assess land cover change over the entire study period, as this was not possible with the Landsat 8 and Sentinel-2 datasets. The land cover from MCD12Q1 is a global land cover dataset with several supervised classification options including the leaf area index (LAI) or fPAR, net primary productivity (NNP), and plant functional type (PFT). Land cover for the study extent was determined using PFT classification technique which has 11 land cover classes, but only five were present within the study area (broad-leaf crops, cereal crops, deciduous broadleaf trees, grass and shrub). Although the MCD12Q1 dataset is typically used for global land cover classification, it was used to demonstrate the change of vegetation cover across the full temporal extent of this study.

Landsat 8 OLI and TIRS

Landsat 8 Operational Land Imager (OLI) and Thermal Infrared Sensor (TIRS) dataset with a resolution of 30 m and obtained every 16 days (https://search.earthdata.nasa.gov, accessed 31 July 2018), from which the land cover images from May 2013-2017, the last five study years only, were obtained. Land cover images from May were selected as it represents a period after the summer rainfall and before the major senescence of winter. Although Landsat 8 was launched in February 2013, offering an opportunity to map land cover types for the dates closest to the $Start_T$, $Peak_T$, Mid_T and End_T for most of the growing seasons, cloud cover around most of these dates was too high.

Sentinel-2A

Sentinel-2A Level 1C dataset with a 10 m resolution and a ten-day return frequency (https://scihub.copernicus.eu/, accessed 26 June 2018), from which images of May 2016 and 2017 were obtained. Sentinel-2 was launched in May 2015, allowing for land cover classification of 2016 and 2017, the last two study years only. The land cover was also obtained for dates closest to the $Start_T$ and End_T of the 2016/2017 growing season. The land cover for the $Peak_T$ and Mid_T could not be obtained for this growing season due to high cloud cover during those times.

Land cover types for the Landsat 8 and Sentinel-2 images were classified using supervised classification techniques, where the pixels of known land cover types are classified first, and a land cover image is generated based on those classifications. In order to classify the various land cover classes, training pixels were selected based on Google Earth imagery, and near infrared (NIR) and shortwave infrared (SWIR) images of the study area derived from Landsat 8 and Sentinel-2 datasets. The NIR and SWIR images show healthy growing vegetation as red for NIR and green for SWIR, and the "healthier" the vegetation, the deeper the red or green. Additionally, a deeper red or green is also indicative of broadleaf vegetation, while lighter red or green shows grasslands or sparsely vegetated areas. Seven land cover classes were identified across the study area; riparian woody vegetation; dense shrub, shrub, open shrub, sparse vegetation, bare ground and water.

Spatial comparisons

The proportion of pixels that were classified under different land cover classes were determined for the study sites for all three land cover remote sensing platforms and the respective differences in cover were compared between the two sides of the fence using paired Wilcoxon signed rank tests. Although bare ground was recorded within the sites for most of the growing seasons, the proportion of pixels was negligible and thus excluded from the analysis.

Temporal comparisons

A constrained ordination technique, redundancy analysis, was used to investigate land cover classes in relation to land use (protected area and communal land) and austral year for each of the land cover platforms. The temporal aspect for MODIS included annual land cover images from 2011-2017 (seven years), Landsat 8 included images from 2013-2017 (five years) and Sentinel-2 (two years) included images from 2016/2017. The percentages for all the land cover classes obtained from the eight sites on either side of the fence (Chapter 2, pg. 15) were averaged for each austral year to produce one value per land cover class per land use, or land cover per year, which was represented by numbers; for MODIS n = 14 (2011-2017), Landsat 8 n = 10 (2013-2017) and Sentinel-2 n = 4 (2016 and 2017). The ordination axes are a combination of variables that explain land cover class ("species") abundance using a multivariate gradient analysis (Ter Braak 1986). Austral year and land use were treated as the environmental variables.

Altitude

The range in altitude for the communal land and protected area was compared using a paired Wilcoxon signed rank test.

2.4. Analytical software

Statistical analyses and MODIS, Landsat 8 and Sentinel-2 image analyses were performed using Rstudio (R Core Team 2014, version 1.1.423) and ArcGIS respectively (ESRI 2011).

3. Results

3.1. Spatial comparison- Effect of land use on land cover

MODIS

The MODIS derived land cover classification yielded five classes within the study sites (broad-leaf crops, cereal crops, deciduous broadleaf trees, grass and shrub). While these classes were all present within the communal land, only the deciduous broadleaf trees and grass were present within the protected area. These two land cover classes common for the communal land and protected area both showed a significant difference across the fence line. The majority of both the communal land and protected area sites were comprised of the grass land cover classification (communal land = 83% and protected area = 95%) (Table 1).

Table 1: Comparison of the percentage of pixels (mean ± SE) that fall within the five land cover classes obtained from the MODIS MCD12Q1 land cover dataset for the protected area and the communal land across the six Austral years (2011-2017) and statistical comparisons between them (paired Wilcoxon signed rank test). Significant differences ($p<0.05$) are shown in bold.

Land cover class	Communal land	Protected area	Paired Wilcoxon signed rank test
Broad-leaf crops	1± 0.495	NA	NA
Cereal crops	2 ± 0.596	NA	NA
Deciduous Broadleaf trees	12± 2.641	5 ± 1.437	v_{55} = 302, $\boldsymbol{p<0.05}$
Grass	83± 3.504	95 ± 1.437	v_{55} = 70, $\boldsymbol{p<0.01}$
Shrub	2 ± 0.596	NA	NA

Landsat

Five land cover classes were derived from the Landsat 8 dataset; dense shrub (communal land = 50% and protected area = 42%) and shrub (communal land = 21% and protected area = 28%) were the most prevalent land cover classes for both land use types . The riparian woody vegetation was the only class to show a significant difference in pixel percentage across the fence, with a greater proportion present within the protected area (Table 2).

Table 2: Comparison of the percentage of pixels (mean ± SE) that fall within the five land cover classes obtained from the Landsat 8 OLI and TIRS land cover dataset for the protected area and the communal land across the six Austral years (2011-2017) and statistical comparisons between them (paired Wilcoxon signed rank test). Significant differences (p<0.05) are shown in bold.

Land cover class	Communal land	Protected area	Paired Wilcoxon signed rank test
Dense shrub	50 ± 5.910	42 ± 4.746	v_{39} = 471, p = 0.261
Open shrub	10 ± 2.231	9± 2.422	v_{39} = 406, p = 0.829
Riparian woody vegetation	14 ± 3.851	17 ± 2.903	v_{39} = 229, **p<0.05**
Shrub	21 ± 3.967	27 ± 4.239	v_{39} = 304, p = 0.158
Sparse vegetation	6 ± 1.256	4. ± 1.262	v_{39} = 292, p = 0.394

Sentinel-2

Dense shrub (communal land = 43% and protected area = 28%) and shrub (communal land = 27% and protected area = 36 %) were also the most prevalent land cover classes for the Sentinel-2 dataset. The riparian woody vegetation was the only class to show a significant difference between the communal land and protected area. However, there was a greater percentage of sparse vegetation (communal land = 23% and protected area = 19%) picked up by the Sentinel-2 dataset (Table 3). The high percentage of sparse vegetation within the protected area, was caused by vegetation changes at different altitudes (communal land = 335 m a.s.l ± 1.90; protected area = 331 m a.s.l ± 4.01) which were not mirrored in the corresponding site across the fence, however the altitude in the sites did not differ significantly overall across the fence line (v_{199} = 10984, p = 0.160). When defining the study areas, the aim was to maintain all sites at least 250 m from rivers, however, sites 7 and 8 of the protected area include a small channel. This is the source of most of the sparse vegetation classified for the protected area.

Table 3: Comparison of the percentage of pixels (mean ± SE) that fall within the five land cover classes obtained from the Sentinel-2A Level 1C land cover dataset for the protected area and the communal land across the six Austral years (2011-2017) and statistical comparisons between them (paired Wilcoxon signed rank test). Significant differences (p<0.05) are shown in bold.

Land cover class	Communal land	Protected area	Paired Wilcoxon signed rank test
Dense shrub	43 ± 9.464	28 ± 6.848	v_{15} = 89, p = 0.298
Open shrub	5 ± 1.373	8± 2.132	v_{15} = 51, p = 0.404
Riparian woody vegetation	2 ± 0.825	9± 1.229	v_{15} = 3, ***p*****<0.001**
Shrub	27 ± 5.341	36 ± 6.242	v_{15} = 45, p = 0.252
Sparse vegetation	23 ± 6.225	19 ± 5.856	v_{15} = 78, p = 0.632

Sentinel-2 Start$_T$ and End$_T$ 2016/2017

The Start$_T$ of the 2016/2017 growing season was 24 December for the communal land and 25 December 2016 for the protected area, the Sentinel-2 image used for the Start$_T$ land cover classification was 23 December 2016. The End$_T$ of the growing season was 18 July for the communal land and 17 July for the protected area, however due to cloud cover over this time the image from 1 July was used to depict the land cover for the end of the 2016/2017 growing season (Figure 1). The dense shrub was the dominant land cover class at the start of the growing season (communal land = 45% and protected area = 44%), by the end of the growing season dense shrub (communal land = 43% and protected area = 28%) and shrub (communal land = 33% and protected area = 40%) comprised of most of the cover across the sites. And as would be expected the proportion of sparse vegetation increased by the end of the growing season (Start$_T$: communal land = 16% and protected area = 6%; End$_T$: communal land = 16% and protected area = 9%) (Table 4 and Figure 1). There was, however, no significant change in the percentage of pixels of each land cover class from the start to the end of the growing season (Table 5). Additionally, neither the StartT or EndT showed a significant difference in pixel percentage for the five land cover classes between the communal land and protected area (Table 5 and Figure 1).

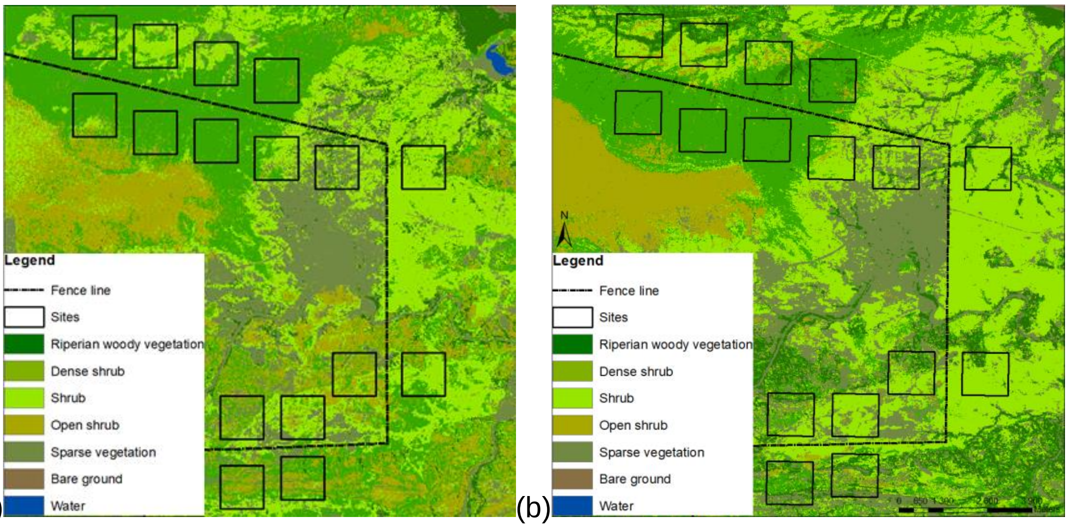

Figure 1: Comparison of the Sentinel-2 derived land cover for the (a) Start$_T$ and (b) End$_T$ of the 2016/2017 growing season. Dense shrub decreased from the start to the end of the growing season, while shrub, sparse vegetation and riparian woody vegetation increased towards the end of the growing season.

Table 4: Comparison of the percentage of pixels (mean ± SE) that fall within the five land cover classes obtained from the Sentinel-2A Level 1C land cover between the protected area and the communal land for the (a) Start$_T$ and (b) End$_T$ of the 2016/2017 growing season (paired t-tests and Wilcoxon signed rank test). Significant differences (p<0.05) are shown in bold.

	(a) Start time		
Land cover type	**Communal land**	**Protected area**	**Paired t-tests and Wilcoxon signed rank test**
Dense shrub	2 ± 0.964	2 ± 1.131	v_{15} = 17, p = 0.945
Open shrub	44 ± 13.127	43 ± 9.344	v_{15} = 18, p = 1
Riparian woody vegetation	25 ± 6.946	39 ± 10.228	v_{15} = 16, p = 0.844
Shrub	13 ± 5.674	10 ± 5.011	v_{15} = 11, p = 0.389
Sparse vegetation	16 ± 6.729	6 ± 1.552	t_{15} = 0.659, p = 0.532
	(b) End time		
	Communal land	**Protected area**	**Paired t-tests and Wilcoxon signed rank test**
Dense shrub	5 ± 1.85	16 ± 2.466	v_{15} = 8, p = 0.195
Open shrub	43 ± 15.912	28 ± 9.155	v_{15} = 19, p = 0.945
Riparian woody vegetation	33 ± 10.642	40 ± 10.535	v_{15} = 15, p = 0.742
Shrub	2 ± 0.818	7 ± 1.645	v_{15} = 12, p = 0.800
Sparse vegetation	17 ± 6.121	9 ± 4.045	t_{15} = 0.606, p = 0.563

Table 5: Statistical comparisons (paired t-tests and Wilcoxon signed rank test) between the $Start_T$ and End_T of the 2016/2017 growing season for the communal land and protected area of the five land cover classes obtained from the Sentinel-2A Level 1C land cover dataset. Significant differences (p<0.05) are shown in bold.

Land cover type	Communal land	Protected area
Dense shrub	v_{15} = 29, p = 0.148	v_{15} = 10, p = 0.313
Open shrub	t_{15} = 0.391, p = 0.707	v_{15} = 19, p = 0.945
Riparian woody vegetation	v_{15} = 20, p = 0.844	v_{15} = 15, p = 0.742
Shrub	v_{15} = 12, p = 0.800	v_{15} = 25, p = 0.383
Sparse vegetation	t_{15} = -0.344, p = 0.741	t_{15} = 0.203, p = 0.845

3.2. Temporal comparison - Effect of extreme climatic events on land cover

The predictive power of the redundancy analysis models was high for MODIS and Sentinel-2, but low for Landsat 8 (percentage of variation explained: MODIS = 93%, Landsat = 29%, and Sentinel-2 = 94%). Additionally, the Landsat 8 land cover data was the only significant model (Table 6). Year was the most important factor influencing land cover change across all three land cover assessments (Figures 2, 3 and 4).

Table 6: Summary statistics of the redundancy analyses (RDA) of the land cover classes and environmental variables for the three land cover assessments; MODIS, Landsat 8 and Sentinel-2. Significant values in bold (p<0.05).

		Axis	
		1	2
MODIS	Accumulated constrained Eigenvalue	71.06	17.02
	Proportion explained	80.68%	19.32%
	Significance	p = 0.283	p = 0.669
Landsat 8	Accumulated constrained Eigenvalue	69.37	0.72
	Proportion explained	98.97%	1.03%
	Significance	***p*< 0.001**	p = 0.201
Sentinel-2	Accumulated constrained Eigenvalue	201.74	57.29
	Proportion explained	77.88%	22.12%
	Significance	p = 0.333	p = 0.083

	Full model variance	Significance
MODIS	88.072	p = 0.225
Landsat 8	70.092	***p*< 0.001**
Sentinel-2	259.032	p = 0.333

MODIS

Deciduous broadleaf trees and grass showed a strong negative correlation across the growing seasons. Deciduous broadleaf trees showed a strong negative correlation with year, while grass showed a strong positive correlation to year (Figure 2). Thus, from 2011/2012 to 2016/2017, deciduous broadleaf trees decreased while grass cover increased. Shrub, cereal crops and broadleaf crops showed strong positive correlations with each other. However, they had a low correlation to the deciduous broadleaf trees, grass and year (Figure 2). Which indicates that the progression in austral years had a minimal effect on the cover of shrub, cereal crops and broadleaf crops. The percentages for all the land cover classes obtained from the eight sites on either side of the fence was averaged for each austral year to produce one value per land cover class per land use. These were classified as the land cover per year for both sides of the fence. Numbers 1-7 represent years 2011-2017 in the communal land and numbers 8-14 represent years 2011-2017 in the protected area (Figure 2). Land cover for each year of the communal land (1-7) were clustered together as was the land cover per year of the protected area (8-14). Numbers 3 and 10 represented the flood year for the communal land and protected area respectively, while numbers 5, 6 and 12, 13 represented the drought years for the two sites. The flood and drought years showed dissimilarity for both the protected area and communal land. Additionally, drought years for the communal land showed high similarity, as did the drought years of the protected area. Based on the Euclidean distances between these numbers, the land cover changed very little between 2011-2013. However, there was increased change from 2013 to 2014. This indicated that the flood event of 2013 led to a shift in land cover for both the communal land and protected area. Additionally, land cover changed from 2014 to 2015, after the first drought season. There was no change in land cover within the communal land and protected area from 2015-2017 (Figure 2).

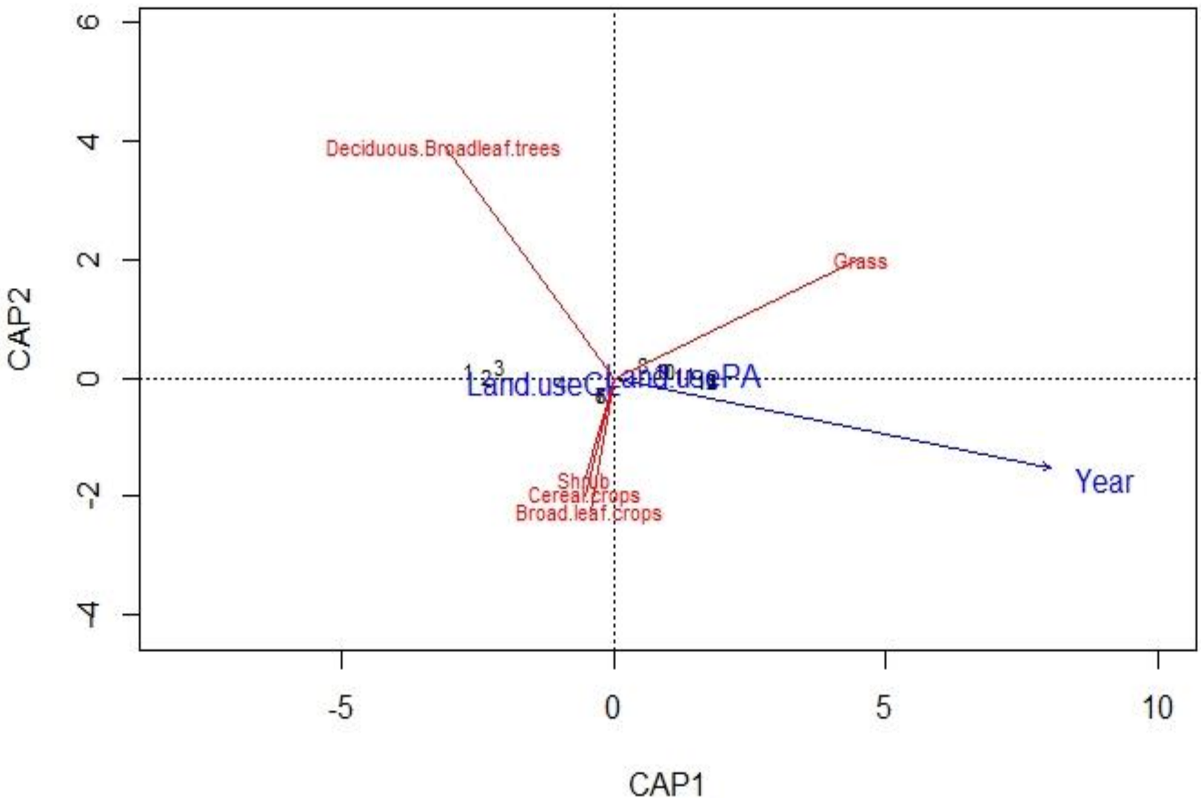

Figure 2: Redundancy analysis (RDA) of land cover classes derived from the 500 m MODIS land cover dataset (MCD12Q1) in relation to land use (protected area (PA) and communal land (CL)) and austral year (2011-2017). The percentages for all the land cover classes obtained from the eight sites on either side of the fence were averaged for each austral year to produce one value per land cover class per land use. These were classified as the land cover per year. Numbers 1-7 indicate sites within the communal land, while 8-14 show sites within the protected area. Numbers 3 and 10 are the sites for the flood year for the communal land and protected area respectively. Numbers 5, 6 and 12,13 represent the drought years for the communal land and protected area respectively.

Landsat 8

Dense shrub and riparian woody vegetation showed a strong negative correlation and open shrub and sparse vegetation showed a fairly strong negative correlation (Figure 3), indicating that when one class decreases the other increases. Conversely, dense shrub and sparse vegetation and riparian woody vegetation and shrub were predicted to have moderate positive correlations (Figure 3), suggesting that when one class increases so will the other. However, dense shrub and open shrub, dense shrub and shrub, as well as open shrub and riparian woody vegetation were predicted to have fairly low negative correlations between each pair. Suggesting that any change experienced for one of these classes is not likely to affect the other. Open shrub and year showed a strong negative correlation, while shrub and year and sparse vegetation and year showed moderate positive correlations. Dense shrub and riparian woody vegetation both showed low, near zero, correlation with year (Figure 3). This indicates that as austral years progressed, open shrub decreased, while sparse vegetation and shrub increased, and there was minimal change in the cover of riparian woody vegetation and dense shrub. The communal land numbers (1-5) were clustered together, however, number 7 of the protected area showed the greatest dissimilarity to the remaining protected area numbers, which were clustered. Number 1 and 6 represented the flood year (2012/2013) for the communal land and protected area respectively, and numbers 3 and 4 and 8 and 9 represented the two drought years (2014/2015 and 2015/2016) for the communal land and protected area respectively (Figure 3). In the communal land, flood and drought years showed dissimilarity and drought years showed high similarity. For the protected area however, the flood year showed very high dissimilarity to the second drought year. The first drought year had similar Euclidean distances to the flood year and the second drought year, being slightly closer to the second drought year, suggesting that the land cover was as different between the first drought year and the flood year as it was for the first and second drought years. These patterns indicated that there was a change in land cover after the flood event in 2013 on both sides of the fence. Although there was minimal change in land cover between the two drought years in the communal land, there was increased change in land cover after the drought event for both sides of the fence. The protected area experienced noticeable change in land cover after both drought years (Figure 3).

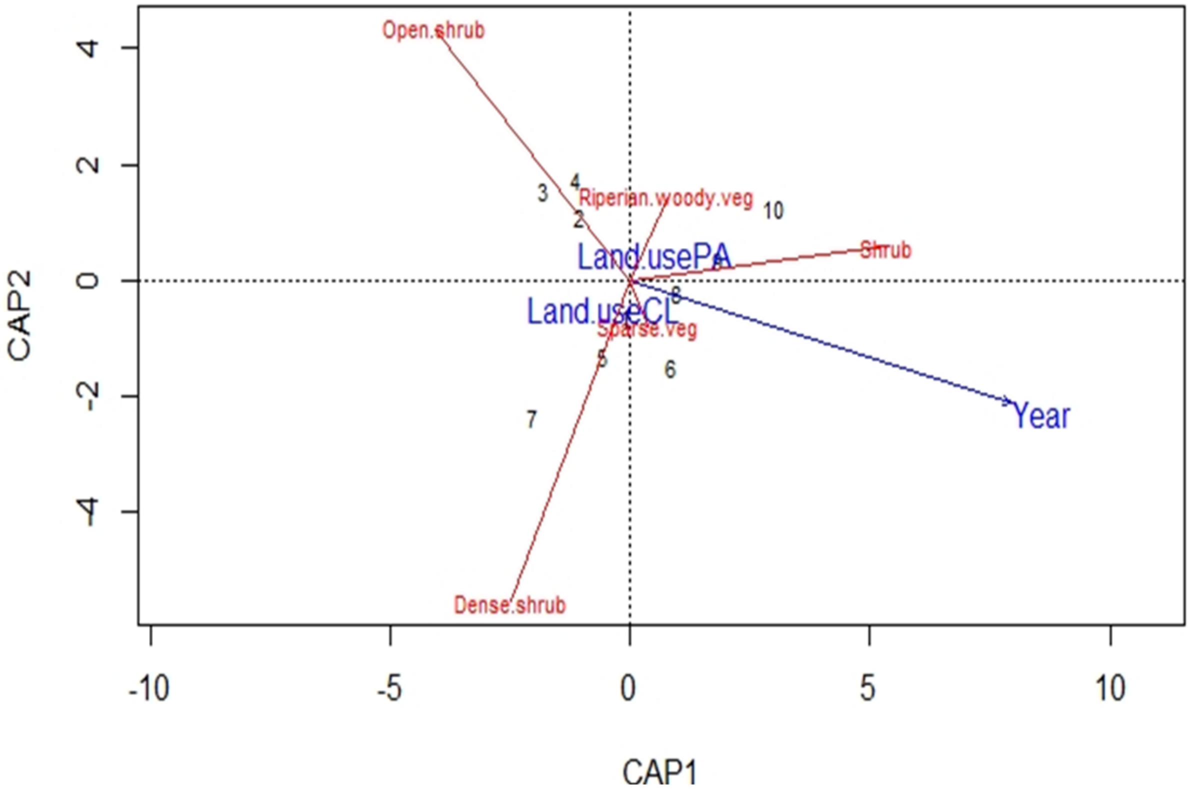

Figure 3: Redundancy analysis (RDA) of land cover classes derived from the 30 m Landsat 8 land cover dataset in relation to land use (protected area (PA) and communal land (CL)) and austral year (2011-2017). The percentages for all the land cover classes obtained from the eight sites on either side of the fence was averaged for each austral year to produce one value per land cover class per land use, these were classified as the land cover per year. Numbers 1-5 indicate sites within the communal land, while 6-10 are within the protected area. Numbers 1 and 6 represent the flood year for the communal land and protected area respectively; numbers 3, 4 and 8, 9 represent the drought years for the communal land and protected area respectively.

Sentinel-2

As predicted for the Landsat 8 assessment, dense shrub and riparian woody as well as open shrub and sparse vegetation showed strong negative correlations. However, sparse vegetation and shrub showed a moderate negative correlation (Figure 4), indicating that when one increased the other would decrease. Riparian woody vegetation and shrub were predicted to have a moderate positive correlation, suggesting both classes would increase simultaneously. Dense shrub and open shrub, dense shrub and sparse vegetation as well as open shrub and riparian woody vegetation were predicted to have fairly low negative correlations between each pair. Sparse vegetation and year were predicted to have a strong negative correlation, while open shrub and year showed a strong positive correlation, similarly, shrub and year showed a moderate positive correlation (Figure 4). Thus, after the drought event, sparse vegetation decreased while open shrub and shrub increased. Both dense shrub and riparian woody vegetation were predicted to have low, near zero, correlations with year, indicating very little change in these land cover classes after the drought event. The high Euclidean distances for the numbers from both sides of the fence suggest considerable land cover change between 2015/2016 and 2016/2017 (Figure 4).

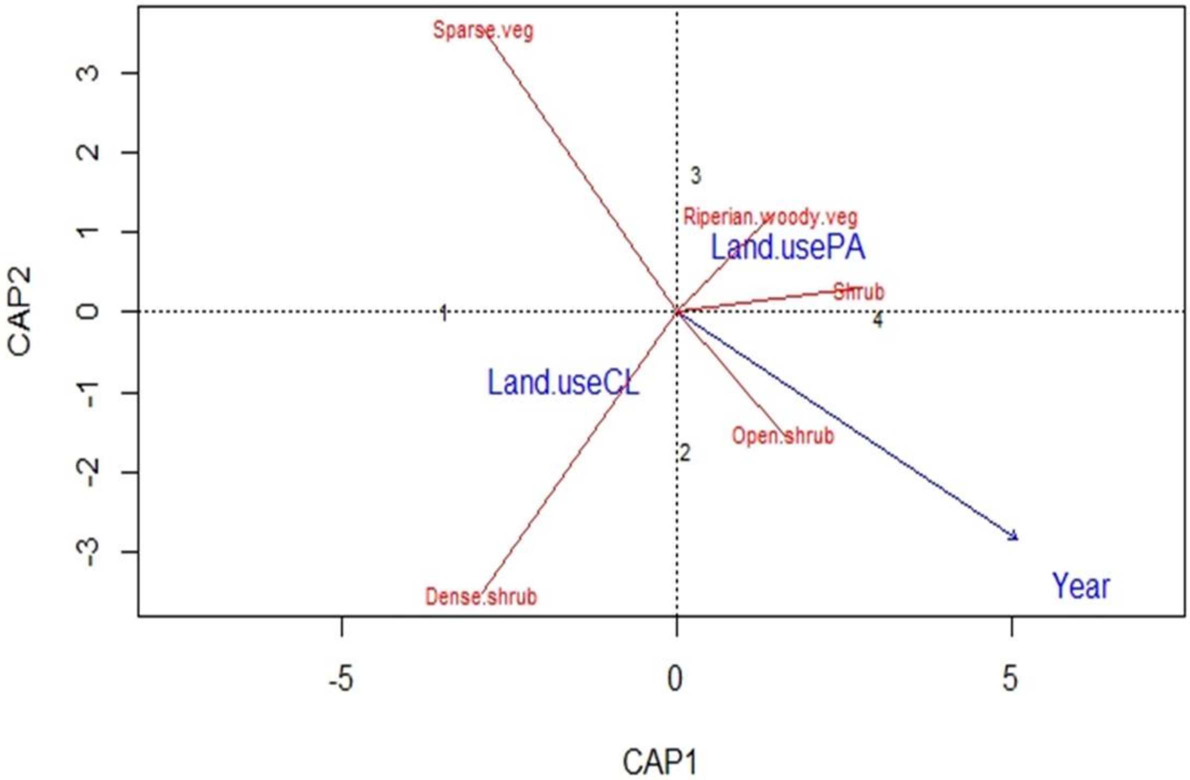

Figure 4: Redundancy analysis (RDA) of land cover classes derived from the 10 m Sentinel-2 land cover dataset in relation to land use (protected area (PA) and communal land (CL)) and austral year (2011-2017). Numbers 1-2 refer to land cover per year within the communal land, while 3-4 represent the protected area.

3.3. Effect of extreme climatic events on land cover

MODIS

The flood year exhibits the greatest proportion of deciduous broadleaf trees (communal land = 20%; protected area = 7%), which decreased in proportion on both sides of the fence during the 2014/2015 (communal land = 15%; protected area = 6%) and 2015/2016 (communal land = 11%; protected area = 4%) drought years (Table 5 and Figure 5).

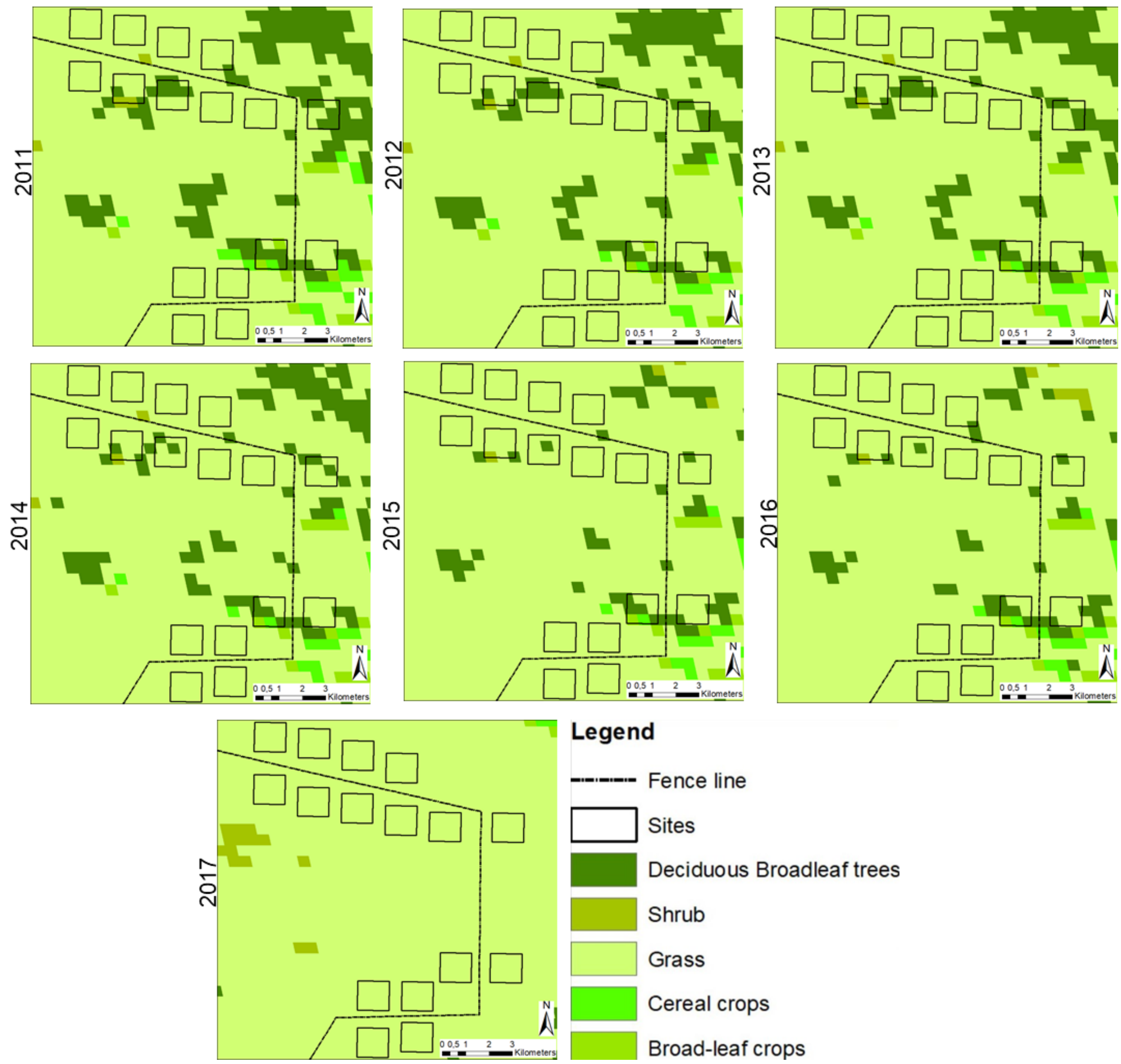

Figure 5: Land cover classification of the study sites along the north western fence line of the Greater Kruger National Park derived from the 500 m MCD12Q1 MODIS land cover type product for 2011-2017.

Table 5: Comparison of the percentage of pixels (mean ± SE) that fall within the five land cover classes obtained from the MODIS MCD12Q1 dataset for 2011-2017, for the two sites across the fence line, the protected area and the communal land. The broad-leaf crops, shrub and cereal crops classification classes occurred in the communal land only.

	Broad-leaf crops		Cereal crops		Deciduous broadleaf trees	
Austral year	Communal land	Protected area	Communal land	Protected area	Communal land	Protected area
2011	1 ± 1.757	NA	1 ± 1.757	NA	18 ± 11.984	8 ± 8.036
2012	1 ± 1.757	NA	3 ± 3.514	NA	16 ± 11.071	6 ± 6.473
2013	1 ± 1.757	NA	1 ± 1.757	NA	16 ± 11.071	6 ± 6.473
2014	1 ± 1.757	NA	1 ± 1.757	NA	12 ± 7.642	4 ± 4.911
2015	1 ± 1.757	NA	1 ± 1.757	NA	9 ± 6.9200	3 ± 3.348
2016	1 ± 1.757	NA	1 ± 1.757	NA	9 ± 6.9200	3 ± 3.348
2017	1 ± 1.757	NA	1 ± 1.757	NA	9 ± 6.9200	3 ± 3.348

	Grass		Shrub	
Austral year	Communal land	Protected area	Communal land	Protected area
2011	77 ± 14.800	92 ± 7.906	3 ± 3.514	NA
2012	78 ± 14.441	94 ± 6.036	1 ± 1.757	NA
2013	80 ± 13.268	94 ± 6.036	1 ± 1.757	NA
2014	84 ± 10.990	97 ± 2.781	1 ± 1.757	NA
2015	87 ± 10.433	97 ± 2.781	1 ± 1.757	NA
2016	87 ± 10.433	97 ± 2.781	1 ± 1.757	NA
2017	87 ± 10.433	97 ± 2.781	1 ± 1.757	NA

Landsat 8

Dense shrub and shrub were the most prominent land cover types for the six growing seasons for both sides of the fence, with the flood and drought years having the highest percentage in the communal land (2013/2014 flood year = 62%; 2014/2015 drought year = 67%; 2015/2016 drought year = 63%). Dense shrub and open shrub were the most prominent land cover classes within the protected area for the flood year (dense shrub = 44%, open shrub = 36%), while both drought years showed dense shrub and shrub to be the most dominant classes (2014/2015 drought year: dense shrub = 54%, shrub = 30%; 2015/2016 drought year: dense shrub = 44%, shrub = 34%). The 2015/2016 drought year experienced the greatest proportion of sparse vegetation, as one might expect, for both sides of the fence (communal land = 15%, protected area = 16%) (Table 7 and Figure 6).

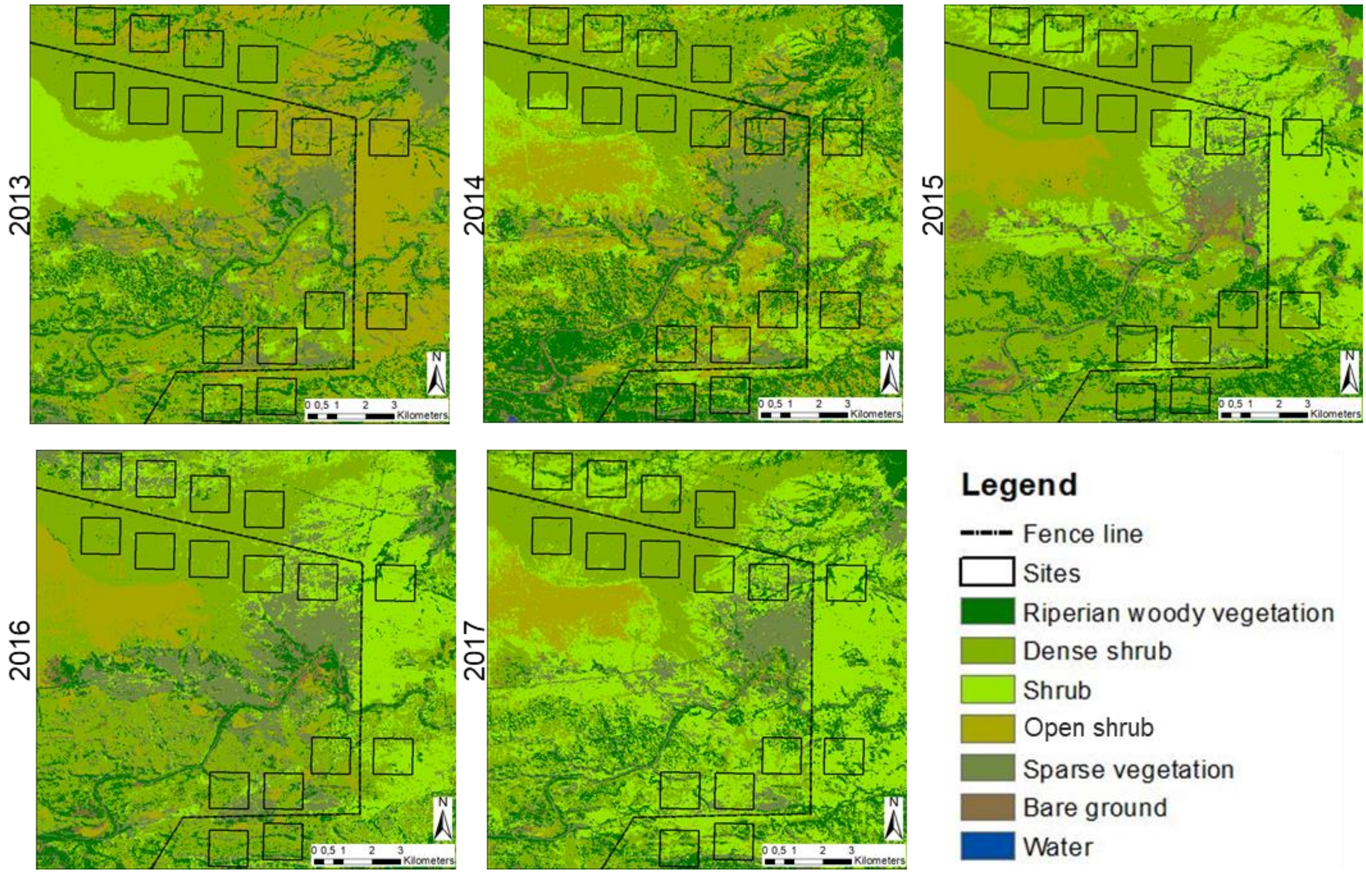

Figure 6: Landsat 8 derived land cover classification of the study sites along the north western fence line of the Greater Kruger National Park for May 2013-2017.

Table 7: Comparison of the percentage of pixels (mean ± SE) that fall within the five land cover classes obtained from the Landsat 8 OLI and TIRS land cover dataset for 2013-2017, for the two sites across the fence line, the protected area and the communal land.

	Dense shrub		**Open shrub**		**Riparian woody vegetation**	
Austral year	**Communal land**	**Protected area**	**Communal land**	**Protected area**	**Communal land**	**Protected area**
2012/2013	50 ± 16.636	43 ± 13.486	10 ± 3.779	20 ± 10.873	9 ± 4.225	13 ± 4.653
2013/2014	40 ± 18.332	38 ± 14.926	20 ± 8.989	19 ± 5.627	24 ± 11.407	23 ± 8.943
2014/2015	55 ± 17.917	54 ± 12.25	5 ± 5.146	1 ± 0.624	19 ± 15.246	14 ± 6.086
2015/2016	64 ± 14.769	44 ± 13.282	10 ± 6.644	7 ± 5.298	3 ± 1.907	9 ± 3.205
2016/2017	40 ± 17.508	32 ± 14.504	4 ± 4.52	1 ± 0.635	17 ± 14.64	25 ± 13.581

	Shrub		**Sparse vegetation**	
Austral year	**Communal land**	**Protected area**	**Communal land**	**Protected area**
2012/2013	27 ± 13.791	21 ± 13.069	5 ± 3.143	2 ± 1.200
2013/2014	11 ± 6.196	16 ± 4.233	6 ± 4.891	5 ± 2.355
2014/2015	20 ± 12.349	31 ± 13.482	1 ± 0.805	0.4 ± 0.241
2015/2016	15 ± 7.987	31 ± 13.423	8 ± 4.953	10 ± 6.718
2016/2017	35 ± 13.067	39 ± 13.221	4 ± 2.366	4 ± 2.575

Sentinel-2

The dense shrub decreased from 2015/2016 (communal land = 45%, protected area = 29%) to 2016/2017 (communal land = 45%, protected area = 44%). However, 2015/2016 had nearly double the proportion of sparse vegetation (communal land = 31%, protected area = 26%) compared to 2016/2017 (communal land = 16%, protected area = 6%). These shifts in vegetation cover led to greater proportions of open shrub (communal land = 13%, protected area = 10%), and shrub in 2016/2017 (communal land = 25%, protected area = 39%), compared to 2015/2016 (open shrub: communal land = 3%, protected area = 2%; shrub: communal land = 20%, protected area = 35%) (Figure 8 and Table 7). The 2015/2016 growing season was the second and final year of the drought, 2016/2017 experienced above average rainfall (Chapter 3, Table 4, page 65) which aided in vegetation recovery after the drought.

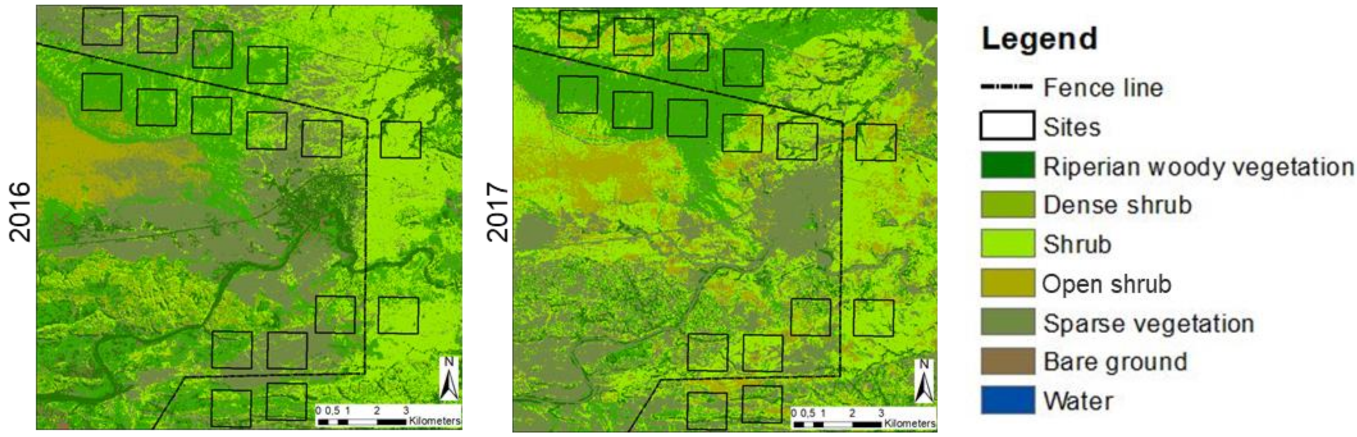

Figure 7: Sentinel-2 derived land cover classification (a) of the study sites along the north western fence line of the Greater Kruger National Park in May 2016 and 2017.

Table 8: Comparison of the percentage of pixels (mean ± SE) that fall within the five land cover classes obtained from the Sentinel-2A Level 1C land cover dataset for 2016/2017, for the two sites across the fence line, the protected area and the communal land.

	Dense shrub		**Open shrub**		**Riparian woody vegetation**	
Austral year	**Communal land**	**Protected area**	**Communal land**	**Protected area**	**Communal land**	**Protected area**
2015/2016	45 ± 16.071	29 ± 12.379	3 ± 1.116	2 ± 1.021	2 ± 1.554	8 ± 1.964
2016/2017	42 ± 18.841	26 ± 12.939	7 ± 3.068	13 ± 3.978	3 ± 1.464	11 ± 2.21

	Shrub		**Sparse vegetation**	
Austral year	**Communal land**	**Protected area**	**Communal land**	**Protected area**
2015/2016	20 ± 6.519	35 ± 13.15	31 ± 13.944	26 ± 12.493
2016/2017	34 ± 11.414	37 ± 9.681	15 ± 6.287	12 ± 7.512

4. Discussion

4.1. Land use effect on land cover

The MODIS platform classified most of the sites as grass, with very little broad leaf trees, which is inaccurate for this region. Although it is a savanna, the northern sites fall within a mopane dominated vegetation type where the herbaceous cover is poor, and the southern sites fall into a vegetation type with a co-dominance of both grass and tree species (Mucina and Rutherford 2006). Many studies have found the land cover assessments of heterogenous vegetation structures such as savannas and small patch sizes of the various savanna intermediates to be easily misclassified with many land cover classification platforms (Latifovic and Olthof 2004, Gessner *et al.* 2013). The MODIS Land Cover Type

(MCD12Q1) has revealed errors in mixed and heterogenous land cover classes (Gessner *et al.* 2013, Adole *et al.* 2018), especially for mixed trees, shrublands, and herbaceous vegetation (Herold *et al.* 2008, Gessner *et al.* 2013).

The MODIS Land Cover Type (MCD12Q1) was simply used in order to assess land cover change over the entire study period, as this was not possible with the Landsat 8 and Sentinel-2 datasets. The MODIS platform may have had the most-coarse spatial resolution (500 m) with high misclassification, but this assessment highlighted differences across the fence line for all five represented land cover classes. The land cover classes of cereal crops and broad leaf crops were only present within the communal land and were detected within a site just south of Bende Mutale, the village that borders Pafuri. This site was the closest site to the village. The presence of the cereal and broad leaf crop classes is likely indicative of the subsistence crop farming that is known to occur within the rural communities in Venda (Paumgarten *et al.* 2018). The difference in proportion of dense shrub across the fence line was not significantly different, for either the Landsat 8 or Sentinel-2 assessments. However, the greater proportion of dense shrub for both assessments was detected in the communal land. The mean pixel percentages differed by 8% for Landsat 8, however, for Sentinel-2, the communal land had 16% more dense shrub. This slight difference may be indicative of the higher utilisation of woody species for browsing and coppicing after wood harvesting within the communal land. Thinning of *C. mopane,* in particular, tends to increase the canopy diameter of the existing trees, by reducing inter-tree competition (Smit 2014). Depending on the ratio of coppicing to herbivory this slightly higher dense shrub cover may also be indicative of intensive coppicing or bush encroachment. *Terminalia sericea*, a common woody species that would be found within the northern and southern sites, displays vigorous coppiced regrowth when harvested by humans (Neke *et al.* 2006) and is prone to encroachment in heavily grazed areas (Papanastasis 2009). The insignificant differences in land cover between the protected area and communal land, as detected by Landsat 8 and Sentinel-2 suggests that differences in land use in this semi-arid savanna system may not always induce changes in land cover. As much as the village itself has converted land cover from naturally vegetated to what would be classified as bare ground in this study, the study suggests that the land cover of the surrounding communal land was generally similar to that of the protected area, when only focused on the five land cover classes identified.

Some studies that compared vegetation cover between communal lands and protected areas used tree cover as a proxy for vegetation cover change (Nacoulma *et al.* 2011, Wessels *et al.* 2011). These studies have found significant differences in vegetation cover between protected areas and communal rangelands. However, the results differ depending on the intensity of the disturbances experienced on either side of the fence. Wessels *et al.* (2011) compared multiple communal land and protected area sites around Sabie Sands and Kruger National Park and found that heavily utilised sites showed a reduction in woody cover compared to the protected area site. However, they also found two communal land sites to have double the woody cover compared to the protected area sites. They believed this to be a result of tree damage and removal due to the high elephant densities within the protected areas (Wessels *et al.* 2011, Mograbi *et al.* 2017). Similarly, Nacoulma *et al.* (2011) compared parts of the W National Park and adjacent communal lands, in the south-eastern part of Burkina Faso. A reduction of woody vegetation cover was found in the communal lands compared to the protected area. However, they established and highlighted that traditional land use does not always result in land cover change and degradation. This statement supports the results of this study, where little evidence of land cover change between the protected area and communal land was found based on the five classification classes used for Landsat 8 and Sentinel-2. The lack of a considerable difference in land cover may be due to near equal damage to, or loss of, woody vegetation within the communal land caused by woody harvesting and elephant damage within the protected area. Fisher *et al.* (2015) conducted a fence line study in the southern part of KNP, comparing woody structure between a communal land and the protected area. They found that the communal land had more than double the number of tall trees, which may have been due to the conservation of larger trees for cultural reasons. On the other hand, the protected area showed major decreases in trees, to which Fisher *et al.* (2015) attributed to the elephant damage. Additionally, woody vegetation shifts to short woodlands, with low large tree densities, in landscapes with high elephant densities, as elephants generally have an impact on tree structure rather than the composition of species (Trollope *et al.* 1998) which may account for the slightly lower dense shrub cover in the protected area. Although the Landsat 8 and Sentinel-2 results suggested little significant differences in land cover across the fence, these studies show that the response of vegetation in the form of vegetation cover change between protected areas and communal lands depends on the severity and frequency of disturbances in the form of herbivory and human activities.

4.2. Land cover change due to extreme climatic events

Anthropogenic activities are the most direct cause of land cover change; however, land cover still changes in response to alterations in climatic variables (Dube and Pickup 2001, Wessels *et al.* 2004, Vanacker *et al.* 2005). Additionally, land cover change is affected by drivers at different scales. Local scale drivers of land cover change include heavy grazing as a result of high stocking (Archer *et al.* 1995, Van Langevelde *et al.* 2003, Gillson 2004), different fire regimes (Trollope 1982, Briggs *et al.* 2005), and the exclusion of fire and herbivory (Silva *et al.* 2001, Wigley *et al.* 2010). Fire does not play as great a role in defining the savanna structure in the Pafuri region, as there is a very long fire return of more than ten years (Du Toit *et al.* 2003). Changing climate conditions, including increased rainfall variability, changing temperatures, and elevated CO_2 concentrations are among the global scale drivers of land cover change (Wigley *et al.* 2010). Land cover change may be a result of only local drivers or only global drivers, or both, and the degree of change will most likely depend on the resilience of the savanna system and that of the species within it.

The redundancy analyses conducted for each of the three land cover assessments suggests that inter-annual variability in rainfall and possibly temperature, is resulting in changes in land cover within the semi-arid region this study focused on. More specifically, the occurrence of extreme climatic events led to shifts in land cover in both the communal land and protected area during the seven years that were investigated. Landsat 8 showed that land cover change was evident after both extreme events. The year after the flood showed a decrease in dense shrub and shrub while open shrub, riparian woody vegetation and sparse vegetation increased. In general, both drought years showed an increase in dense shrub and shrub and a decrease in open shrub, shrub and riparian woody vegetation. Sparse vegetation decreased during the first drought year but increased during the second drought year. However, MODIS only picked up change after the flood year with a decrease in in deciduous broadleaf trees and an increase in grass for both the protected area and communal land. Sentinel-2 showed land cover changes after the final drought year, with a decrease in dense shrub and sparse vegetation and an increase in the remaining land cover classes. MODIS and Landsat 8 both showed evidence of a decrease in woody cover after the flood year. Similarly, Landsat 8 and Sentinel-2 showed evidence of an increase in woody cover after the drought. There is some evidence supporting these findings, where spatial patterns of land cover change is influenced by short-term variability in rainfall (Lambin and Ehrlich 1997, Fensham *et al.* 2005, Vanacker *et al.* 2005, Garrard *et al.* 2016). Wigley *et al.* (2010) assessed thicket expansion under different land use pressures between sites within communal lands, a commercial farming area and a protected area in the Hluhluwe region using aerial photographs from 1937, 1960 and 2004. Regardless of land use, there was similar woody cover change across the sites over a relativity short time, indicating common global drivers influencing woody cover. These finding align with those of the significant Landsat 8 model in this study, indicating an increase of dense shrub across the growing seasons, in other words, a bush encroachment signal. Conversely, Aleman *et al.* (2016) established land use to be the main cause of woody cover change, rather than due to changes in rainfall, across sub-Saharan Africa. Typically, land cover change due to anthropogenic activities develop in the short term compared to land use change induced by changing environmental factors which develop over a longer period (Davies-Barnard *et al.* 2015). Although the study period was very short in relation to other studies that assess vegetation response to environmental variables, the occurrence of both a flood and drought event and the resultant very high rainfall variability (interannual CV = 45%) is likely why all the land cover models yielded time (year) to be the most important factor. The redundancy analysis for Sentinel-2 may be used as an indicator of how the land cover altered after the drought. The 2016/2017 growing season experienced the second greatest total annual rainfall (after that of the flood year) for the study extent (Chapter 3, Table 4, page 65). Thus, the final season of the study can be seen as a “recovery” growing season, and the analysis suggests that the interannual change, most likely due to the increase in rainfall, resulted in considerable change in land cover for both the protected area and communal land. Vegetation productivity can recover quickly after a drought if the succeeding growing seasons have sufficient rainfall (Vetter 2009).

Although the models yielded by the three land cover assessments showed contradictory changes in vegetation over time -either an increase or decrease in woody vegetation over time- all the models suggested short-term change in the tree-grass ratio of the savanna. Overall, MODIS suggested a reduction on woody cover and an increase in grassy cover. Similarly, Sentinel-2 suggested a reduction in dense woody cover, after the drought, while Landsat 8 suggested an increase in dense woody cover. Then again, the images obtained from these three platforms represent different temporal scales, and these differences between the models are most likely due to interannual change in land cover, as the land cover from the three assessments responded similarly to the flood and drought events.

4.3. Study limitations

For fine scale studies, such as this one, ground truthing would be highly beneficial to better evaluate the accuracy of the land cover classification. This addition may also provide an opportunity for more classification classes, which could show differences across the fence line as well as provide more detailed insight into the response of vegetation cover to extreme climatic events. The Landsat 8 and Sentinel-2 classes did not include an agricultural crop class or a grass/herbaceous layer class, however, these could have been added with the aid of ground truthing. This would likely show a stronger difference across the fence line due to the agricultural crops and likely difference in herbivore densities, as the MODIS images highlighted. Adding a grass class may have highlighted differences across the fence line in the southern sites where *Digitaria eriantha, Panicum maximum* and *Pogonarthria* *squarrosa* are some of the common grass species found within the Makuleke Sandy Bushveld vegetation type (Mucina and Rutherford 2006). Unfortunately, the short duration site visit in November 2017 could not afford any ground truthing, thus the Landsat 8 and Sentinel-2 classifications were aided only by Google Earth, NIR and SWIR imagery of the sites, from which it was difficult to identify agricultural crops, a grass/herbaceous layer and anything other than the five classes that were used. It would be premature to conclude that there is no difference in land cover across the fence until more land cover classes, including agricultural crops and grass/herbaceous layer, have been added. Vegetation type was also not taken into account for the land cover classifications. The effect of vegetation type on vegetation phenology was tested in Chapter 2, where it was found to significantly influence phenology, however, the two dominant vegetation types, Musina Mopane Bushveld (northern sites) and Makuleke Sandy Bushveld (southern sites) were nearly equally distributed across the protected area and communal land, and so vegetation type was not included in the land cover analyses.

5. Conclusion

All three land cover assessments showed change in land cover across the austral seasons from 2011-2017. MODIS and Landsat 8 showed changes in land cover after the flood year for both the communal land and protected area with a decrease in woody cover in the year after the flood. Landsat 8 and Sentinel-2 displayed changes in land cover after the drought event with an increase in woody vegetation cover for both sides of the fence. Of the three land cover assessments, only MODIS yielded significant differences in land cover due to land use. Although agricultural crops were evident in the communal lands, which were not distinguished for the Landsat 8 and Sentinel-2 assessments, the MODIS land cover classification misclassified grass to be the dominant vegetation class (communal land = 83%, protected area = 95%) across the study sites. It would be premature, however, to conclude that there is no significant difference in land cover between the protected area and communal land in this region until a grass/herbaceous layer class as well as an agricultural crop class is added to the Landsat 8 and Sentinel-2 assessments. Variability in rainfall, in terms of mean annual rainfall and distribution, of semi-arid savannas is expected to increase with the increasing effects of climate change over time (Chamaille-Jammes *et al.* 2006). Thus, understanding how land cover changes at local scales in response to interannual variation, as well as extreme climatic events, will help to develop mitigation strategies to deal with any negative changes in vegetation cover that will affect the livelihoods of local communities and landscape level biodiversity and conservation efforts (Bewket and Abebe 2013, Muhati *et al.* 2018).

Chapter 5

Synthesis

1. Synthesis and summary of major findings

Savannas are complex systems with varying proportions of trees and grass depending on several ecological and environmental factors including rainfall, temperature, and the degree of disturbances such as fire and herbivory as well as how these variables interact. These ecological and environmental factors interact creating heterogeneity at a range of temporal and spatial scales (Gillson 2004). Gillson (2004) created a spatio-temporal framework, based on the Hierarchical Patch Dynamic Paradigm, to assess how savanna vegetation dynamics at various spatial scales are influenced by these factors (Figure 1). This framework can also be applied to the findings of this study to aid in the understanding of how the vegetation dynamics (phenology and land cover) interact with small scale and broad scale factors (land use and climatic variables).

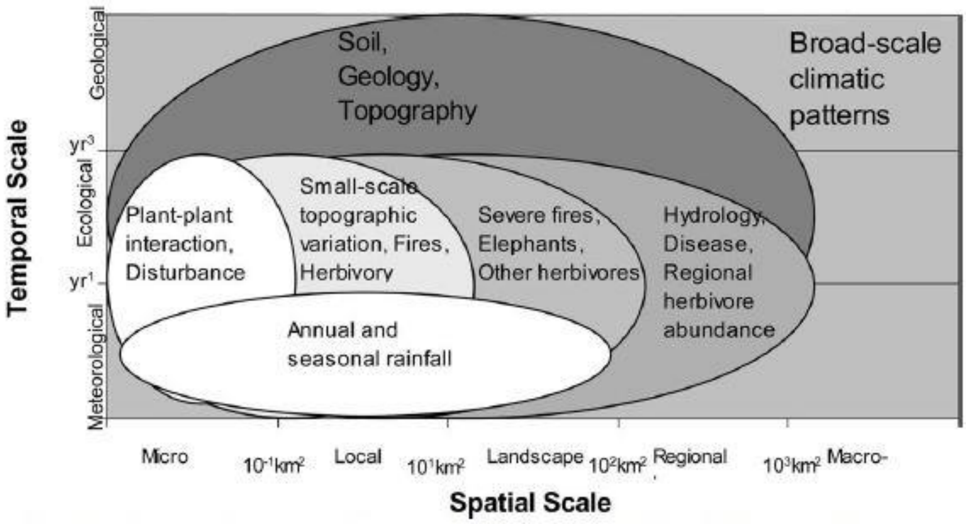

Figure 1: Spatio-temporal framework diagram, based on the Hierarchical Patch Dynamic Paradigm, used to assess how savanna vegetation dynamics are influenced by the interaction of ecological and environmental variables and multiple temporal and spatial scales (Gillson 2004).

1.1. Vegetation response to land use during growing seasons with extreme climatic events

Vegetation response to land use

The spatial aspect of this study was used to determine how vegetation phenology (Chapter 2) and land cover (Chapter 4) differed under different land management practices of a communal rangeland and an adjacent protected area. Land use and management practice has a top down effect on vegetation dynamics through human related and -typically- greater 'herbivory' (utilization) disturbances within communal land, and elephant and other herbivore disturbances within the protected area. These disturbances would influence vegetation phenology at the micro and local scales, while land cover is more susceptible to change at the local and landscape scales (Figure 1). This study established that although vegetation type (landscape scale) significantly influenced vegetation phenology, land use was the main driver of the significant differences in phenology in the semi-arid savanna that was assessed. The communal land had the significantly earlier $Start_T$ of six days, a longer growing season of five days and 1% greater productivity compared to the protected area. However, the protected area was the "greener" side of the fence with 1% more seasonally active vegetation (Chapter 2).

Although the phenology showed change in response to land use at the local scale, land cover change across the fence line was not as clear cut. Only the MODIS land cover classification showed a large significant difference in land cover between the communal land and protected area, with the communal land showing a greater proportion of woody vegetation. However, the MODIS assessment misclassified most of the study area as grass (communal land = 83%, protected area = 95%) (Chapter 4). Riparian woody vegetation was the only land cover class to show a significant difference between the protected area and communal land for Landsat 8 and Sentinel-2, however this represents a very small proportion of land cover for both sides of the fence (Landsat 8: communal land = 14%, protected area = 17%; Sentinel-2: communal land = 3%, protected area = 9%). Nevertheless, the presence of this class does indicate vegetation that is more water dependent, and found within low lying areas, along small tributaries or small valleys within the study area, with species such as *Hyphaene natalensis, Lonchocarpus capassa*, and *Acacia xanthoploea* (Mucina and Rutherford 2006). While not significantly different across the fence for either Landsat 8 or Sentinel-2, dense shrub was the dominant land cover class for both assessments (Landsat 8: communal land = 50%, protected area = 42%; Sentinel-2: communal land = 43%, protected area = 28%). It would, however, be premature to conclude that there were no significant differences in land cover across the fence, as grass and crop agriculture were not included in the land cover classifications for the Landsat 8 and Sentinel-2 assessments. This was due to the method used to establish training pixels for the classification classes. Without ground truthing the classes were established using Goggle Earth, SWIR and NIR images of the study area. With these images crop agriculture and grass were difficult to distinguish (Chapter 4).

Vegetation response to conditions associated with floods and drought

In terms of this study, the broad scale climatic patterns would be the ENSO episodes and the associated changes in rainfall and temperature, and the local climate of the Pafuri region which has highly variable annual rainfall (CV >40 (Mucina and Rutherford 2006)), but would fall under the local scale climatic patterns. As savannas in southern Africa are naturally drought prone and flooding does occur occasionally (Gibberd 1996), the interaction of the broad scale and local scale climatic variables is what determines the severity of extreme events including floods and droughts. Which is depicted in the Gillson (2004) framework by the influence of the broad scale climatic patterns on the remaining variables and the smaller scales (Figure 1). In Chapter 3 and part of Chapter 4 the temporal aspects of vegetation response were assessed- how vegetation phenology (Chapter 3) and land cover (Chapter 4) responded to conditions associated with flood and drought events. This study found no major correlations between EVI and the environmental variables that were selected (rainfall, temperature and photoperiod; Chapter 3), and rainfall only showed a weak positive relationship with EVI, which is contradictory to most phenological studies. The onset of rainfall and the onset of the growing seasons showed no correlation, likely due to the contrasting phenologies of the prominent woody species. Nevertheless, rainfall variability across the growing seasons significantly influenced changes in most of the phenometrics. Unsurprisingly, the flood year showed the longest growing season (protected area: 229 days; communal land: 244 days; $p<0.05$) and yielded the greatest vegetation productivity (flood year to first drought year: protected area= 13% decrease; communal land= 13% decrease, $p<0.05$; flood year to second drought year: protected area= 9% decrease; communal land= 8% decrease, $p<0.05$) despite the presence of high cloud cover over the period when the peak in EVI should have occurred. Which most likely led to an inaccurate $Start_T$ and peak EVI and would have affected many of the remaining phenometrics. There was some evidence of land use influencing the response of vegetation phenology to the conditions associated with the flood and drought years. $Start_T$, $Peak_T$ and Mid_T were the only phenometrics to show significant differences between the communal land and protected area as a result of the conditions associated with the flood year and first drought year (Chapter 3). However, the results from the land cover analysis (Chapter 4) showed land use to have minor differences and minimal effect on land cover change across the growing seasons. However, both the phenological analysis (Chapter 3) and the land cover analysis (Chapter 4) highlight the greater effect of the 2013 flood episode -above average rainfall- for both the communal land and protected area. Land cover change across the austral seasons, 2011-2017, was detected by all three land cover assessments (Chapter 4). The land cover derived from MODIS did not change after the drought event. However, as with the Landsat 8 assessment, change was detected after the flood year showing a decrease in woody cover for both sides of the fence. Land cover change after the drought was detected by Landsat 8 and Sentinel-2, suggesting an increase in woody vegetation cover for both the protected area and communal land.

The broad scale ENSO patterns, variability of seasonal rainfall and local scale variables interacted to drive the response of vegetation under different land uses to conditions associated with extreme climatic events. Changes in both land cover and phenology will in turn have an effect on albedo, carbon sequestration, evapotranspiration and productivity, which could create a feedback effect on the interaction of the broad scale and local scale climatic variables.

2. Implications for local communities and protected areas

Worldwide, millions of people rely on ecosystem services provided by savannas particularly for livestock grazing, fuel wood harvesting, and harvesting of non-timber forest products (NTFP) (Wessels *et al.* 2011, Jurisch *et al.* 2012). In southern Africa, the tree-grass ratio and structure of a savanna is typically established through interactions between soil type, climate and disturbance regimes, particularly fire and herbivory (Sankaran *et al.* 2005). However anthropogenic activities change the impact these regimes have on savanna vegetation (Aleman *et al.* 2016). Short term disturbances within the local scale in the form of fire, herbivory or human activity may have beneficial or adverse effects on savannas depending on the severity and frequency of the disturbance. Beneficial effects may include increased nutrient cycling, greater seedling establishment, longer growing seasons, increased productivity and increased species diversity (Denslow 1980, Mladenoff 1987, Dean and Milton 1991, Shackleton *et al.* 1994). While adverse effects could include reduced canopy cover, delayed onset of growing season, decreased productivity and increased soil erosion (Rao *et al.* 1990, Shackleton *et al.* 1994). This study suggests that bush encroachment may be the reason for the increased productivity in the communal land as well as the difference in dense shrub between the two sites. The increases of woody plant cover in savannas, typically due to bush encroachment, reduces grazing availability, which affects livestock in communal areas as well as grazers in protected areas. Changes in land cover as a result of communal land use would depend on the size of the settlement, the population, and the likelihood of its expansion based on locality.

The study area falls within the Limpopo river catchment area (Sitoe *et al.* 2015), and although the study area received above average rainfall in mid-January 2013 (Chapter 3), the flood event itself was not considered severe for the nearby rivers. However, it was devastating for low lying areas of Mozambique into which these rivers feed further downstream (Manhique *et al.* 2015). Similarly, the drought event was not nearly as severe as was experienced slightly further south in the northern parts of Mpumalanga which incorporate the southern section of the Kruger National Park. Nevertheless, vegetation phenology and land cover still responded notably to the changes caused by these events. If these differences are being detected in response to less severe flooding and drought events, there may be extreme vegetation change in response to the more severe and frequent climatic events predicted for the future, potentially threatening biodiversity and food security in savannas. This would affect the livelihoods of rural communities and self-sufficient farmers throughout southern Arica and impact land managers within commercial, rural and conservation settings. This uneven distribution of extreme climatic events across similar landscapes highlights the necessity of monitoring the responses of various vegetation types as well as vegetation under different land use pressures and disturbances to increased climatic variability typically associated with extreme climatic events. This study shows that the effects of these disturbances will also vary depending on the land use and management practices, as well as the influence of broad scale and local scale climatic variables.

3. Vulnerability of savannas under the predicted changes

Changes in global climate are leading to extreme climatic events, such as floods and droughts, becoming more severe and frequent (Bloor *et al.* 2010). Among increases in global temperature, increasing atmospheric CO_2 concentrations and changes in regional rainfall patterns; human activity is leading to changes in vegetation dynamics worldwide. This study has shown that land use, as well as shifts in climatic variables, have the potential to change vegetation phenology and land cover. Natural vegetation stands little chance against extreme land use change, such as large agricultural conversions and urban developments. However, vegetation has the potential to adapt to less intrusive land use and minor changes in climate. This adaption may result in shifts in the tree-grass ratios of savannas, leading to biome shifts which ultimately influence conservation, land use and human livelihoods and regional climate (Wigley *et al.* 2010). Although, this study suggests that the change in land use generally led to longer growing seasons and increased productivity, the occurrence of drought led to a reduction in growing season length and productivity for not only the communal lands but the protected area too. However, the growing season following the drought had increased productivity, growing season length and some evidence of vegetation cover recovery as a result of the increased rainfall. In southern Texas, USA, the drought of the 1950's resulted in significant woody cover loss, yet in the post-drought years there was a considerable increase in woody cover, which led to an overall net increase of woody vegetation from 1941 to 1983 (Archer *et al*. 1988). Anchang *et al.* (2019) found the same response in woody vegetation cover over 32 years in savannas of West Africa, after the droughts of the 1970's and 1980's. If the frequency and severity of droughts are predicted to increase, this recovery of woody species after drought events may not occur or there may not be sufficient time for the woody vegetation to recover, and hence over time a reduction in woody cover may follow. In contrast, bush encroachment is an increasing threat to savannas due to changes in rainfall distribution and increasing temperatures, high intensity grazing and exclusion of fire (Shackleton *et al.* 1994). Bush encroachment of *Eucalyptus* in the semi-arid savanna of north-western New South Wales, Australia, tends to happen in wet periods when soil moisture is appropriate for seedlings to outcompete the grassy layer. It is believed that historically hot fires fuelled by the increased grass biomass created during these wet periods would have reduced the success of the *Eucalyptus* recruitment and maintained the savanna structure (Hodgkinson 1991, Fensham *et al.* 2005). However, these hot fires were controlled and reduced by management. Bush encroachment is a common adaption by woody vegetation after increased herbivory or increases in CO_2 concentrations (Skarpe 1990, Scheiter and Higgins 2009, Wigley *et al.* 2010, Higgins and Scheiter 2012). Studies predicting changes in global and regional climate conditions predict that these changes have the potential of increasing woody cover. Atmospheric CO_2 and increases in temperature are more likely to lead to the increase of woody species rather than grasses (Scheiter and Higgins 2009).The change in vegetation structure of savannas also has knock-on effects for phenology. More severe changes in land cover will lead to extreme changes in savanna systems, which may include reduced productivity and biodiversity. Savannas in the Brazilian *cerrado* are among several highly threatened biomes due to large-scale agricultural conversion to mainly cattle and soybean farming. These land use changes have had considerable impact on fire regimes, water pollution and have led to biodiversity loss. In the last 50 years more than 50% of the *cerrado* has been transformed due to land use change (Klink and Machado 2005).

How the drivers of vegetation change will interact within and between the various spatial and temporal scales is still uncertain. Due to their complexity, savannas are predicted to be influenced extensively by changes in land use, climate, nitrogen deposition, atmospheric CO_2 and biotic exchange (Sala *et al.* 2000). Effective mitigation planning will rely on understanding as much about the response of various savannas to land use change of various intensities as well as to the predicated changes in climate. How savannas inevitably respond to these changes will depend on the resilience of the species and the system, in terms of the disturbance and pressures it experiences.

4. Study limitations and suggestions for future research

Limitations

A major limitation to this study was cloud cover. Cloud cover over the time in which the flood years EVI peak was expected to occur resulted in a plateaued EVI curve for that season due to degraded time series data.. The underestimated peak in EVI would have influenced most of the phenometrics for that growing season- fortunately, many of the phenometrics still highlighted the difference in phenology to that of the drought years. Due to cloud cover the establishment of land cover change from the StartT to the EndT based on the Landsat images for the flood and drought years was not possible.

Ground truthing for both the phenology and land cover aspects would be highly recommended for small scale, localised studies such as this one. Correlating the most recent seasons' remotely sensed phenology with phenology measured at the study sites would have assessed the accuracy of the phenological measurements that were acquired from the MODIS EVI data. And ground truthing would have been extremely beneficial for the land cover assessment. Training pixels for the land cover analysis were only based on NIR, SWIR and Google Earth images of the study site. Although the NIR and SWIR provides some insight into differentiating between broadleaf and "greener" vegetation, it is likely that some areas were inaccurately classified. Vegetation sampling for physiognomic type (i.e. grass, shrub or taller woody vegetation) as well as broad species identification aided by the known vegetation types may produce more accurate land cover classes that may highlight the changes across the seasons as well as establish if there is any land cover change between the two land use types.

Suggestions for future research

Although the influence of vegetation type on phenology across the fence line was assessed, the effect of vegetation type across the seasons was not assessed. The Musina Mopane Bushveld (northern sites) and Makuleke Sandy Bushveld (southern sites) suggested different phenology and may have responded differently to the conditions associated with flooding and drought. Correlating EVI and the phenometrics from the northern and southern sites separately with the environmental variables may have shown different responses. It is likely that combining these two vegetation types may have clouded the responses.

The location of this study provides an interesting opportunity to study vegetation response to not only the contrast between communal land and protected area, but rather the transition of a communal land to protected area. The Makuya Nature Reserve was established in 1987 (Medvey 2010), when the original fence line between existing communal lands and Kruger National Park was dropped. Expanding this study to incorporate the contrast created by the original fence line between Kruger National Park and the now Makuya Nature Reserve, would thus create three different contrasts as opposed to two.

The local scale of this study allows for more focus on the influence of villages on the boundary of one of Africa's largest conservation areas. The impact of such a development is likely to vary depending on population size, scale of natural resource use, grazing and browsing pressure and rainfall variability. Thus, similar studies along the rainfall, as well as population gradient within savannas would benefit future monitoring and predictions of land cover response to the predicted increase in climate variability. Communal lands that border KNP further south provide several opportunities to replicate this study in conjunction with higher mean annual rainfall and population size in the local communities. Fire in these areas will also need to be included in assessing vegetation response to land use and climatic variables.

5. Conclusion

The main aim of this study was to assess vegetation response to land use and conditions associated with extreme climatic events in a southern African savanna. This was broken down into quantifying how land use and conditions associated with floods and drought influenced (1) vegetation phenology and (2) land cover change along the north-western fence line of the Greater Kruger National Park. This study has shown that differences in phenology across the fence line were driven by land use. However, there was insufficient evidence to conclude that land use had a significant effect on land cover change, yet there was evidence of more woody cover within the communal land. Both the phenology and land cover findings highlight the changes in vegetation dynamics as a result of the conditions associated with flood and drought events. This study highlights the impacts of extreme climatic events and the response of vegetation under different land management strategies to these events, as well as providing important insight for land managers and conservation practitioners, given the prediction of more frequent extreme climatic events across South Africa in the future (Figure 2).

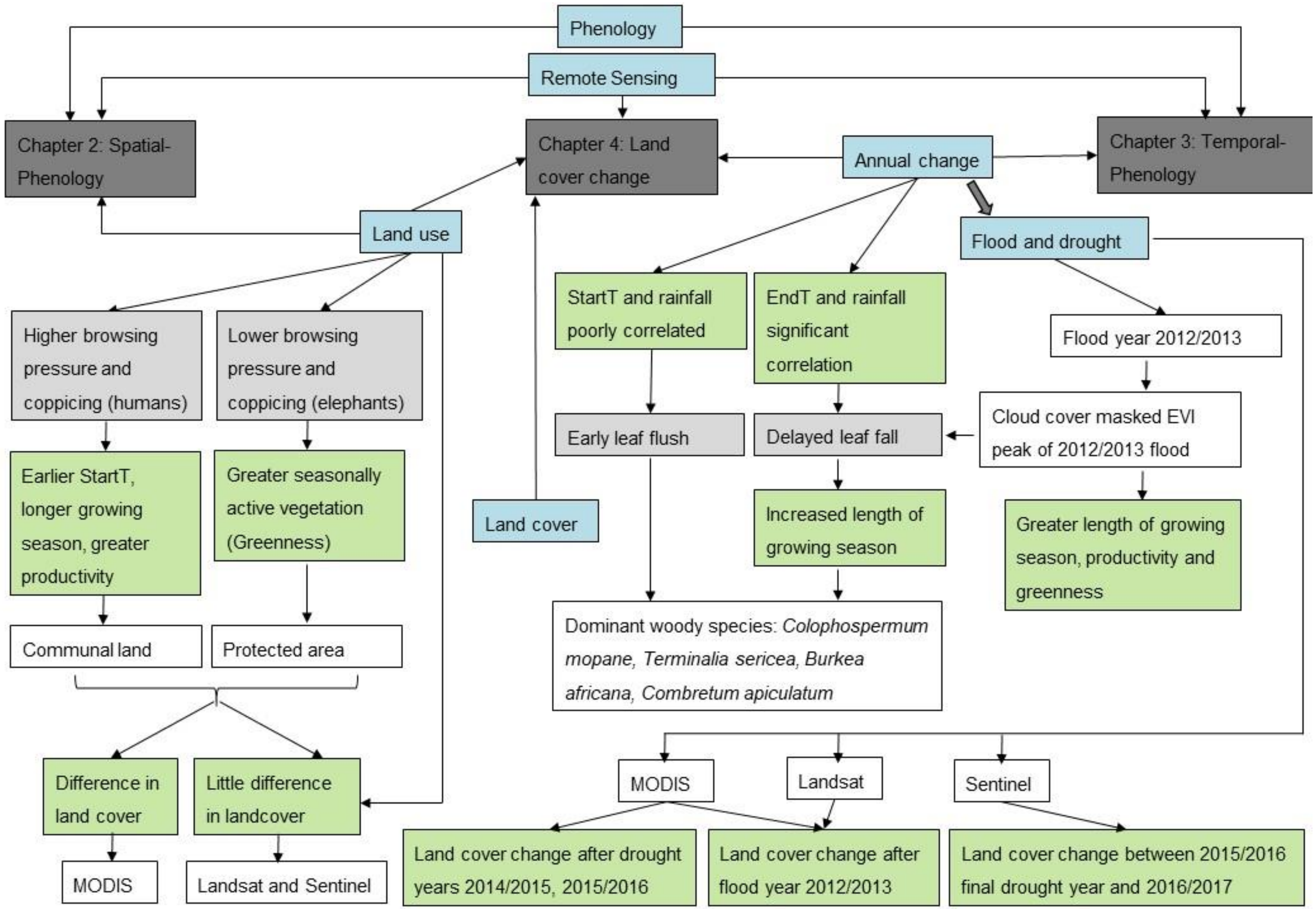

Figure 2: Graphical summary of the major findings of this study (green), what their likely causes are (light grey) and shared topics between chapters (blue) .

References:

Adole, T., Dash, J., and Atkinson, P.M., 2016. A systematic review of vegetation phenology in Africa. *Ecological Informatics*, 34:117–128.

Adole, T., Dash, J., and Atkinson, P.M., 2018. Characterising the land surface phenology of Africa using 500 m MODIS EVI. *Applied Geography*, 90:187–199.

Ainslie, A., 1999. When 'community' is not enough: Managing common property natural resources in rural South Africa. *Development Southern Africa*, 16:375–401.

Alados, C.L., Barroso, F.G., and García, L., 1997. Effects of early season defoliation on above-ground growth of Anthyllis cytisoides, a Mediterranean browse species. *Journal of Arid Environments*, 37:269–283.

Aleman, J.C., Blarquez, O., and Staver, C.A., 2016. Land-use change outweighs projected effects of changing rainfall on tree cover in sub-Saharan Africa. *Global Change Biology*, 22:3013–3025.

Anchang, J.Y., Prihodko, L., Kaptué, A.T., Ross, C.W., Ji, W., Kumar, S.S., Lind, B., Sarr, M.A., Diouf, A.A., and Hanan, N.P., 2019. Trends in woody and herbaceous vegetation in the savannas of West Africa. *Remote Sensing*, 11:576-593.

Anderson, T.M., Ritchie, M.E., Mayemba, E., Eby, S., Grace, J.B., and McNaughton, S.J., 2007. Forage Nutritive Quality in the Serengeti Ecosystem: The Roles of Fire and Herbivory. *The American* Naturalist, 170:343–357.

Anthony, B.P., 2006. A View from the other side of the fence: Tsonga communities and the Kruger National Park, South Africa. Unpublished doctoral dissertation, Central European University, Budapest, Hungary.

Anttonen, S., Piispanen, R., Ovaska, J., Mutikainen, P., Saranpää, P., and Vapaavuori, E., 2002. Effects of defoliation on growth, biomass allocation, and wood properties of Betula pendula clones grown at different nutrient levels. *Canadian Journal of Forest Research*, 32:498–508.

Anyamba, A., Tucker, C.J., and Mahoney, R., 1999. From El Nino to La Nina: vegetation response patterns over east and southern Africa during the 1997–2000 period. *Journal of Climate*, 15:3096-3103.

Archer, S., Boutton, T.W., and Hibbard, K.A., 2001. Trees in grasslands: biogeochemical consequences of woody plant expansion. *In*: Global biogeochemical cycles in the climate system. *Elsevier*, 115–137.

Archer, S., Schimel, D.S., and Holland, E.A., 1995. Mechanisms of shrubland expansion: land use, climate or CO_2? *Climatic Change*, 29:91–99.

Archer, S., Scifres, C., Bassham, CR., Maggio, R., 1988. Autogenic succession in a subtropical savanna: conversion of grassland to thorn woodland. *Ecological Monographs,* 58:111–127.

Archibald, S. and Scholes, R.J., 2007. Leaf green-up in a semi-arid African savanna-separating tree and grass responses to environmental cues. *Journal of Vegetation Science*, 18:583–594.

Atzberger, C., Klisch, A., Mattiuzzi, M., and Vuolo, F., 2013. Phenological metrics derived over the European continent from NDVI3g data and MODIS time series. *Remote Sensing*, 6:257–284.

Augustine, D.J. and McNaughton, S.J., 1998. Ungulate effects on the functional species composition of plant communities: Herbivore selectivity and plant tolerance. *The Journal of Wildlife Management*, 62:1165–1183.

Augustine, D.J. and McNaughton, S.J., 2006. Interactive effects of ungulate herbivores, soil fertility, and variable rainfall on ecosystem processes in a semi-arid savanna. *Ecosystems*, 9:1242-1256.

Ault, T.R., Henebry, G.M., de Beurs, K.M., Schwartz, M.D., Betancourt, J.L., and Moore, D., 2013. The False Spring of 2012, Earliest in North American Record. *Eos, Transactions American Geophysical Union,* 94:181–182.

Badeck, F.-W., Bondeau, A., Böttcher, K., Doktor, D., Lucht, W., Schaber, J., and Sitch, S., 2004. Responses of spring phenology to climate change. *New Phytologist,* 162:295–309.

Bagan, H., Wang, Q., Watanabe, M., Yang, Y., and Ma, J., 2005. Land cover classification from MODIS EVI times-series data using SOM neural network. *International Journal of Remote Sensing*, 26:4999–5012.

Bartholomé, E. and Belward, A.S., 2005. GLC2000: a new approach to global land cover mapping from Earth observation data. *International Journal of Remote Sensing*, 26:1959–1977.

Baruch, Z., 1994. Responses to drought and flooding in tropical forage grasses. *Plant and Soil*, 164:97–105.

Bate, G. C., Furniss, P. R. and Pendle, P. G., 1982. Water relations in southern African savannas. *In:* Skarpe, C., 1990. Structure of the woody vegetation in disturbed and undisturbed arid savanna, Botswana. *Vegetatio,* 87:11–18.

Baudoin, M.-A., Vogel, C., Nortje, K., and Naik, M., 2017. Living with drought in South Africa: lessons learnt from the recent El Niño drought period. *International Journal of Disaster Risk Reduction*, 23:128–137.

Beater, M.M.T., Garner, R.D. and Witkowski, E.T.F., 2008. Impacts of clearing invasive alien plants from 1995 to 2005 on vegetation structure, invasion intensity and ground cover in a temperate to subtropical riparian ecosystem. *South African Journal of Botany*, 74(3):495-507.

Beck, P.S., Atzberger, C., Høgda, K.A., Johansen, B., and Skidmore, A.K., 2006. Improved monitoring of vegetation dynamics at very high latitudes: A new method using MODIS NDVI. *Remote Sensing of Environment*, 100:321–334.

Behnke, R.H., 1985. Measuring the benefits of subsistence versus commercial livestock production in Africa. *Agricultural Systems*, 16:109–135.

Beinart, W., 2008. *The Rise of Conservation in South Africa: settlers, livestock, and the environment* Oxford University Press, 1770-1950.

Bendix, J., Hupp, C.R., and others, 2000. Hydrological and geomorphological impacts on riparian plant communities. *Hydrological Processes*, 14:2977–2990.

Beniston, M. and Stephenson, D.B., 2004. Extreme climatic events and their evolution under changing climatic conditions. *Global and Planetary Change*, 44:1–9.

Benjaminsen, T.A., Rohde, R., Sjaastad, E., Wisborg, P., and Lebert, T., 2006. Land reform, range ecology, and carrying capacities in Namaqualand, South Africa. *Annals of the Association of American Geographers*, 96:524–540.

Berger, M., Moreno, J., Johannessen, J.A., Levelt, P.F., and Hanssen, R.F., 2012. ESA's sentinel missions in support of Earth system science. *Remote Sensing of Environment*, 120:84–90.

Bergström, R., Skarpe, C., and Danell, K., 2000. Plant responses and herbivory following simulated browsing and stem cutting of Combretum apiculatum. *Journal of Vegetation Science*, 11:409–414.

Bewket, W. and Abebe, S., 2013. Land-use and land-cover change and its environmental implications in a tropical highland watershed, Ethiopia*. International Journal of Environmental Studies*, 70:126–139.

Bloor, J.M.G., Pichon, P., Falcimagne, R., Leadley, P., and Soussana, J.-F., 2010. Effects of warming, summer drought, and CO_2 enrichment on aboveground biomass production, flowering phenology, and community structure in an upland grassland ecosystem. *Ecosystems*, 13:888–900.

Boke-Olén, N., Lehsten, V., Ardö, J., Beringer, J., Eklundh, L., Holst, T., Veenendaal, E., and Tagesson, T., 2016. Estimating and analyzing savannah phenology with a lagged time series model. *PLOS ONE,* 11:e0154615.

Borel, C.C. and Gerstl, S.A.W., 1994. Nonlinear spectral mixing models for vegetative and soil surfaces. *Remote Sensing of Environment*, 47:403–416.

Boschetti, M., Stroppiana, D., Brivio, P.A., and Bocchi, S., 2009. Multi-year monitoring of rice crop phenology through time series analysis of MODIS images. *International Journal of Remote Sensing*, 30:4643–4662.

Botha, J., Witkowski, E.T.F., and Shackleton, C.M., 2002. A comparison of anthropogenic and elephant disturbance on Acacia xanthophloea (fever tree) populations in the Lowveld, South Africa. *Koedoe*, 45:9-18.

Brannstrom, C., Jepson, W., Filippi, A.M., Redo, D., Xu, Z., and Ganesh, S., 2008. Land change in the Brazilian Savanna (Cerrado), 1986–2002: Comparative analysis and implications for land-use policy. *Land Use Policy*, 25:579–595.

Breshears, D.D., Cobb, N.S., Rich, P.M., Price, K.P., Allen, C.D., Balice, R.G., Romme, W.H., Kastens, J.H., Floyd, M.L., Belnap, J., and others, 2005. Regional vegetation die-off in response to global-change-type drought. *Proceedings of the National Academy of Sciences of the United States of America*, 102:15144–15148.

Brida, A.-B., Owiyo, T., and Sokona, Y., 2013. Loss and damage from the double blow of flood and drought in Mozambique. *International Journal of Global Warming*, 5:514–531.

Briggs, J.M. and Knapp, A.K., 1995. Interannual variability in primary production in tallgrass prairie: climate, soil moisture, topographic position, and fire as determinants of aboveground biomass. *American Journal of Botany*, 82:1024–1030.

Briggs, J.M., Knapp, A.K., Blair, J.M., Heisler, J.L., Hoch, G.A., Lett, M.S., and McCarron, J.K., 2005. An ecosystem in transition: Causes and consequences of the conversion of mesic grassland to shrubland. *BioScience*, 55:243–254.

Brown, M.E., de Beurs, K., and Vrieling, A., 2010. The response of African land surface phenology to large scale climate oscillations. *Remote Sensing of Environment*, 114:2286–2296.

Bruner, A.G., Gullison, R.E., Rice, R.E., and Da Fonseca, G.A., 2001. Effectiveness of parks in protecting tropical biodiversity. *Science,* 291:125–128.

Carter, A.J. and Rogers, K.H., 1995. A Markovian approach to investigating landscape change in the Kruger National Park rivers. *In:* Parsons, M., McLoughlin, C.A., Rountree, M.W., and Rogers, K.H., 2006. The biotic and abiotic legacy of a large infrequent flood disturbance in the Sabie River, South Africa. *River Research and Applications,* 22:187–201.

Chamaille-Jammes, S., Fritz, H., and Murindagomo, F., 2006. Spatial patterns of the NDVI–rainfall relationship at the seasonal and interannual time scales in an African savanna. *International Journal of Remote Sensing*, 27:5185–5200.

Chambers, L.E., Altwegg, R., Barbraud, C., Barnard, P., Beaumont, L.J., Crawford, R.J.M., Durant, J.M., Hughes, L., Keatley, M.R., Low, M., Morellato, P.C., Poloczanska, E.S., Ruoppolo, V., Vanstreels, R.E.T., Woehler, E.J., and Wolfaardt, A.C., 2013. Phenological changes in the southern hemisphere. *PLoS ONE*, 8:e75514.

Chen, J., Chen, J., Liao, A., Cao, X., Chen, L., Chen, X., He, C., Han, G., Peng, S., Lu, M., Zhang, W., Tong, X., and Mills, J., 2015. Global land cover mapping at 30m resolution: A POK-based operational approach. *ISPRS Journal of Photogrammetry and Remote Sensing*, 103:7–27.

Chen, P.-Y., Fedosejevs, G., Tiscareño-LóPez, M., and Arnold, J.G., 2006. Assessment of MODIS-EVI, MODIS-NDVI and VEGETATION-NDVI composite data using agricultural measurements: an example at corn fields in Western Mexico. *Environmental Monitoring and Assessment,* 119:69–82.

Chen, S., Jiang, H., Jin, J., and Wang, Y., 2017. Changes in net primary production in the Tianmu Mountain Nature Reserve, China, from 1984 to 2014. *International Journal of Remote Sensing*, 38: 211–234.

Chidumayo, E.N., 2001. Climate and Phenology of Savanna Vegetation in Southern Africa. *Journal of Vegetation Science*, 12:347-354.

Childes, S.L., 1988. Phenology of nine common woody species in semi-arid, deciduous Kalahari Sand vegetation. *Vegetatio*, 79:151–163.

Chmielewski, F.-M. and Rötzer, T., 2001. Response of tree phenology to climate change across Europe. *Agricultural and Forest Meteorology*, 108:101–112.

Chmielewski, F.-M., Müller, A., and Bruns, E., 2004. Climate changes and trends in phenology of fruit trees and field crops in Germany, 1961–2000. *Agricultural and Forest Meteorology*, 121:69–78.

Clark, M.L., 2017. Comparison of simulated hyperspectral HyspIRI and multispectral Landsat 8 and Sentinel-2 imagery for multi-seasonal, regional land-cover mapping. *Remote Sensing of Environment*, 200:311–325.

Cleland, E., Chuine, I., Menzel, A., Mooney, H., and Schwartz, M., 2007. Shifting plant phenology in response to global change. *Trends in Ecology and Evolution*, 22:357–365.

Coetzer, K.L., Erasmus, B.F.N., Witkowski, E.T.F., and Bachoo, A.K., 2010. Land-cover change in the Kruger to Canyons Biosphere Reserve (1993– 2006): A first step towards creating a conservation plan for the subregion. *South African Journal of Science*, 106:1-10.

Cousins, B., 1994. Livestock production and agrarian reform in South Africa. *In;* Dovie, D.B.K., Shackleton, C.M., and Witkowski, E.T.F., 2006. Valuation of communal area livestock benefits, rural livelihoods and related policy issues. *Land Use Policy*, 23:260–271.

Csillag, F. and Kabos, S., 2002. Wavelets, boundaries, and the spatial analysis of landscape pattern. *Écoscience*, 9:177–190.

Cubasch, U., Meehl, G.A., Boer, G.J., Stouffer, R.J., Dix, M., Noda, A., Senior, C.A., Raper, S., and Yap, K.S., 2001. Projections of future climate change. *In:* Climate Change 2001: The scientific basis. Contribution of WG1 to the Third Assessment Report of the IPCC (TAR). *Cambridge University Press,* 525-582.

Cullen, B.R., Chapman, D.F., and Quigley, P.E., 2006. Comparative defoliation tolerance of temperate perennial grasses. *Grass and Forage Science,* 61 (4):405–412.

Dadashpoor, H., Azizi, P., and Moghadasi, M., 2019. Land use change, urbanization, and change in landscape pattern in a metropolitan area. *Science of The Total Environment*, 655:707–719.

Dai, A., 2011. Drought under global warming: a review. *Wiley Interdisciplinary Reviews: Climate Change*, 2: 45-65.

Danell, K., Bergström, R., and Edenius, L., 1994. Effects of large mammalian browsers on architecture, biomass, and nutrients of woody plants. *Journal of Mammalogy*, 75 (4):833–844.

Dang, N.M., Babel, M.S., and Luong, H.T., 2011. Evaluation of food risk parameters in the day river flood diversion area, Red River delta, *Vietnam. Natural Hazards,* 56:169–194.

Davies-Barnard, T., Valdes, P.J., Singarayer, J.S., Wiltshire, A.J., and Jones, C.D., 2015. Quantifying the relative importance of land cover change from climate and land use in the representative concentration pathways. *Global Biogeochemical Cycles*, 29:842–853.

Dean, W.R.J. and Milton, S.J., 1991. Disturbances in semi-arid shrubland and arid grassland in the Karoo, South Africa: mammal diggings as germination sites. *African Journal of Ecology*, 29:11–16.

Defourny, P., Kirches, G., Brockmann, C., Boettcher, M., Peters, M., Bontemps, S., Lamarche, C., Schlerf, M., and Santoro, M., 2012. Land cover CCI. Product User Guide Version, 2. *In:* Yang, Y., Xiao, P., Feng, X., and Li, H., 2017. Accuracy assessment of seven global land cover datasets over China. *ISPRS Journal of Photogrammetry and Remote Sensing*, 125:156–173.

DeFries, R. and Bounoua, L., 2004. Consequences of land use change for ecosystem services: A future unlike the past. *GeoJourna*l, 61:345–351.

Dekker, B. and Smit, G.N., 1996. Browse production and leaf phenology of some trees and shrubs in different Colophospermum mopane savanna communities. *African Journal of Range and Forage Science*, 13:15–23.

Denslow, J.S., 1980. Patterns of plant species diversity during succession under different disturbance regimes. *Oecologia*, 46:18–21.

Di Gregorio, A., and L. Jansen. 2005. Land Cover Classification System. Report. Accessed June 12:2014. *In:* Grekousis, G., Mountrakis, G., and Kavouras, M., 2015. An overview of 21 global and 43 regional land-cover mapping products. *International Journal of Remote Sensing*, 36:5309–5335.

Dieppois, B., Pohl, B., Rouault, M., New, M., Lawler, D. and Keenlyside, N., 2016. Interannual to interdecadal variability of winter and summer southern African rainfall, and their teleconnections. *Journal of Geophysical Research: Atmospheres*, 121:6215-6239.

Dodd, D.E.S. and Jolliffe, I.T., 2001. Early detection of the start of the wet season in semiarid tropical climates of western Africa. *International Journal of Climatology*, 21:1251–1262.

Dovie, D.B., Witkowski, E.T., and Shackleton, C.M., 2003. Direct-use value of smallholder crop production in a semi-arid rural South African village. *Agricultural Systems*, 76:337–357.

Dovie, D.B.K., Shackleton, C.M., and Witkowski, E.T.F., 2006. Valuation of communal area livestock benefits, rural livelihoods and related policy issues. *Land Use Policy*, 23:260–271.

Drusch, M., Del Bello, U., Carlier, S., Colin, O., Fernandez, V., Gascon, F., Hoersch, B., Isola, C., Laberinti, P., Martimort, P., Meygret, A., Spoto, F., Sy, O., Marchese, F., and Bargellini, P., 2012. Sentinel-2: ESA's optical high-resolution mission for GMES operational services. *Remote Sensing of Environment*, 120:25–36.

Du Toit, J.T., Biggs, H.C., and Rogers, K.H., 2003. *The Kruger experience: ecology and management of savanna heterogeneity*. Island Press.

Dube, O.P. and Pickup, G., 2001. Effects of rainfall variability and communal and semi-commercial grazing on land cover in southern African rangelands. *Climate Research*, 17:195–208.

Duncan, A.J., Hartley, S.E., and Iason, G.R., 1998. The effect of previous browsing damage on the morphology and chemical composition of Sitka spruce (*Picea sitchensis*) saplings and on their subsequent susceptibility to browsing by red deer (*Cervus elaphus*). *Forest Ecology and Management*, 103: 57–67.

Eamus, D., 1999. Ecophysiological traits of deciduous and evergreen woody species in the seasonally dry tropics. Trends in *Ecology and Evolution*, 14:11–16.

February, E.C., Higgins, S.I., Bond, W.J., and Swemmer, L., 2013. Influence of competition and rainfall manipulation on the growth responses of savanna trees and grasses. *Ecology*, 94:1155–1164.

Fensham, R.J., Fairfax, R.J., and Archer, S.R., 2005. Rainfall, land use and woody vegetation cover change in semi-arid Australian savanna. *Journal of Ecology*, 93:596–606.

Fisher, J., Erasmus, B.F.N., Witkowski, E., van Aardt, J., Asner, G., Kennedy-Bowdoin, T., Knapp, D., Mathieu, R., and Wessels, K., 2009. Three-dimensional woody vegetation structure across different land-use types and -land-use intensities in a semi-arid savanna. *In:* 2009 IEEE International Geoscience and Remote Sensing Symposium. Presented at the 2009 *IEEE International Geoscience and Remote Sensing Symposium, Cape Town, South Africa*: IEEE, II-198-II–210.

Fisher, J.T., Erasmus, B.F.N., Witkowski, E.T.F., Van Aardt, J., Asner, G.P., Wessels, K.J. and Mathieu, R., 2014. Management approaches of conservation areas: Differences in woody vegetation structure in a private and a national reserve. *South African Journal of Botany*, 90:146-152.

Fisher, J.T., Witkowski, E.T.F., Erasmus, B.F.N., Mograbi, P.J., Asner, G.P., van Aardt, J.A.N., Wessels, K.J., and Mathieu, R., 2015. What lies beneath: detecting sub-canopy changes in savanna woodlands using a three-dimensional classification method. *Applied Vegetation Science*, 18 (3), 528–540.

Fitchett, J.M., Grab, S.W., and Thompson, D.I., 2015. Plant phenology and climate change: Progress in methodological approaches and application. *Progress in Physical Geography*, 39: 460–482.

Friedl, M., McIver, D., Hodges, J.C., Zhang, X., Muchoney, D., Strahler, A., Woodcock, C., Gopal, S., Schneider, A., Cooper, A., Baccini, A., Gao, F., and Schaaf, C., 2002. Global land cover mapping from MODIS: Algorithms and early results. *Remote Sensing of Environment*, 83:287–302.

Friedl, M.A., Sulla-Menashe, D., Tan, B., Schneider, A., Ramankutty, N., Sibley, A., and Huang, X., 2010. MODIS Collection 5 global land cover: Algorithm refinements and characterization of new datasets. *Remote Sensing of Environment*, 114:168–182.

Friedman, J.M. and Auble, G.T., 2000. *Floods, flood control, and bottomland vegetation. Inland Flood Hazards: Human, Riparian, and Aquatic Communities*. Cambridge University Press, Cambridge, UK, 219–237.

Fynn, R., Morris, C., and Kirkman, K., 2005. Plant strategies and trait trade-offs influence trends in competitive ability along gradients of soil fertility and disturbance. *Journal of Ecology*, 93 (2), 384–394.

Gadd, M.E., Young, T.P., and Palmer, T.M., 2001. Effects of simulated shoot and leaf herbivory on Garrard, R., Kohler, T., Price, M.F., Byers, A.C., Sherpa, A.R., and Maharjan, G.R., 2016. Land Use and Land Cover Change in Sagarmatha National Park, a World Heritage Site in the Himalayas of Eastern Nepal. *Mountain Research and Development*, 36:299–310.

Geerken, R., Zaitchik, B., and Evans, J.P., 2005. Classifying rangeland vegetation type and coverage from NDVI time series using Fourier Filtered Cycle Similarity. *International Journal of Remote Sensing*, 26:5535–5554.

Gessner, U., Knauer, K., Kuenzer, C., and Dech, S., 2015. Land surface phenology in a West African Savanna: impact of land use, land cover and fire. In: Remote Sensing Time Series. Springer, 203–223.

Gessner, U., Machwitz, M., Conrad, C., and Dech, S., 2013. Estimating the fractional cover of growth forms and bare surface in savannas. A multi-resolution approach based on regression tree ensembles. *Remote Sensing of Environment*, 129:90–102.

Gibberd, V., 1996. Drought risk management in southern Africa: the potential of long lead climate forecasts for improved drought management. University of Greenwich, Natural Resources Institute.

Gillson, L., 2004. Evidence of hierarchical patch dynamics in an East African savanna? *Landscape Ecology*, 19 (8), 883–894.

Giri, C. and Long, J., 2014. Land cover characterization and mapping of South America for the year 2010 using Landsat 30 m satellite data. *Remote Sensing*, 6:9494–9510.

Gong, P., Wang, J., Yu, L., Zhao, Y., Zhao, Y., Liang, L., Niu, Z., Huang, X., Fu, H., Liu, S., Li, C., Li, X., Fu, W., Liu, C., Xu, Y., Wang, X., Cheng, Q., Hu, L., Yao, W., Zhang, H., Zhu, P., Zhao, Z., Zhang, H., Zheng, Y., Ji, L., Zhang, Y., Chen, H., Yan, A., Guo, J., Yu, L., Wang, L., Liu, X., Shi, T., Zhu, M., Chen, Y., Yang, G., Tang, P., Xu, B., Giri, C., Clinton, N., Zhu, Z., Chen, J., and Chen, J., 2013. Finer resolution observation and monitoring of global land cover: first mapping results with Landsat TM and ETM+ data. *International Journal of Remote Sensing*, 34:2607–2654.

Grekousis, G., Mountrakis, G., and Kavouras, M., 2015. An overview of 21 global and 43 regional land-cover mapping products. *International Journal of Remote Sensing*, 36:5309–5335.

Guy, P.R., Mahlangu, Z., and Charidza, H., 1979. Phenology of some trees and shrubs in the Sengwa Wildlife Research Area, Zimbabwe- Rhodesia. *South African Journal of Wildlife Research*, 9:47-54.

Hachigonta, S., Reason, C.J.C., and Tadross, M., 2008. An analysis of onset date and rainy season duration over Zambia. *Theoretical and Applied Climatology*, 91:229–243.

Hall-Martin, A.J. and Fuller, N.G., 1975. Observations on the phenology of some trees and shrubs of the Lengwe National Park, Malawi. *South African Journal of Wildlife Research*, 5:83-86.

Hansen, M.C., Defries, R.S., Townshend, J.R.G., and Sohlberg, R., 2000. Global land cover classification at 1 km spatial resolution using a classification tree approach. *International Journal of Remote Sensing*, 21:1331–1364.

Hao, Z., Hao, F., Singh, V.P., and Zhang, X., 2018. Quantifying the relationship between compound dry and hot events and El Niño–southern Oscillation (ENSO) at the global scale. *Journal of Hydrology*, 567:332–338.

Heritage, G.L., Moon, B.P., Jewitt, G.P., Large, A.R.G., and Rountree, M., 2001. The February 2000 floods on the Sabie River, South Africa: an examination of their magnitude and frequency. *Koedoe*, 44:37–44.

Herold, M., Mayaux, P., Woodcock, C. E., Baccini, A., and Schmullius, C., 2008. Some challenges in global land cover mapping: An assessment of agreement and accuracy in existing 1 km datasets. *Remote Sensing of Environment*, 112:2538–2556.

Heumann, B.W., Seaquist, J.W., Eklundh, L., and Jönsson, P., 2007. AVHRR derived phenological change in the Sahel and Soudan, Africa, 1982–2005. *Remote Sensing of Environment*, 108:385–392.

Higgins, S.I. and Scheiter, S., 2012. Atmospheric CO_2 forces abrupt vegetation shifts locally, but not globally. *Nature*, 488:209–212.

Higgins, S.I., Delgado-Cartay, M.D., February, E.C., and Combrink, H.J., 2011. Is there a temporal niche separation in the leaf phenology of savanna trees and grasses? *Journal of Biogeography*, 38:2165–2175.

Higgins, S.I., Shackleton, C.M., and Robinson, E.R., 1999. Changes in woody community structure and composition under constrasting landuse systems in a semi-arid savanna, South Africa. *Journal of Biogeograph*y, 26:619–627.

Hodgkinson, K.C., 1991. Shrub recruitment response to intensity and season of fire in a semi-arid woodland. *Journal of Applied Ecology*, 1:60–70.

Hoell, A. and Cheng, L., 2018. Austral summer Southern Africa precipitation extremes forced by the El Niño-Southern oscillation and the subtropical Indian Ocean dipole. *Climate Dynamics*, 50 :3219–3236.

Hoffman, M.T., Skowno, A., Bell, W., and Mashele, S., 2018. Long-term changes in land use, land cover and vegetation in the Karoo drylands of South Africa: implications for degradation monitoring. *African Journal of Range and Forage Science*, 35: 209–221.

Horritt, M., 2003. Waterline mapping in flooded vegetation from airborne SAR imagery. *Remote Sensing of Environment*, 85:271–281.

Huete, A., Justice, C., and Liu, H., 1994. Development of vegetation and soil indices for MODIS-EOS. *Remote Sensing of Environment*, 49:224–234.

Hulme, M., Barrow, E.M., Arnell, N.W., Harrison, P.A., Johns, T.C., and Downing, T.E., 1999. Relative impacts of human-induced climate change and natural climate variability. *Nature*, 397:688-691.

Hunter, A.F. and Lechowicz, M.J., 1992. Predicting the Timing of Budburst in Temperate Trees. *Journal of Applied Ecology*, 29:597–604.

Illius, A.W. and O'connor, T.G., 1999. On the relevance of nonequilibrium concepts to arid and semiarid grazing systems. *Ecological applications*, 9:798–813.

Immitzer, M., Atzberger, C., and Koukal, T., 2012. Tree Species Classification with Random Forest Using Very High Spatial Resolution 8-Band WorldView-2 Satellite Data. *Remote Sensing*, 4:2661–2693.

Jarnagin, S.T., 2004. Regional and global patterns of population, land use, and land cover change: an overview of stressors and impacts. *GIScience and Remote Sensing*, 41:207–227.

Jewitt, D., Goodman, P.S., Erasmus, B.F., O'Connor, T.G., and Witkowski, E.T., 2015. Systematic land-cover change in KwaZulu-Natal, South Africa: Implications for biodiversity. *South African Journal of Science*, 111:01–09.

Ji, L. and Peters, A.J., 2003. Assessing vegetation response to drought in the northern Great Plains using vegetation and drought indices. *Remote Sensing of Environment*, 87:85–98.

Jia, K., Wei, X., Gu, X., Yao, Y., Xie, X., and Li, B., 2014. Land cover classification using Landsat 8 Operational Land Imager data in Beijing, China. *Geocarto International*, 29:941–951.

Jin, C., Xiao, X., Merbold, L., Arneth, A., Veenendaal, E., and Kutsch, W.L., 2013. Phenology and gross primary production of two dominant savanna woodland ecosystems in Southern Africa. *Remote Sensing of Environment*, 135:189–201.

Jolly, W.M. and Running, S.W., 2004. Effects of precipitation and soil water potential on drought deciduous phenology in the Kalahari. *Global Change Biology*, 10:303–308.

Jolly, W.M., Nemani, R., and Running, S.W., 2005. A generalized, bioclimatic index to predict foliar phenology in response to climate. *Global Change Biology*, 11:619–632.

Jönsson, A.M., Eklundh, L., Hellström, M., Bärring, L., and Jönsson, P., 2010. Annual changes in MODIS vegetation indices of Swedish coniferous forests in relation to snow dynamics and tree phenology. *Remote Sensing of Environment*, 114:2719–2730.

Jönsson, P. and Eklundh, L., 2004. TIMESAT—a program for analyzing time-series of satellite sensor data. *Computers and Geosciences*, 30:833–845.

Joubert, A.M., Mason, S.J., and Galpin, J.S., 1996. Droughts over southern Africa in a doubled-CO climate. *International Journal of Climatology*, 16:1149–1156.

Junk, W.J., Bayley, P.B., Sparks, R.E., and others, 1989. The flood pulse concept in river-floodplain systems. *Canadian special publication of fisheries and aquatic sciences,* 106:110–127.

Jurisch, K., Hahn, K., Wittig, R., and Bernhardt-Römermann, M., 2012. Population Structure of woody plants in relation to land use in a semi-arid savanna, West Africa. *Biotropica*, 44:744–751.

Kalema, V.N., Witkowski, E.T.F., Erasmus, B.F.N., and Mwavu, E.N., 2015. The impacts of changes in land use on woodlands in an equatorial African savanna: land use changes in an equatorial African savanna. *Land Degradation and Development*, 26: 632–641.

Kamusoko, C. and Aniya, M., 2007. Land use/cover change and landscape fragmentation analysis in the Bindura District, Zimbabwe. *Land Degradation and Development*, 18:221–233.

Kariyeva, J., van Leeuwen, W.J., and Woodhouse, C.A., 2012. Impacts of climate gradients on the vegetation phenology of major land use types in Central Asia (1981–2008). *Frontiers of Earth Science*, 6:206–225.

Kelly, R.D. and Walker, B.H., 1976. The effects of different forms of land use on the ecology of a semi-arid region in south-eastern Rhodesia. *The Journal of Ecology*, 553–576.

Kiguli, L.N., Palmer, A.R., and Avis, A.M., 1999. A description of rangeland on commercial and communal land, Peddie district, South Africa. *African Journal of Range and Forage Science*, 16:89–95.

Klink, C.A. and Machado, R.B., 2005. Conservation of the Brazilian cerrado. *Conservation biology*, 19:707–713.

Knapp, A.K., Briggs, J.M., and Koelliker, J.K., 2001. Frequency and extent of water limitation to primary production in a mesic temperate grassland. *Ecosystems*, 4:19–28.

Kruger, A. c., 1999. The influence of the decadal-scale variability of summer rainfall on the impact of El Niño and La Niña events in South Africa. *International Journal of Climatology*, 19 :59–68.

Lambin, E.F. and Ehrlich, D., 1997. Land-cover changes in sub-saharan Africa (1982–1991): Application of a change index based on remotely sensed surface temperature and vegetation indices at a continental scale. *Remote Sensing of Environment*, 61:181–200.

Lambin, E.F., Turner, B.L., Geist, H.J., Agbola, S.B., Angelsen, A., Bruce, J.W., Coomes, O.T., Dirzo, R., Fischer, G., Folke, C., George, P.S., Homewood, K., Imbernon, J., Leemans, R., Li, X., Moran, E.F., Mortimore, M., Ramakrishnan, P.S., Richards, J.F., Skånes, H., Steffen, W., Stone, G.D., Svedin, U., Veldkamp, T.A., Vogel, C., and Xu, J., 2001. The causes of land-use and land-cover change: Moving beyond the myths. *Global Environmental Change,* 11:261–269.

Latifovic, R. and Olthof, I., 2004. Accuracy assessment using sub-pixel fractional error matrices of global land cover products derived from satellite data. *Remote sensing of Environment*, 90:153–165.

Latifovic, R., Homer, C., Ressl, R., Pouliot, D., Hossain, S.N., Colditz, R.R., Olthof, I., Giri, C.P., and Victoria, A., 2016. North American land-change monitoring system. *In:* Remote sensing of land use and land cover. *CRC Press,* 322–343.

Lausch, A., Blaschke, T., Haase, D., Herzog, F., Syrbe, R.-U., Tischendorf, L., and Walz, U., 2015. Understanding and quantifying landscape structure – A review on relevant process characteristics, data models and landscape metrics. *Ecological Modelling*, 295:31–41.

Lehtilä, K., Haukioja, E., Kaitaniemi, P., and Laine, K.A., 2000. Allocation of resources within mountain birch canopy after simulated winter browsing. *Oikos*, 90:160–170.

Lieth, H., 1974. Purposes of a Phenology Book. *In:* H. Lieth, ed. *Phenology and Seasonality Modeling*. Springer Berlin Heidelberg, 3–19.

Lin, Y., Deng, X., and Jin, Q., 2013. Economic effects of drought on agriculture in North China. *International Journal of Disaster Risk Science*, 4:59–67.

Linderman, M., Rowhani, P., Benz, D., Serneels, S., and Lambin, E.F., 2005. Land-cover change and vegetation dynamics across Africa. *Journal of Geophysical Research: Atmospheres*, 110:1-15.

Lindesay, J.A. and Vogel, C.H., 1990. Historical evidence for Southern Oscillation-southern African rainfall relationships. *International Journal of Climatology*, 10:679–689.

Little, P.D., Stone, M.P., Mogues, T., Castro, A.P., and Negatu, W., 2006. 'Moving in place': Drought and poverty dynamics in South Wollo, Ethiopia. *Journal of Development Studies*, 42:200–225.

Liu, X., Li, X., Chen, Y., Tan, Z., Li, S., and Ai, B., 2010. A new landscape index for quantifying urban expansion using multi-temporal remotely sensed data. *Landscape Ecology*, 25:671–682.

Lobo, F. de A., Campelo Junior, J.H., Rodríguez-Ortíz, C.E., Lucena, I.C. de, and Vourlitis, G.L., 2008. Leaf and fruiting phenology and gas exchange of Mangabeira in response to irrigation. *Brazilian Journal of Plant Physiology*, 20:1–10.

Loveland, T.R., Reed, B.C., Brown, J.F., Ohlen, D.O., Zhu, Z., Yang, L., and Merchant, J.W., 2000. Development of a global land cover characteristics database and IGBP DISCover from 1 km AVHRR data. *International Journal of Remote Sensing*, 21:1303–1330.

Lu, P.-L., Yu, Q., Liu, J.-D., He, Q.-T., and others, 2006. Effects of changes in spring temperature on flowering dates of woody plants across China. *Botanical Stud*ies, 47 (2), 153–161.

Luoga, E.J., Witkowski, E.T.F., and Balkwill, K., 2000. Differential utilization and ethnobotany of trees in kitulanghalo forest reserve and surrounding communal lands, eastern Tanzania. *Economic Botany*, 54 (3), 328–343.

Madzibane, J. and Potgieter, M.J., 1999. Uses of Colophospermum mopane (Leguminosae: Caesalpinioideae) by the Vhavenda. *South African Journal of Botany*, 65 (5–6), 440–444.

Manhique, A.J., Reason, C.J.C., Silinto, B., Zucula, J., Raiva, I., Congolo, F., and Mavume, A.F., 2015. Extreme rainfall and floods in southern Africa in January 2013 and associated circulation patterns. *Natural Hazards*, 77:679–691.

Mapaure, I., 1994. The distribution of *Colophospermum mopane* (Leguminosae-caesalpinioideae) in Africa. *Kirkia*, 1–5.

Masia, N.D., Stevens, N., and Archibald, S., 2018. Identifying phenological functional types in savanna trees. *African Journal of Range and Forage Science*, 35:81–88.

Matthews, H.D., Weaver, A.J., Meissner, K.J., Gillett, N.P., and Eby, M., 2004. Natural and anthropogenic climate change: incorporating historical land cover change, vegetation dynamics and the global carbon cycle. *Climate Dynamics*, 22:461–479.

McLoughlin, C.A., Deacon, A., Sithole, H., and Gyedu-Ababio, T., 2011. History, rationale, and lessons learned: Thresholds of potential concern in Kruger National Park river adaptive management. *Koedoe*, 53:69-95.

McNaughton, S.J., 1979. Grazing as an optimization process: grass-ungulate relationships in the Serengeti. *American Naturalist*, 113:691–703.

McNaughton, S.J., 1987. Adaptation of herbivores to seasonal changes in nutrient supply. Nutrition of herbivores/edited by JB Hacker and JH Ternouth. *In:* Dekker, B. and Smit, G.N., 1996. Browse production and leaf phenology of some trees and shrubs in different Colophospermum mopane savanna communities. *African Journal of Range and Forage Science*, 13:15–23.

Medvey, J., 2010. Benefits or burden? Community participation in natural resource management in the Greater Kruger Park area. *Citeseer.*

Menzel, A., Sparks, T.H., Estrella, N., Koch, E., Aasa, A., Ahas, R., Alm-Kübler, K., Bissolli, P., Braslavská, O., Briede, A., and others, 2006. European phenological response to climate change matches the warming pattern. *Global Change Biology*, 12:1969–1976.

Mladenoff, D.J., 1987. Dynamics of nitrogen mineralization and nitrification in hemlock and hardwood treefall gaps. *Ecology,* 68:1171–1180.

Mograbi, P.J., Asner, G.P., Witkowski, E.T.F., Erasmus, B.F.N., Wessels, K.J., Mathieu, R., and Vaughn, N.R., 2017. Humans and elephants as treefall drivers in African savannas. *Ecography*, 40:1274–1284.

Mucina, L. and Rutherford, M.C., 2006. *The vegetation of South Africa, Lesotho and Swaziland.* South African National Biodiversity Institute.

Mueller, R.C., Scudder, C.M., Porter, M.E., Talbot Trotter III, R., Gehring, C.A., and Whitham, T.G., 2005. Differential tree mortality in response to severe drought: evidence for long-term vegetation shifts. *Journal of Ecology*, 93:1085–1093.

Mugalavai, E.M., Kipkorir, E.C., Raes, D., and Rao, M.S., 2008. Analysis of rainfall onset, cessation and length of growing season for western Kenya. *Agricultural and Forest Meteorology*, 148:1123–1135.

Muhati, G.L., Olago, D., and Olaka, L., 2018. Land use and land cover changes in a sub-humid Montane forest in an arid setting: A case study of the Marsabit forest reserve in northern Kenya. *Global Ecology and Conservation*, 16,:e00512.

Mwavu, E.N. and Witkowski, E.T.F., 2008. Land-use and cover changes (1988-2002) around budongo forest reserve, NW Uganda: implications for forest and woodland sustainability. *Land Degradation and Development*, 19:606–622.

Myers, B.A., Williams, R.J., Fordyce, I., Duff, G.A., and Eamus, D., 1998. Does irrigation affect leaf phenology in deciduous and evergreen trees of the savannas of northern Australia? *Australian Journal of Ecology,* 23:329–339.

Nacoulma, B.M.I., Schumann, K., Traoré, S., Bernhardt-Römermann, M., Hahn, K., Wittig, R., and Thiombiano, A., 2011. Impacts of land-use on West African savanna vegetation: A comparison between protected and communal area in Burkina Faso. *Biodiversity and Conservation*, 20:3341–3362.

Nash, D., 2017. Changes in precipitation over southern Africa during recent centuries.

Naughton-Treves, L., Holland, M.B., and Brandon, K., 2005. The role of protected areas in conserving biodiversity and sustaining local livelihoods. *Annual Review of Environment and Resources*, 30:219–252.

Neke, K.S., Owen-Smith, N., and Witkowski, E.T.F., 2006. Comparative resprouting response of Savanna woody plant species following harvesting: the value of persistence. *Forest Ecology and Managemen*t, 232:114–123.

Nemani, R.R., Keeling, C.D., Hashimoto, H., Jolly, W.M., Piper, S.C., Tucker, C.J., Myneni, R.B., and Running, S.W., 2003. Climate-driven increases in global terrestrial net primary production from 1982 to 1999. *Science*, 300:1560–1563.

News24 2017. *They are tourists in their land.* *https://www.news24.com/SouthAfrica/-News/they-are-tourists-in-their-land-20171118. Accessed 26 May 2019.*

Nord, E.A. and Lynch, J.P., 2009. Plant phenology: A critical controller of soil resource acquisition. *Journal of Experimental Botany*, 60:1927–1937.

O'Connor, T.G., 1995. Transformation of a savanna grassland by drought and grazing. *African Journal of Range and Forage Science*, 12:53–60.

O'Connor, T.G., 1998. Impact of sustained drought on a semi-arid *Colophospermum mopane* savanna. *African Journal of Range and Forage Science,* 15:83–91.

Odekunle, T.O., 2004. Rainfall and the length of the growing season in Nigeria. *International Journal of Climatology*, 24:467–479.

Ogallo, L.A., 1997. Validity of the ENSO-related impacts in Eastern and Southern Africa. *In:* Ogutu, J.O., Piepho, H.-P., Dublin, H.T., Bhola, N., and Reid, R.S., 2008. El Niño-Southern Oscillation, rainfall, temperature and Normalized Difference Vegetation Index fluctuations in the Mara-Serengeti ecosystem. *African Journal of Ecology*, 46 :132–143.

Oguntunde, P.G., Lischeid, G., Abiodun, B.J., and Dietrich, O., 2014. Analysis of spatial and temporal patterns in onset, cessation and length of growing season in Nigeria. *Agricultural and Forest Meteorology*, 194:77–87.

Ogutu, J.O. and Owen-Smith, N., 2003. ENSO, rainfall and temperature influences on extreme population declines among African savanna ungulates. *Ecology Letters*, 6:412–419.

Ogutu, J.O., Piepho, H.-P., Dublin, H.T., Bhola, N., and Reid, R.S., 2008. El Niño-Southern Oscillation, rainfall, temperature and Normalized Difference Vegetation Index fluctuations in the Mara-Serengeti ecosystem. *African Journal of Ecology*, 46 :132–143.

Pacifici, F., Chini, M., and Emery, W.J., 2009. A neural network approach using multi-scale textural metrics from very high-resolution panchromatic imagery for urban land-use classification. *Remote Sensing of Environmen*t, 113:1276–1292.

Papanastasis, V.P., 2009. Restoration of degraded grazing lands through grazing management: can it work? *Restoration Ecology,* 17:441–445.

Parmesan, C. and Yohe, G., 2003. A globally coherent fingerprint of climate change impacts across natural systems. *Nature*, 421:37–42.

Parry, D., 1989. Some effects of the 1981-87 drought on woody plants in Botswana. *Botswana Notes and Records*, 20:155–159.

Parsons, M., McLoughlin, C.A., Kotschy, K.A., Rogers, K.H., and Rountree, M.W., 2005. The effects of extreme floods on the biophysical heterogeneity of river landscapes. *Frontiers in Ecology and the Environment,* 3:487–494.

Parsons, M., McLoughlin, C.A., Rountree, M.W., and Rogers, K.H., 2006. The biotic and abiotic legacy of a large infrequent flood disturbance in the Sabie River, South Africa. *River Research and Applications,* 22:187–201.

Paumgarten, F., Locatelli, B., and Witkowski, E.T.F., 2018. Wild Foods: Safety Net or Poverty Trap? A South African Case Study. *Human Ecology*, 46:183–195.

Peel, M.J.S., Biggs, H., and Zacharias, P.J.K., 1998. The evolving use of stocking rate indices currently based on animal number and type in semi-arid heterogeneous landscapes and complex land-use systems. *African Journal of Range and Forage Science*, 15:117–127.

Peters, A.J., Walter-Shea, E.A., Ji, L., Vina, A., Hayes, M., and Svoboda, M.D., 2002. Drought monitoring with NDVI-based standardized vegetation index. *Photogrammetric Engineering and Remote Sensing,* 68:71–75.

Petit, C., Scudder, T., and Lambin, E., 2001. Quantifying processes of land-cover change by remote sensing: Resettlement and rapid land-cover changes in south-eastern Zambia. *International Journal of Remote Sensing*, 22:3435–3456.

Poggio, L., Gimona, A. and Brown, I., 2012. Spatio-temporal MODIS EVI gap filling under cloud cover: An example in Scotland. *ISPRS journal of photogrammetry and remote sensing*, 72:56-72.

Polgar, C.A. and Primack, R.B., 2011. Leaf-out phenology of temperate woody plants: from trees to ecosystems. *New Phytologist*, 191:926–941.

Primack, R.B., Ibáñez, I., Higuchi, H., Lee, S.D., Miller-Rushing, A.J., Wilson, A.M., and Silander, J.A., 2009. Spatial and interspecific variability in phenological responses to warming temperatures. *Biological Conservation*, 142:2569–2577.

Prins, H.H.T., 1988. Plant Phenology Patterns in Lake Manyara National Park, Tanzania. *Journal of Biogeography,* 15:465-480.

Rao, P., Barik, S.K., Pandey, H.N., and Tripathi, R.S., 1990. Community composition and tree population structure in a sub-tropical broad-leaved forest along a disturbance gradient. *Vegetatio*, 88:151–162.

Ray, T.W. and Murray, B.C., 1996. Nonlinear spectral mixing in desert vegetation*. Remote Sensing of Environment,* 55:59–64.

Recha, C.W., Makokha, G.L., Traore, P.S., Shisanya, C., Lodoun, T., and Sako, A., 2012. Determination of seasonal rainfall variability, onset and cessation in semi-arid Tharaka district, Kenya*. Theoretical and Applied Climatology*, 108:479–494.

Reich, P.B. and Borchert, R., 1984. Water Stress and Tree Phenology in a Tropical Dry Forest in the Lowlands of Costa Rica. *The Journal of Ecology*, 72:61.

Reid, R.S., Kruska, R.L., Muthui, N., Taye, A., Wotton, S., Wilson, C.J., and Mulatu, W., 2000. Land-use and land-cover dynamics in response to changes in climatic, biological and socio-political forces: the case of southwestern Ethiopia. *Landscape Ecology*, 15:339–355.

Ren, Y., Lü, Y., Comber, A., Fu, B., Harris, P., and Wu, L., 2019. Spatially explicit simulation of land use/land cover changes: Current coverage and future prospects. *Earth-Science Reviews,* 190:398–415.

Richard, Y., Fauchereau, N., Poccard, I., Rouault, M. and Trzaska, S., 2001. 20th century droughts in southern Africa: spatial and temporal variability, teleconnections with oceanic and atmospheric conditions. *International Journal of Climatology*, 21:873-885.

Richardson, A.D., Keenan, T.F., Migliavacca, M., Ryu, Y., Sonnentag, O., and Toomey, M., 2013. Climate change, phenology, and phenological control of vegetation feedbacks to the climate system. *Agricultural and Forest Meteorology*, 169:156–173.

Romo-Leon, J.R., van Leeuwen, W.J.D., and Castellanos-Villegas, A., 2016. Land Use and Environmental Variability Impacts on the Phenology of Arid Agro-Ecosystems. *Environmental Management*, 57:283–297.

Rooke, T. and Bergström, R., 2007. Growth, chemical responses and herbivory after simulated leaf browsing in Combretum apiculatum. *Plant Ecology*, 189:201–212.

Rossi, L., 2009. Very High Resolution Satellites. *In:* Desertification and Risk Analysis Using High and Medium Resolution Satellite Data. *Springer Science and Business Media, Dordrecht*, 217–228.

Rouault, M. and Richard, Y., 2005. Intensity and spatial extent of droughts in southern Africa. *Geophysical Research Letters*, 32: L15702.

Ryan, C.M., Williams, M., Grace, J., Woollen, E., and Lehmann, C.E.R., 2017. Pre-rain green-up is ubiquitous across southern tropical Africa: implications for temporal niche separation and model representation. *New Phytologist,* 213:625–633.

Ryan, C.M., Williams, M., Hill, T.C., Grace, J., and Woodhouse, I.H., 2014. Assessing the Phenology of Southern Tropical Africa: A Comparison of Hemispherical Photography, Scatterometry, and Optical/NIR Remote Sensing. *IEEE Transactions on Geoscience and Remote Sensing,* 52:519–528.

Sala, O.E., Chapin, F.S., Armesto, J.J., Berlow, E., Bloomfield, J., Dirzo, R., Huber-Sanwald, E., Huenneke, L.F., Jackson, R.B., and Kinzig, A., 2000. Global biodiversity scenarios for the year 2100. *Science*, 287:1770–1774.

Sankaran, M., Hanan, N.P., Scholes, R.J., Ratnam, J., Augustine, D.J., Cade, B.S., Gignoux, J., Higgins, S.I., Le Roux, X., and Ludwig, F., 2005. Determinants of woody cover in African savannas. *Nature*, 438:846.

Satellite Imaging Corporation. 20017. https://www.satimagingcorp.com/satellite-sensors/quickbird/. Accessed 27 May 2019.

Scheiter, S. and Higgins, S.I., 2009. Impacts of climate change on the vegetation of Africa: an adaptive dynamic vegetation modelling approach. *Global Change Biology*, 15:2224–2246.

Schmidt, H. and Karnieli, A., 2000. Remote sensing of the seasonal variability of vegetation in a semi-arid environment. *Journal of Arid Environments,* 45:43–59.

Scholes, R.J. and Walker, B.H., 2004. *An African savanna: synthesis of the Nylsvley study*. Cambridge University Press.

Schwartz, M.D., Ahas, R., and Aasa, A., 2006. Onset of spring starting earlier across the Northern Hemisphere. *Global Change Biology*, 12:343–351.

Seki, H.A., Shirima, D.D., Mustaphi, C.J.C., Marchant, R., and Munishi, P.K.T., 2018. The impact of land use and land cover change on biodiversity within and adjacent to Kibasira Swamp in Kilombero Valley, Tanzania. *African Journal of Ecology*, 56:518–527.

Sellers, P.J., Dickinson, R.E., Randall, D.A., Betts, A.K., Hall, F.G., Berry, J.A., Collatz, G.J., Denning, A.S., Mooney, H.A., and Nobre, C.A., 1997. Modeling the exchanges of energy, water, and carbon between continents and the atmosphere. *Science*, 275:502–509.

Seydack, A.H., Grant, C.C., Smit, I.P., Vermeulen, W.J., Baard, J., and Zambatis, N., 2012. Large herbivore population performance and climate in a South African semi-arid savanna. *Koedoe*, 54:1–20.

Shackleton, C.M., 2000. Comparison of plant diversity in protected and communal lands in the Bushbuckridge lowveld savanna, South Africa. *Biological Conservation*, 94:273–285.

Shackleton, C.M., Griffin, N.J., Banks, D.I., Mavrandonis, J.M., and Shackleton, S.E., 1994. Community structure and species composition along a disturbance gradient in a communally managed South African savanna. *Vegetatio*, 115:157–167.

Shackleton, C.M., Guthrie, G., and Main, R., 2005. Estimating the potential role of commercial over-harvesting in resource viability: a case study of five useful tree species in South Africa. *Land Degradation and Development*, 16:273–286.

Shackleton, C.M., Shackleton, S.E., and Cousins, B., 2001. The role of land-based strategies in rural livelihoods: The contribution of arable production, animal husbandry and natural resource harvesting in communal areas in South Africa. *Development Southern Africa*, 18:581–604.

Shackleton, S.E., Shackleton, C.M., Netshiluvhi, T.R., Geach, B.S., Ballance, A., and Fairbanks, D.H.K., 2002. Use patterns and value of savanna resources in three rural villages in South Africa. *Economic Botany,* 56:130–146.

Sharma, C.S., Behera, M.D., Mishra, A., and Panda, S.N., 2011. Assessing flood induced land-cover changes using remote sensing and fuzzy approach in Eastern Gujarat (India). *Water Resources Management*, 25:3219.

Sibanda, M., Mutanga, O. and Rouget, M., 2017. Testing the capabilities of the new WorldView-3 space-borne sensor's red-edge spectral band in discriminating and mapping complex grassland management treatments. *International Journal of Remote Sensing*, 38:1-22.

Silva, J.F., Zambrano, A., and Fariñas, M.R., 2001. Increase in the woody component of seasonal savannas under different fire regimes in Calabozo, Venezuela. *Journal of Biogeography*, 28:977–983.

Sims, N.C. and Thoms, M.C., 2002. What happens when flood plains wet themselves: Vegetation response to inundation on the lower Balonne flood plain. *International Association of Hydrological Sciences*, Publication, 276:195–202.

Sitoe, S.R., Risberg, J., Norström, E., Snowball, I., Holmgren, K., Achimo, M., and Mugabe, J., 2015. Paleo-environment and flooding of the Limpopo River-plain, Mozambique, between c. AD 1200–2000. *Catena,* 126:105–116.

Sivakumar, M.V.K., 1988. Predicting rainy season potential from the onset of rains in Southern Sahelian and Sudanian climatic zones of West Africa. *Agricultural and Forest Meteorology*, 42:295–305.

Skarpe, C., 1990. Structure of the woody vegetation in disturbed and undisturbed arid savanna, Botswana. *Vegetatio,* 87:11–18.

Smallie, J.J. and O'Connor, T.G., 2000. Elephant utilization of *Colophospermum mopane*: possible benefits of hedging. *African Journal of Ecology,* 38:352-359.

Smit, G.N. and Rethman, N.F.G., 1998. The influence of tree thinning on the reproduction dynamics of *Colophospermum mopane*. *South African Journal of Botany*, 64:25–29.

Smit, G.N., 1994. The Influence of intensity of tree thinning on mopani veld. PhD thesis, University of Pretoria, Pretoria, South Africa. *In:* Smit, G.N., 2003. The coppicing ability of *Acacia erubescens* and *Combretum apiculatum subsp. apiculatum* in response to cutting. *African Journal of Range and Forage Science*, 20:21–27.

Smit, G.N., 2003. The coppicing ability of *Acacia erubescens* and *Combretum apiculatum subsp. apiculatum* in response to cutting. *African Journal of Range and Forage Science*, 20:21–27.

Smit, G.N., 2005. Tree thinning as an option to increase herbaceous yield of an encroached semi-arid savanna in South Africa. *BMC Ecology*, 15:4.

Smit, N., 2014. Response of *Colophospermum mopane* to different intensities of tree thinning in the Mopane Bushveld of southern Africa. *African Journal of Range and Forage Science*, 31:173–177.

Statistics South Africa, S.S., 2016. Statistics South Africa | The South Africa I Know, The Home I Understand. http://www.statssa.gov.za/

Steenkamp, K., Wessels, K., Archibald, S., and Von Maltitz, G., 2008. Long-term phenology and variability of Southern African vegetation. *In:* Geoscience and Remote Sensing Symposium, 2008. *IGARSS 2008. IEEE International.* IEEE, III–816.

Stephenson, N.L., 1990. Climatic control of vegetation distribution: the role of the water balance. *The American Naturalist*, 135:649–670.

Stevens, N., Archibald, S.A., Nickless, A., Swemmer, A., and Scholes, R.J., 2016. Evidence for facultative deciduousness in *Colophospermum mopane* in semi-arid African savannas: Leaf Drop in C. mopane. *Austral Ecology*, 41:87–96.

Styles, C.V. and Skinner, J.D., 1997. Seasonal variations in the quality of mopane leaves as a source of browse for mammalian herbivores. *African Journal of Ecology*, 35:254–265.

Swemmer, A.M., Bond, W.J., Donaldson, J., Hempson, G.P., Malherbe, J., and Smit, I.P.J., 2018. The ecology of drought – a workshop report. *South African Journal of Science*, 114:1-3.

Thompson, J. G., 1960. A description of the growth habits of Mopane in relation to soil and climatic conditions. *Proceedings of the First Federal Science Congress, Salisbury*, 181-186.

Todd, S.W. and Hoffman, M.T., 1999. A fence-line contrast reveals effects of heavy grazing on plant diversity and community composition in Namaqualand, South Africa. *Plant Ecology*, 142:169–178.

Todd, S.W. and Hoffman, M.T., 2009. A fence line in time demonstrates grazing-induced vegetation shifts and dynamics in the semiarid Succulent Karoo. *Ecological Applications*, 19:1897–1908.

Trollope, W.S.W., 1982. Ecological effects of fire in South African savannas. In: Ecology of tropical savannas. *Springer*, 292–306.

Trollope, W.S.W., Trollope, L.A., Biggs, H.C., Pienaar, D., and Potgieter, A.L.F., 1998. Long-term changes in the woody vegetation of the Kruger National Park, with special reference to the effects of elephants and fire. *Koedoe*, 41:103–112.

Tucker, C.J., Goff, T.E., and Townshend, J.R.G., 1985. African land-cover classification using satellite data. *Science,* 227:369–375.

Unganai, L.S. and Kogan, F.N., 1998. Drought monitoring and corn yield estimation in Southern Africa from AVHRR data. *Remote Sensing of Environment*, 63:219-232.

Usman, M.T. and Reason, C.J.C., 2004. Dry spell frequencies and their variability over southern Africa. *Climate Research*, 26:199–211.

van de Koppel, J., Rietkerk, M., van Langevelde, F., Kumar, L., Klausmeier, C.A., Fryxell, J.M., Hearne, J.W., van Andel, J., de Ridder, N., Skidmore, A., Stroosnijder, L., and Prins, H.H.T., 2002. Spatial Heterogeneity and Irreversible Vegetation Change in Semiarid Grazing Systems. *The American Naturalist*, 159:209–218.

Van der Colff, H. 2017. Personal communication. Manager at the Awelani Lodge.

Van Heerden, J., Terblanche, D.E., and Schulze, G.C., 1988. The southern oscillation and South African summer rainfall. *Journal of Climatology*, 8:577–597.

Van Langevelde, F., Van De Vijver, C.A., Kumar, L., Van De Koppel, J., De Ridder, N., Van Andel, J., Skidmore, A.K., Hearne, J.W., Stroosnijder, L., and Bond, W.J., 2003. Effects of fire and herbivory on the stability of savanna ecosystems. *Ecology*, 84:337–350.

Van Leeuwen, W.J.D., Davison, J.E., Casady, G.M., and Marsh, S.E., 2010. Phenological characterization of Desert Sky Island vegetation communities with remotely sensed and climate time series data. *Remote Sensing*, 2:388–415.

Van Loon, A.F., 2015. Hydrological drought explained. *Wiley Interdisciplinary Reviews: Water*, 2:359-392.

van Marrewijk, L., 2011. Climate Smart Agriculture in the Mutale Basin, South Africa, MSc.-thesis IVMVU Amsterdam.

Van Voorthuizen, E.G., 1976: The mopane tree. *Botswana Notes and Records*, 8:223-230.

Vanacker, V., Linderman, M., Lupo, F., Flasse, S., and Lambin, E., 2005. Impact of short-term rainfall fluctuation on interannual land cover change in sub-Saharan Africa. *Global Ecology and Biogeography,* 14:123–135.

Vanak, A.T., Thaker, M. and Slotow, R., 2010. Do fences create an edge-effect on the movement patterns of a highly mobile mega-herbivore? *Biological Conservation* 143:2631–2637.

Veenendaal, E.M., Kolle, O., and Lloyd, J., 2004. Seasonal variation in energy fluxes and carbon dioxide exchange for a broad-leaved semi-arid savanna (Mopane woodland) in Southern Africa. *Global Change Biology*, 10:318–328.

Venter, F.J., Naiman, R.J., Biggs, H.C., and Pienaar, D.J., 2008. The Evolution of Conservation Management Philosophy: Science, Environmental Change and Social Adjustments in Kruger National Park. *Ecosystems,* 11:173–192.

Venter, F.J., Scholes, R.J., and Eckhardt, H.C., 2003. The abiotic template and its associated vegetation pattern. The Kruger experience: *Ecology and management of savanna heterogeneit*y, 83:129.

Venter, S.M. and Witkowski, E.T.F., 2010. Baobab (*Adansonia digitata L.*) density, size-class distribution and population trends between four land-use types in northern Venda, South Africa. *Forest Ecology and Management*, 259:294–300.

Venter, S.M. and Witkowski, E.T.F., 2013. Fruits of our labour: contribution of commercial baobab (*Adansonia digitata L.*) fruit harvesting to the livelihoods of marginalized people in northern Venda, South Africa. *Agroforestry Systems*, 87:159–172.

Vetter, S., 2009. Drought, change and resilience in South Africa's arid and semi-arid rangelands. *South African Journal of Science*, 105:29–33.

Viljoen, A.J., 1995. The influence of the 1991/92 drought on the woody vegetation of the Kruger National Park. *Koedoe*, 38: 85–97.

Vintrou, E., Bégué, A., Baron, C., Seen, D.L., Alexandre, S., and Traoré, S., 2012. Analysing MODIS phenometrics quality on cropped land in West Africa. *In: Processions of the ESA Sentinel-2 Preparatory Symposium.*

Vogel, C. and van Zyl, K., 2016. Drought: In search of sustainable solutions to a persistent, 'wicked'problem in South Africa. In: Climate Change Adaptation Strategies–An Upstream-downstream Perspective. *Springer,* 195–211.

Waldner, F., Hansen, M.C., Potapov, P.V., Löw, F., Newby, T., Ferreira, S., and Defourny, P., 2017. National-scale cropland mapping based on spectral-temporal features and outdated land cover information. *PLOS ONE*, 12:e0181911.

Walker, B.H., 1980. A review of browse and its role in livestock production in southern Africa. Browse in Africa. *The current state of knowledge. ILCA: Addis Ababa, Ethiopia*, 7-24.

Wallace, C.S., Villarreal, M.L., and Riper III, C., 2013. Influence of monsoon-related riparian phenology on yellow-billed cuckoo habitat selection in Arizona. *Journal of Biogeography*, 40:2094–2107.

Wang, Q. and Tenhunen, J.D., 2004. Vegetation mapping with multitemporal NDVI in North Eastern China transect (NECT). *International Journal of Applied Earth Observation and Geoinformation,* 6:17–31.

Ward, P.J., Jongman, B., Kummu, M., Dettinger, M.D., Sperna Weiland, F.C., and Winsemius, H.C., 2014. Strong influence of El Nino Southern Oscillation on flood risk around the world. *Proceedings of the National Academy of Sciences*, 111:15659–15664.

Ward, P.J., Kummu, M., and Lall, U., 2016. Flood frequencies and durations and their response to El Niño Southern Oscillation: Global analysis. *Journal of Hydrology*, 539:358–378.

Wells, M.P., 1996. The social role of protected areas in the new South Africa. *Environmental Conservation*, 23:322–331.

Wessels, K., Prince, S., Frost, P., and van Zyl, D., 2004. Assessing the effects of human-induced land degradation in the former homelands of northern South Africa with a 1 km AVHRR NDVI time-series. *Remote Sensing of Environment*, 91:47–67.

Wessels, K.J., Mathieu, R., Erasmus, B.F.N., Asner, G.P., Smit, I.P.J., van Aardt, J.A.N., Main, R., Fisher, J., Marais, W., Kennedy-Bowdoin, T., Knapp, D.E., Emerson, R., and Jacobson, J., 2011. Impact of communal land use and conservation on woody vegetation structure in the Lowveld savannas of South Africa. *Forest Ecology and Management*, 261:19–29.

Wessels, K.J., Prince, S.D., Malherbe, J., Small, J., Frost, P.E., and VanZyl, D., 2007. Can human-induced land degradation be distinguished from the effects of rainfall variability? A case study in South Africa. *Journal of Arid Environments,* 68: 271–297.

Wessels, K.J., Steenkamp, K., Von Maltitz, G., Archibald, S., Scholes, R.J., Miteff, S., and Bachoo, A., 2009. Remotely sensed phenology for mapping biomes and vegetation functional types. *In:* Geoscience and Remote Sensing Symposium, 2009 IEEE International, *IGARSS 2009*. IEEE, IV–1034.

Whitecross, M.A., Witkowski, E.T.F. and Archibald, S., 2016. No two are the same: Assessing variability in broad-leaved savanna tree phenology, with watering, from 2012 to 2014 at Nylsvley, South Africa. *South African Journal of Botany*, 105:123-132.

Whitecross, M.A., Witkowski, E.T.F. and Archibald, S., 2017b. Savanna tree-grass interactions: A phenological investigation of green-up in relation to water availability over three seasons. *South African Journal of Botany*, 108:29-40.

Whitecross, M.A., Witkowski, E.T.F., and Archibald, S., 2017a. Assessing the frequency and drivers of early-greening in broad-leaved woodlands along a latitudinal gradient in southern Africa. *Austral Ecology*, 42 :341–353.

Wigley, B.J., Bond, W.J., and Hoffman, M.T., 2010. Thicket expansion in a South African savanna under divergent land use: local vs. global drivers? *Global Change Biology*, 16:964–976.

Wilhite, D.A., 1993. *Planning for drought: A methodology. In Drought assessment, management, and planning: Theory and case studies.* Springer, Boston, MA, 87-108.

Wischmeier, W.H. and Smith, D.D., 1978. *Predicting rainfall erosion losses-a guide to conservation planning*. Predicting rainfall erosion losses-a guide to conservation planning.

Witkowski, E.T.F. and O'Connor, T.G., 1996. Topo-edaphic, floristic and physiognomic gradients of woody plants in a semi-arid African savanna woodland. *Vegetatio,* 124:9–23.

Xie, Y., Sha, Z., and Yu, M., 2008. Remote sensing imagery in vegetation mapping: a review. *Journal of Plant Ecology,* 1:9–23.

Yang, Y., Xiao, P., Feng, X., and Li, H., 2017. Accuracy assessment of seven global land cover datasets over China. *ISPRS Journal of Photogrammetry and Remote Sensing*, 125:156–173.

Yu, L., Wang, J., and Gong, P., 2013. Improving 30 m global land-cover map FROM-GLC with time series MODIS and auxiliary data sets: a segmentation-based approach. *International Journal of Remote Sensing*, 34:5851–5867.

Zambatis, N. and Biggs, H.C., 1995. Rainfall and temperatures during the 1991/92 drought in the Kruger National Park. *Koedoe*, 38:1–16.

Zhang, X., A., M., Tan, B., D., M., and Yu, Y., 2012. Long-Term Detection of global vegetation phenology from satellite instruments*. In: Phenology and Climate Change*. InTechOpen.

Zhao, M., Peng, C., Xiang, W., Deng, X., Tian, D., Zhou, X., Yu, G., He, H., and Zhao, Z., 2013. Plant phenological modelling and its application in global climate change research: Overview and future challenges. *Environmental Reviews*, 21:1–14.